1-1-2011

High Speed Wireless Networking for 60GHz

Candy Yiu
Portland State University

Let us know how access to this document benefits you.

High Speed Wireless Networking for 60GHz

by

Candy Yiu

A dissertation submitted in partial fulfillment of the
requirements for the degree of

Doctor of Philosophy
in
Computer Science

Dissertation Committee:
Suresh Singh, Chair
Sergio Antoy
Fei Xie
Bryant York
Lisa Zurk

Portland State University
2011

Abstract

This thesis examines the problem of providing high data-rate wireless connectivity to users in indoor environments. The goal is to be able to reach Gbps/user rates even when there are multiple users present. The technology that we study is to use the 60 GHz spectrum whose special propagation properties make it ideally suited to this task. The approaches developed include using multiple spatially distributed smart antennas in a room or multiple co-located antennas to provide coverage where needed and when needed. All the antennas are connected to a single access point which allows us to dynamically change spectrum and link allocation among the users (as they move or as their needs change). The innovations in this work include the exploitation of the special properties of 60 GHz and the corresponding design of algorithms for efficient spectrum allocation. We use detailed simulations to demonstrate that very high data rates are indeed achievable.

Dedication

I dedicate this thesis to my parents and my husband, without their patience and support, it would not been possible.

Acknowledgements

Contents

List of Tables

List of Figures

Chapter 1

INTRODUCTION

The opening of the 60GHz ISM (Industrial Scientific Medical) band has triggered intense interest in industry as well as academia on exploring different ways to exploit the available 5-7GHz bandwidth. The large amount of bandwidth available makes it possible to deploy very high data rate links. Some use models being studied include point-to-point links between buildings (similar to free space optics), high data rate wireless networks in buildings, and as a replacement for wires within computers. Our focus in this thesis is on wireless networks though the solutions developed can be applied generally to any high frequency channel in the tens of GHz or 100s of GHz range.

From a network design point of view, this frequency band offers a specific challenge not seen at lower ends of the spectrum (for instance the bands we are more familiar with, between 2-5GHz). At 60GHz, the signal attenuation is high because of oxygen absorption and absorption by many materials commonly used in construction. Therefore, reflected components of a signal tend to be significantly attenuated as compared to a direct path. Furthermore, given the high frequency, there is also significant attenuation with distance (88 dB/10m as compared with 60 dB/10m for 2.5 GHz). Therefore, as [15] points out, technologies such as MIMO (Multiple Input Multiple Output) that rely on a rich multi-path environment are not useful at this frequency. Indeed, typical WLAN (Wireless Local Area Network) architectures used at lower frequencies (which exploit multi-path) are not suitable

for 60GHz networks. This leads to the design challenge of how best to architect WLANs at this frequency so as to provide high data rate coverage indoors.

The approach proposed by various authors is to build a WLAN around the idea of highly directional smart antennas at the access points (AP) and users. The benefit of these antennas is the high gain and adaptive beamforming. But the drawbacks are many. For instance, links can be easily broken by obstacles as the user moves behind an obstruction or if another person comes in the Line of Sight (LoS) path between the user and AP (the high water content of the body is a very good absorber of this frequency).

1.1 RESEARCH CONTRIBUTIONS

In this thesis we examine various design trade offs in building 60 GHz WLANs. Some major challenges to overcome, and the problems we examine, are:

- 60 GHz is primarily targeted for indoor applications such as office and factory environments. However, these environments have numerous obstructions such as partitions, walls, metallic objects like filing cabinets, plasterboard walls, glass walls, etc. All of these obstructions either completely block 60 GHz signals or attenuate them by 5-15dB. As a result, providing full coverage in such complex spaces is a challenging problem where the constraint is to minimize the number of access points deployed while also maximizing throughput.

- While poor propagation of 60 GHz causes coverage problems, it also gives us the opportunity to dramatically increase throughput by spatially re-using the spectrum. For instance, two users located in the same room but separated by a partition or in different directional beams of the AP's antenna can use the same spectrum with minimal interference. This is unlike 2-5 GHz where

reflections are not severely attenuated and thus it is impossible to re-use the same spectrum at close quarters. We study innovative ways of maximizing spectrum re-use when APs are equipped with smart antennas.

- Given a deployed indoor WLAN, it is still possible for coverage to be intermittent due to changes in orientation of obstructions or due to people walking around (since people are composed mainly of water, their bodies act as excellent absorbers of this frequency). The problem we study is how to design the coverage and spectrum allocation of a room to account for all potential future disruptions.

The solutions to these challenges are based on a combination of careful AP placement in the room, efficient resource allocation (where the resources are spatial and frequency channels) and provisioning indirect paths to mitigate intermittent link breakages.

The main contributions of this research are as follows:

- Design of optimal algorithms for providing 100% coverage in rooms with arbitrary collections of obstructions [52, 48].

- Algorithms for ad hoc communication between arbitrary collection of devices (without WLAN infrastructure) [51].

- Different architectures and resource allocation algorithms for maximizing throughput per user and link repair algorithms [53, 50, 54, 49].

1.2   THESIS ORGANIZATION

In the next chapter, we provide a detailed literature survey. In Chapter 2, we summarize the technical background related to this thesis. Chapter 3 reviews the

60GHz properties. In Chapter 4, a summary of smart antennas is provided and we describe the two types of antenna configurations we study for 60 GHz. The access point placement study for 100% coverage given static obstructions is given in chapter 5. Chapters 6 and 7 examine different architectures and resource allocations to maximize throughput. Finally, the problem of maintaining connectivity even in the presence of mobile obstructions (or link repair) is studied in chapter 8 followed by our conclusions in chapter 9.

Chapter 2

RELATED WORK

2.1 TECHNIQUES FOR HIGH-SPEED WIRELESS

Over the past several years, many technologies have been developed to deliver high data rates over wireless channels. Typically, the techniques developed exploit some aspect of the particular frequency band or propagation environment under consideration. Since the focus of the current work is on 60 GHz WLANs, it is instructive to examine if and how existing technologies can be applied to this new frequency regime.

Delivering high data rates to each user translates to the problem of maximizing the *Number of bits/Hz*. Two of the factors that significantly degrade this metric include, competition for the channel by multiple users and poor channel quality resulting in lower spectral efficiency. The former problem is a MAC (Medium Access Control) problem whereas the latter problem lies at the Physical Layer. Our focus in this thesis is not on the MAC layer but rather on the physical layer and the intersection between the MAC layer and the physical layer. Therefore, to enable a comprehensive discussion of issues, we provide a quick summary of the main issues at the MAC layer as they related to high data rate WLANs. In the wireless domain, the number of users and the channel load offered by each user are unknown (indeed, unknowable) quantities. Therefore, if n users have packets to send or receive at some instant, determining who gets channel access is a difficult problem to solve. Numerous solutions have been proposed in the past and they can

5

be classified as either being random access or managed access. Examples of random access include the CSMA/CA (Carrier Sense Multiple Access/Collision Avoidance) used in 802.11 networks while example of managed access include splitting the channel in time or frequency or code and statically allocating these sub-channels to registered users. In random access solutions, a great deal of the channel is wasted in contention for the channel while in managed access, since the sub-channels are statically assigned, the inefficiencies come about when there is a load imbalance between users. Thus, lightly loaded users barely use the sub-channel assigned to them while heavy users see high delays since the capacity of sub-channels is lower. As a result, the average bits/Hz is reduced.

The physical layer challenge has to do with the problem of improving channel quality by exploiting properties of the channel itself. Imagine a simple model where the AP and user are both equipped with single omni-directional antennas. The channel between them will then consist of the strongest multi-path component between them. Thus, obstructions that cause loss of a direct line of sight path will result in a weaker signal being received (and hence lower data rate). Furthermore, if there is another user present, then the problem is compounded because of MAC layer contention between these two users for channel access. Some of the techniques studied to enable high-speed wireless access are described below.

2.1.1 Time Division Multiple Access (TDMA)

A well known way to deal with the problem of contention for channel access is to split the channel into time slots where a 'master' emits pulses to indicate time boundaries and nodes transmit only in their assigned slot. The slots may be allocated statically to individual users or dynamically using some form of periodic reservation scheme. This technique lies at the boundary of the physical layer and

MAC layer and is used in all modern cellular phone systems. The benefit of TDMA is that it eliminates the problem of channel contention (that can consume a large portion of the channel). However, uneven loading and the problem of having very accurate clocks at users and the master (who emits the periodic pulses to indicate time boundaries) render this solution unpalatable for many applications.

Despite these drawbacks, TDMA is an attractive solution at high frequencies where the channel bandwidth is large. To understand the reason for this it is best to see why random access techniques are a poor choice. Given a large bandwidth (several Ghz, for example), the length of a packet, as measured in time, is very short. For instance, if the channel bandwidth is 3 GHz, and we use a simple modulation of 8 bits/Hz, we can transmit at 24 Gbps. If users are in a room (say 15m long) then the round trip time between a pair is 10^{-7} seconds. In order for random access techniques to work well, the packet length needs to be greater than the round trip time. This means that the smallest packet we can have will be longer than 2400 bits or 300 bytes. In typical Ethernet communication the smallest packet is 64 Bytes. Thus, we will need to pad these packets to make them 300 Bytes long resulting in enormous wastage of bandwidth.

Therefore, TDMA has been proposed as the ideal technology to use at the frequency bands available for WLANs at 19 and 25 GHz [20]. By using TDMA we can ensure that packet transmissions do not collide and the protocols work correctly. Furthermore, given > 1 GHz available bandwidth, we can easily ensure better than 400Mbps rates for each user (since it is unlikely that more than tens of users will be present in any room).

2.1.2 Orthogonal Frequency Division Multiple Access (OFDM)

A solution related to TDMA is to divide the frequency band into mutually orthogonal channels and assign one channel statically to each user. We can show that TDMA and OFDM are equivalent [38] and therefore the kind of data rates achieved are similar. Note, however, that in OFDM the frequency sub-channels are not as wide and therefore a packet length lasts much longer. As an example, by dividing a channel into 16, we have a maximum Ethernet packet size of 32μsec. This means that, in order to use contention based protocols like 802.11, we need to ensure a minimum round trip delay between nodes of 19 meters which is easily attainable. Indeed, OFDM is used in 802.11a/g protocols because it results in better channel efficiency.

2.1.3 Multiple Input Multiple Output (MIMO), Spatial Division Multiple Access (SDMA)

MIMO is an innovative approach to improving channel efficiency by cleverly utilizing multi-path components of a transmission. Typically, a transmission will arrive at the receiver via multiple reflected (and perhaps a direct) paths. In MIMO, each transmitter and receiver has m and n antennas respectively. The transmitter generates m symbol streams and transmits them while the receiver combines the n received signals to extract the transmitted symbols. This technique can result in very high data rates (of the order of $m \times n$ improvement) since we are utilizing more than one transmitted component [32, 8, 12, 44]. Note, however, that this approach relies on high quality reflected components. SDMA refers to the technique where we split the propagation environment spatially. Thus, if two users are located at opposite ends of a room, it is possible for them both to be simultaneously active if the AP

8

uses directional antennas pointed at each of them. This effectively doubles the capacity and bits/Hz of the channel. There are numerous formulations of how to best apply SDMA to a given WLAN [41, 23, 35, 47, 1, 22, 34, 4, 7, 21, 25, 16, 26, 24, 19, 3] but they all share a common underlying model. The idea is, given some placement of n users and some number of antenna elements at the AP, how can we assign spatial channels to each user to maximize throughput. In a later chapter we discuss how directional transmissions can be enabled using smart antennas. For now, it is reasonable to assume that each user can be served by an isolated beam of a directional transmission. Naturally, different transmissions will have very different signal quality (some might be direct paths between the AP and user while others may be reflected). Thus, the problem formulation for maximizing system capacity reduces to one of resource allocation.

2.1.4 Distributed Antenna Systems (DAS)

There have also been some results on using distributed antenna systems (DAS) in WLAN environments. However, the purpose of using these is different from ours (all antennas transmit the same signal in DAS systems). Thus, [43] uses multiple antennas in a room (with appropriate amplification/filtering) to send a high data-rate transmission from one device to another that is across the room. [5] uses multiple antennas in a room to reduce transmit power and hence inter-cell interference between different APs (much like repeaters in today's cellular networks). [30] studies these antenna systems (as used in these other papers) from the point of view of fading degradation due to incoherent signal combining.

2.1.5 Other work

Some other areas peripherally related to our work here include: mesh networks (where resource planning techniques are also reducible to graph coloring problems), downlink scheduling in cellular CDMA networks [42], multi-class WLANs where the problems looked at include transmission scheduling to take into consideration different service requirements, smart antennas and directional antennas in ad hoc networks [37], multi-radio systems [9] (where each user has multiple radios and the challenge is scheduling between multiple channels), efficient AoA (Angle of Arrival) and beamforming algorithms for ad hoc networks.

2.1.6 Discussion

While these numerous techniques do enable higher data rates at various frequency bands, we note that none of them can do the same for the 60 GHz band due to the peculiar features of this frequency. Thus, there are few or no multi-path components at 60 GHz due to absorption by kost building materials. As a result, MIMO is a poor choice to obtain high data rates [32, 44]. For the same reasons, MIMO/SDMA is also a poor choice and cannot ensure high data rates since most reflected have a power that is several dB less than the direct transmission component. DAS is useful in order to ensure uniform propagation of a signal. Unfortunately, it also increases the interference between distant users by repeating the signal widely.

In this work, we utilize multiple smart antennas in a room to create multiple mini-cells and then use SDMA to maximize the channel efficiency. Since 60 Ghz signals do not propagate far or through most obstructions, we can ensure good signal isolation to within cells, thus minimizing interference and maintaining high data rates.

Chapter 3

60GHZ PROPAGATION

In urban environments, signals propagate from a transmitter to a receiver via multiple paths, each of which affects the received signal quality, see Figure 3.1. As shown in the figure, there is a direct path for signals to travel from the AP to Bob as well as a reflected path. The direct path is commonly referred to as Line of Sight (LoS) while reflected and other indirect paths are called multipath. Alice is hidden behind a wall but the signals may travel to her by going through the walls. In this case the received signal strength will be smaller due to absorption by the wall material. Finally, Charlie is behind a wall but near the corner. The signal bends around the edge of the wall and reaches him via a diffracted path.
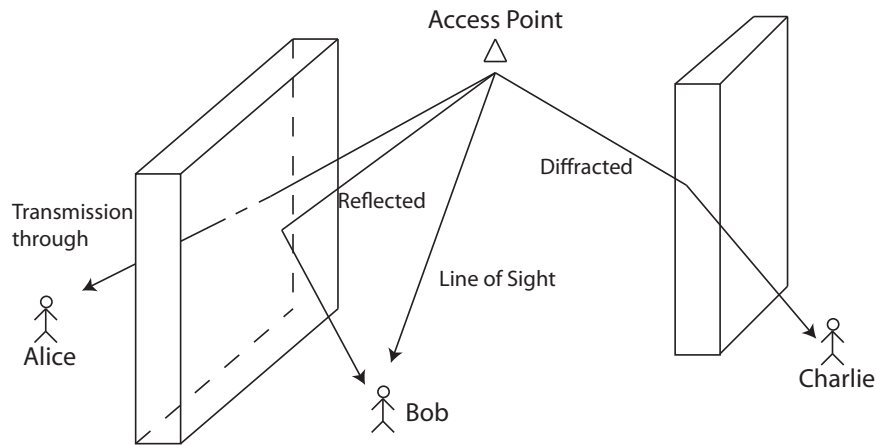
Figure 3.1: Illustration of indoor propagation.

A key factor in determining the achievable data rates is the SINR (Signal to

Interference and Noise Ratio) of the received signal. In the absence of any obstacles (like in outer space), the signal strength density degrades as a factor of distance^2 (imagine the signal energy exists on the surface of an expanding sphere whose radius is the distance between the transmitter and receiver). This is called free space propagation and the number 2 is called the path loss exponent. In urban environments, LoS paths mimic free space propagation with similar exponents. Therefore, in our example, the LoS path to Bob will see signal strength that degrades as square of the distance to the AP. However, reflected signals, diffracted signals, and signals transmitted through materials, see far greater loss in energy as they propagate, with exponents of 3 or 4 being quite common. If signals propagate far via multipath then we may see interference as well from distant transmitters. This further serves to weaken the SINR and hence lower the data rate. Finally, signal quality can also degrade due to ISI (Inter Symbol Interference). ISI occurs when the reflected component of the previous symbol arrives at the same time as the LoS component of the current symbol. Thus, the previous symbol acts as interference for the current symbol. In order to determine how to achieve high data rates at 60 GHz, it is necessary to first understand the propagation behavior of signals at this frequency.

3.1   SURVEY OF MEASUREMENT STUDIES

The propagation characteristics of 60 GHz have been studied by several authors [46, 2, 11, 28] who have noted its ray-like propagation properties which can be modeled as free space propagation with a measured path loss exponent of 2.1. In [29, 11, 15, 10], studies have shown that this frequency band has lack of significant multipath due to absorption, greater signal diffusion (i.e., less specular reflection) and lack of diffraction around obstacles. Furthermore [40, 46] note the small RMS (Root

Mean Square) delay spread for 60GHz indicating little multipath. The authors measured the relative strength of the reflected components with respect to the LoS component. The first-order reflections in typical indoor environments (from windows) were almost 10 dB below the LoS path. If the surface is not polished, then the reflected component is much weaker. Second-order and higher-order reflections are highly attenuated and negligible. The penetration losses are also severe with many building materials such as concrete causing a 35 dB reduction in signal strength. LoS paths, as a result, are the predominant signal. The characteristics of this propagation model makes it ideal for spatial reuse due to lack of interference from other simultaneous separated transmitters [29]. In addition, using highly directional antennas will therefore yield high throughput.

Spatial Division Multi Access, SDMA divides space into multiple cells. By using different frequencies in neighbouring cells, the interference can be reduced resulting in good signal to interference and noise ratio, SINR. SDMA has been studied over the past decade and numerous algorithms have been developed. However, all previous work looks at a much lower frequency (2-5GHz) where multipath components are significant. Thus, a great deal of previous work [36, 45, 18] develops MIMO/SDMA algorithms to identify the strongest multipath components in a room and combine them to achieve high data rates. In our system, since multipath is negligible, these previous algorithms are not applicable.

In terms of the channel, as noted by [40, 31] and others, OFDM (Orthogonal Frequency Division Multiplexing) is a good choice because it partitions a highly frequency selective wideband channel into nonselective narrowband channels. However, [40] notes that a drawback of this frequency is the relatively severe Doppler spread (1200 Hz) even at walking speeds. This puts a minimum lower bound of at least 30 Kilo-symbols/sec per carrier in the OFDM set.

3.2 DISCUSSION

The primary conclusion from all of these measurement studies is that 60 GHz WLANs need to be designed in a way that ensures the existence of a LoS path between the AP and users. Transmissions through materials, even office partitions, degrade the signal severely resulting in very low data rates. While this is a problem in the sense that we need to deploy more APs (or antennas), the benefit is the ease of spatial reuse of spectrum. Thus, the same frequency bands can be used in adjacent rooms with little fear of interference thus considerably boosting achievable data rates. Finally, we note that while most reflected components are highly attenuated, reflections off glass are an exception. We use this observation to create reflected paths to users who lack a LoS to the AP thus extending coverage (particularly in the presence of unintended obstacles to the LoS path).

Perpendicular Polarisation	R	R	R	R	R	R	R	R	T
Material(thickness d [cm];	-dB	-dB	-dB	-dB	-dB	-dB	-dB	Profile	-dB
estimated roughness σ_h [mm])	(10°)	(20°)	(30°)	(40°)	(50°)	(60°)	(70°)	Type	(0°)
Aerated Concrete (5;0.2)	14.1	13.4	12.7	11.0	9.6	7.5	5.1	F	18.9
Concrete (5,0.1)	7.5	7.2	6.7	6.2	5.3	4.1	2.0	F	≥ 30.0
Brick (11; micro 0.3, macro 2)	14.8	12.7	13.4	17.5	12.3	8.6	4.8	M	16.9
Tiles (0.5;0.1)	4.1	3.8	4.1	3.8	5.8	7.6	2.1	M	≥ 30.0
Plasterboard (1.4:0)	14.1	14.1	8.3	5.5	9.8	5.1	1.2	M	2.8
Plasterboard(1;0)	23.8	17.9	8.1	4.5	4.5	8.9	6.9	M	2.1
Plasterboard rough (1;1.7)	≥ 30.0	≥ 30.0	≥ 30.0	≥ 30.0	≥ 30.0	≥ 30.0	16.9	M	≥ 30.0
Plasterboard rough (1;1.2)	≥ 30.0	≥ 30.0	≥ 30.0	≥ 30.0	≥ 30.0	23.8	12.1	M	≥ 30.0
Plasterboard rough (1;1)	≥ 30.0	≥ 30.0	≥ 30.0	≥ 30.0	23.1	14.6	6.9	M	≥ 30.0
Plasterboard smooth(1;0.25)	6.9	6.2	6.9	7.2	6.9	5.0	1.4	M	4.5
Wood Fibreboard (1.2;0.2)	21.0	27.2	15.8	15.5	12.7	10.7	5.5	M	3.4
Hard Fibreboard (0.4;0)	17.9	16.9	14.8	10.7	7.4	4.3	0.7	M	3.4
Wooden Panels (1.9;0)	22.0	21.7	18.4	18.2	15.2	9.3	6.5	M	8.6
Wooded Panels (1.2;0)	16.4	15.8	15.7	14.5	11.9	8.9	4.8	M	7.6
Wooden Chipboard (1.3;0.2)	13.4	10.7	9.5	11.7	7.9	5.5	5.3	M	6.2
Wooden Chipboard(1.6;0)	10.0	10.0	11.4	8.2	7.9	6.2	3.9	M	8.3
Acrylic Glass(0.4;0)	6.2	5.5	5.5	5.5	6.0	7.6	13.1	M	1.7
Glass metalized(0.4)	8.9	4.5	3.1	3.1	2.7	2.7	1.05	M	≥ 30.0

Table 3.1: Reflectivity R and transitivity T [27].

Chapter 4

ANTENNA AND SMART ANTENNA

An antenna converts electrical currents into electromagnetic waves at the transmitter and this process is reversed at the receiver. As a consequence, the received signal strength in a communication channel is very dependent on the nature of the antennas being used. The simplest (theoretical) antenna is modeled as a point source which emits electromagnetic waves uniformly over the surface of a sphere and is called an isotropic antenna. Therefore, the signal strength at some distance d can be written as,

$$P_r = P_t \times G_t G_r \frac{\lambda}{4\pi d^2}$$

here P_t is the transmitted power and P_r is the received power at distance d. G_t and G_r are the transmitter and receiver antenna gains, respectively. For an isotropic antenna, the gain is 1 and thus the antenna gain of any antenna is written relative to the gain of an isotropic antenna. If the antenna gain of an antenna is greater than 1 then we call that a directional antenna. In effect, such an antenna selectively directs the energy in some directions. As an example consider Figure 4.1 where the transmitter antenna focuses most of its energy in the two lobes shown and $G_t^b >> G_t^a$ (these two quantities denote the transmitter antenna gain in the direction of receivers b and a respectively). As a result, the signal strength received by b will be much greater than the signal strength received at a.

In the context of 60 GHz WLANs, given the severe attenuation suffered, it is necessary to use directional transmissions to maximize signal strength at the
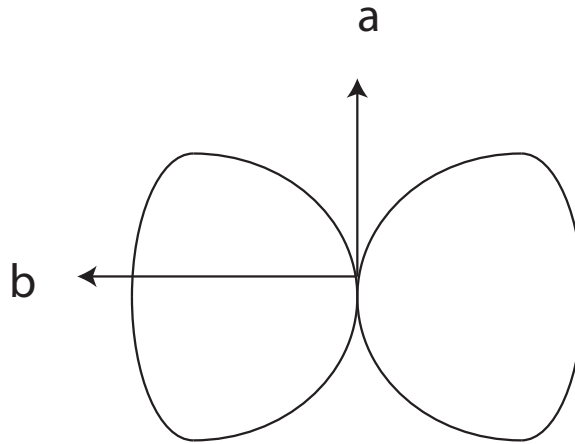
Figure 4.1: Example of directional transmission.

receiver. This will ensure high data rates while simultaneously minimizing the interference at other receivers due to focussed transmissions. In general, there are two ways to build a directional antenna. One way is to carefully place multiple antenna elements and reflectors to provide high gain in some direction(s). The other way is to use an antenna array consisting of multiple antenna elements and then provide directivity by carefully combining signals received (or transmitted) along each element. The signals from each antenna element may be amplified differently prior to combining and may even be phase shifted to obtain specific beam shapes. The benefit of the latter types of antennas (also called Smart Antennas) is that the direction of transmission can be changed as a user moves about the room. The beam is moved by changing the amplification and phase of the signals received/transmitted along each of the array elements. Since we are concerned with providing high data rate channels to users in indoor spaces, this ability to change direction of communication is important. In this thesis we consider two specific topologies (linear and circular) for arranging the antenna elements to obtain different types of beam shapes (and hence directivity) and study how we can share

the channel among users in the room to maximize the throughput as measured in bits/Hz.

4.1 SMART ANTENNAS

Smart antennas give us the ability to form directional beams in any direction, *null* some number of interfering signals, and enable the detection of transmitters by applying algorithms to determine the direction of arrival. Physically, smart antennas consist of multiple antenna elements arranged in some geometry (popular geometries include linear, circular, and rectangular). The output from each antenna element is fed to a *beamforming module* that is responsible for beamforming, nulling and direction of arrival computations. There can be multiple beamforming modules, all attached to the same physical antenna elements. This gives us the capability to form multiple beams in different directions and/or use multiple frequency channels over the same antenna. Of course, each beamforming module connects to a separate RF chain for transmit and receive functions. Additionally, beamforming modules may either be implemented as analog components (lacking flexibility) or digital. In the digital case, the beamforming modules come after the analog-to-digital converter on the receiver side and before the digital-to-analog converter on the transmit side.

Since an antenna array has multiple elements, a signal arriving from a distant transmitter will arrive at slightly different times at each element. This manifests itself as a phase shift between the signals received by different antenna elements allowing for direction of arrival computation. For communication, beamforming at a receiver is done by taking signals received by each antenna element, phase shifting them appropriately and then coherently summing them. At a transmitter, the reverse is done where the signal fed to each antenna element is appropriately

phase shifted to form a beam in some direction.

Figure 4.2 shows a 2 element linear array. Each element is an isotropic antenna (each direction has the same gain = 1). Each element is separated by distance d. Assume that the signal arrives from angle θ. Given sufficient separation between the transmitter and receiver, the signal hitting each element of the antenna can be assumed to travel parallel paths.
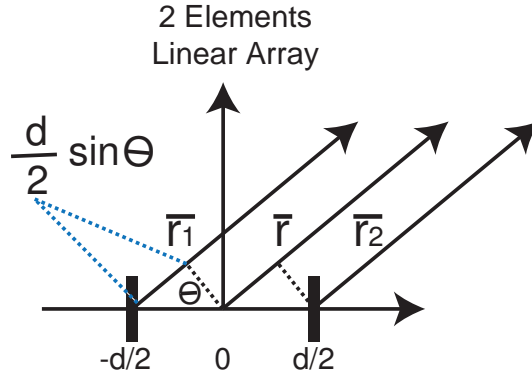
Figure 4.2: Linear array with 2 elements

The antenna gain of a *linear antenna array* with M elements is computed as follows. We calculate the array factor (AF) using the expression below [17],

$$AF = \sum_{i=1}^{M} e^{j(i-1)\kappa d(\sin\theta - \sin\theta_0)} \tag{4.1}$$

where $\kappa = 2\pi/\lambda$ and d is the antenna element spacing. θ_0 is the angle at which we are forming the main beam and θ is the angle at which we are computing the array factor. The gain in any direction is then computed as,

$$E \frac{4\pi U(\theta, \phi)}{\int_0^{2\pi} \int_0^{\pi} U(\theta, \phi) \sin\theta d\theta d\phi} \tag{4.2}$$

where E is the efficiency (that we assume is 1 in this thesis). θ and ϕ are measured as shown in Figure 4.3 and U is the radiation intensity derived from the AF [17].

19
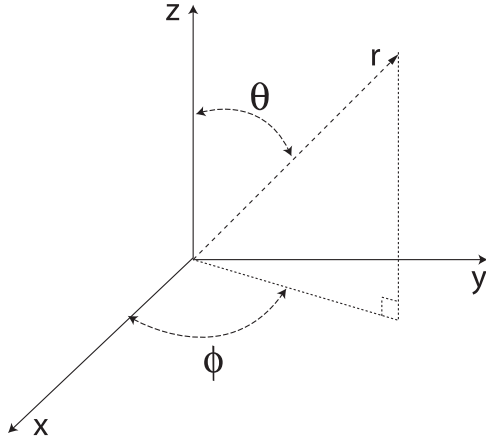
Figure 4.3: 3D angle convention used.

In a similar fashion, the array factor for a *circular antenna array* with M elements when beamforming in a direction (ϕ_0, θ_0) is [17],

$$AF = \sum_{i=1}^{M} e^{-j(\kappa a(\sin\theta\cos(\phi-\phi_i)-\sin\theta_0\cos(\phi_0-\phi_i)))} \qquad (4.3)$$

where we again measure the angles as shown in Figure 4.3. Gain is computed by using equation 4.2. Figure 4.4 shows beam patterns at different angles using 4 and 8 element linear arrays. More number of elements are used to form narrower beams.

Finally, we note that by multiplying each term in the sum in equations 4.1 and 4.3 by a complex weight w_i (this can be thought of as amplification) we can shape the beam differently (without changing the direction) or add nulls (section 4.1.2).

4.1.1 Beam Patterns – Linear and Circular Antenna Arrays

Consider a linear antenna array where the antenna is in the ceiling of a room aligned along the y-axis. The beam formed by this type of an array exhibits a circular symmetry along the main antenna axis. Figure 4.5 shows the *gain* in dBi when the beam is formed towards a user located at coordinates (1.5m, 1.5m, 0.5m).

20

(a) 4 elements 20 degree

(d) 8 elements 20 degree

(b) 60 degree

(e) 60 degree

(c) 90 degree
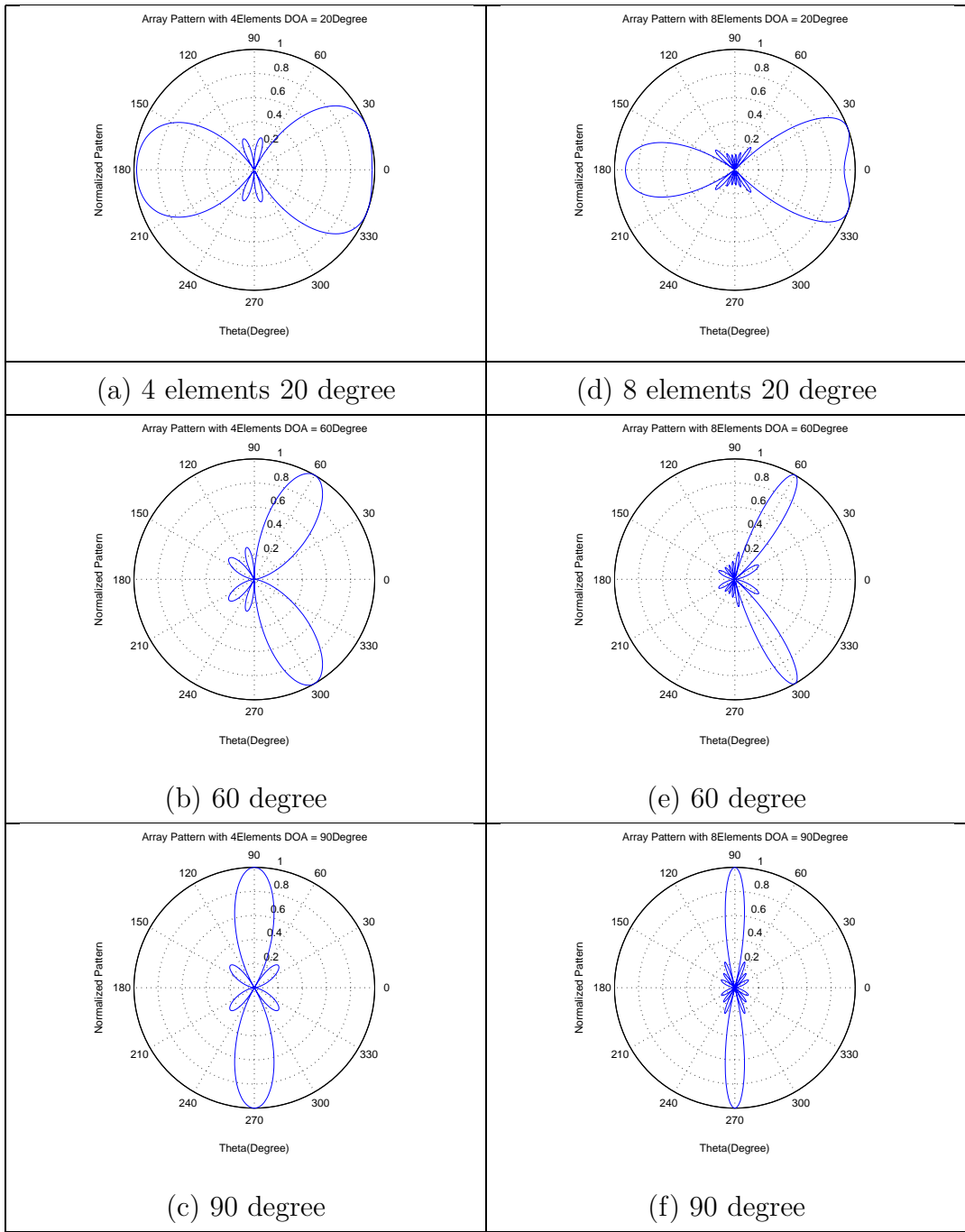
(f) 90 degree

Figure 4.4: Beamforming at 20, 60 and 90 degrees using 4 and 8 element linear array

21

As we can see, the beam covers a large area and is in fact given by the intersection of the x-y plane of the room with the cone whose axis coincides with that of the array and whose angle at the intersection (projected to two dimensions) is 2θ. θ is the angle formed by the intersection of the line connecting the user location to the center of the antenna axis and the antenna axis itself. The implication of this type of beam is that all users located within the same θ of the AP will be spatially inseparable and will therefore have to share the channel using TDMA or other protocols. If we now form a beam using a circular array to the same user located at (1.5m, 1.5m, 0.5m), the gain we see in the room is shown in Figure 4.6. Unlike the linear case, the beam appears to be more focused in this case. Observe the side-lobes in the figures – these are regions where there will be interference. Also, the beam width of the main beam represents the 3dB region (i.e., the signal strength at the boundary is half that of the energy at the boresight).

4.1.2   Nulling

An additional benefit of using smart antennas is the ability to form up to $M-1$ *nulls* when the antenna has M elements. Nulls are formed by appropriately weighting the elements of the array factor from equations 4.1, 4.3. Let us assume that we are beamforming at angle θ_0 and nulling angles $\theta_1, \cdots, \theta_p$. We can write the following set of linear equations for the linear antenna array:

$$\sum_{i=1}^{M} w_i e^{j(i-1)\kappa d \sin\theta_0} = 1$$
$$\sum_{i=1}^{M} w_i e^{j(i-1)\kappa d \sin\theta_1} = 0$$
$$\cdot$$
$$\cdot$$
$$\sum_{i=1}^{M} w_i e^{j(i-1)\kappa d \sin\theta_p} = 0$$
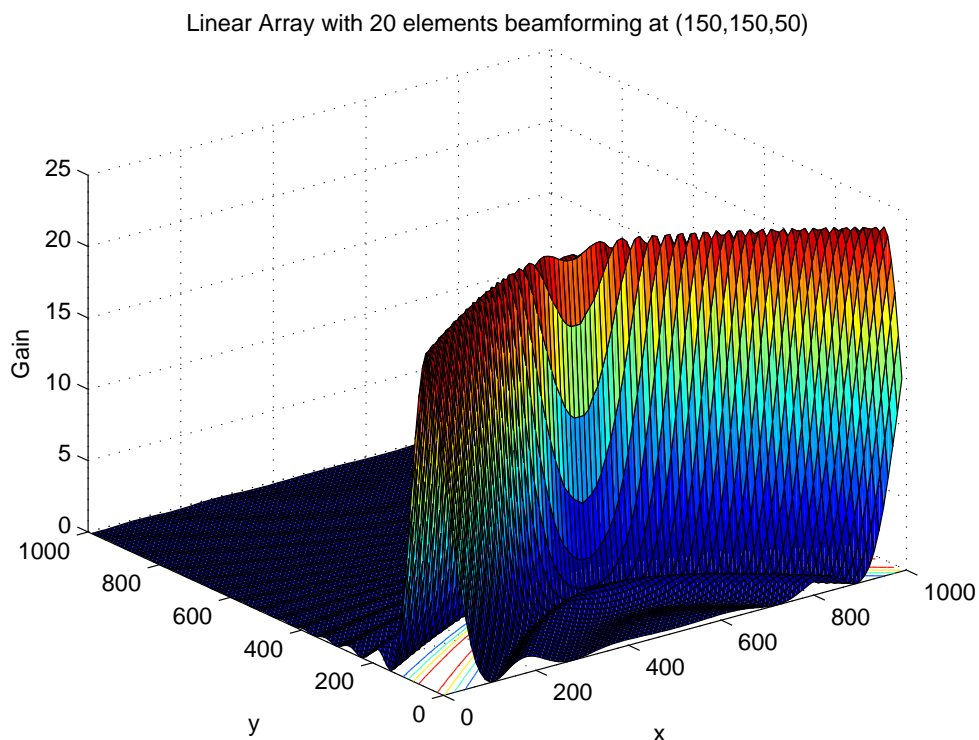
Figure 4.5: Gain with 20-element linear array pointing to (1.5m,1.5m,0.5m) and the axis of the antenna aligned along the y-axis.

Here, each equation describes the desired output of the antenna for the different directions. By solving these equations for w_i, we can beamform towards θ_0 and null the remaining p angles. The criterion used is maximizing SIR (Signal to Interference Ratio) [17]. In matrix form, we can write the above set of equations as $w^H.A = [1, 0, \cdots, 0]^T$ where ^{H} denotes the Hermitian and A is the matrix of array factors. If $p = M - 1$, the above system can be solved in matrix form as:

$$w^H = [1, 0, \cdots, 0]^T.A^{-1} \tag{4.4}$$

23
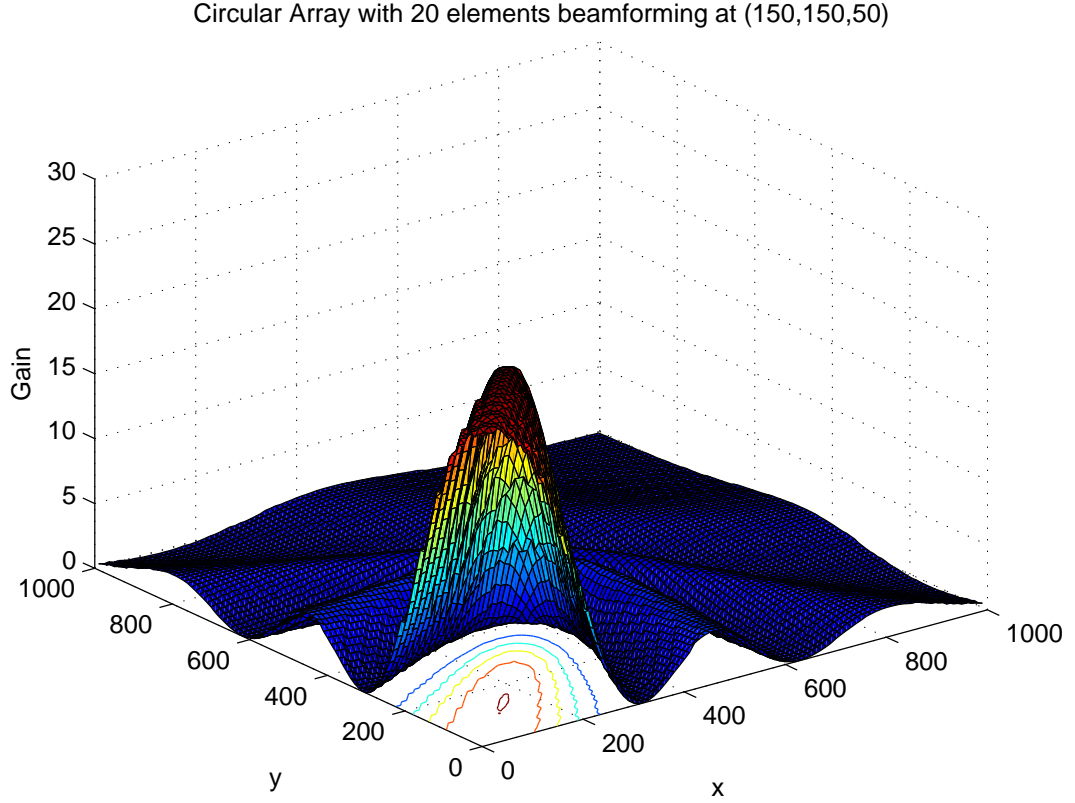
Figure 4.6: Gain with a 20-element circular array pointing to (1.5m,1.5m,0.5m).

Otherwise, if $p < M - 1$ we use an approximation [13] where we make the matrix A square by adding noise terms. The weights are then found as:

$$w^H = [1, 0, \cdots, 0]^T.A^H.(A.A^H + \sigma^2 I)^{-1} \tag{4.5}$$

where σ^2 is the noise variance.

4.1.3 Access Point Model Used

In this thesis we assume that an AP is equipped with either a linear antenna array or with a circular antenna array. The element spacing is $\lambda/2 = 2.5cm$. The length

of a 20 element linear array is thus 47.5cm while the diameter of the circular array with 20 elements is $50/\pi$cm.

Each AP may have one or more beamforming modules (also simply called modules in the text). Each module is capable of forming a beam in a preferred direction and forming up to 19 nulls (with 20 elements). It is noteworthy that each module will have its own associated RF chain (including amplifiers, demodulators, filters, etc.). Thus, if an AP has M modules then it will also have M RF chains and can communicate in M directions simultaneously.

4.2   DISCUSSION

The beam shapes produced by linear and circular antenna arrays intersect the room's floor in different ways. Thus, the linear array forms a beam whose coverage area is a strip across the room while the circular array results in more conical coverage areas. The next question we address is how to perform resource allocation in the room for each of these antenna topologies to maximize data rates. For instance, users located in the same strip will interfere with each other and thus need to share the channel using some MAC protocol like TDMA or CSMA. On the other hand, users located in alternating strips can reuse the same channels since the interference between them will be very small. We consider each of these novel characteristics of smart antennas in the context of 60 GHz propagation next and develop very efficient resource allocation algorithms.

Chapter 5

ACCESS POINT PLACEMENT STUDY

Antenna placement is an important issue for 60GHz wireless networking. Because of the properties of the 60GHz spectrum, there is little or no signal coverage when obstructions block the signal path. This is unlike the 2.4GHz and 5GHz spectrum, where it is easy to have 100% coverage because signals can pass through obstructions and walls. Therefore, we investigate the question of antenna placement with the goal of providing full coverage for the 60GHz spectrum. In this chapter, algorithms are proposed as well as a proof of optimal antenna placement with minimum number of antennas is provided.

The optimal solution for full coverage in the absence of obstructions is simple. We can place one antenna anywhere at a reasonable height, higher than any receiver antenna. However, the challenge comes when there are obstructions present.

Obstructions can be of any shape. However, obstructions usually are of a rectangular shape in office and home environments. To simplify our analysis, we first assume that obstructions are rectangles (similar to partitions in offices) with no thickness. The assumption of zero thickness is reasonable because there is a small amount of diffraction of the signal around sharp corners of the obstruction effectively allowing us to ignore the thickness of most partitions. We develop a antenna placement algorithm for rooms containing partition-like obstructions. We then study the case when obstructions have significant thickness which means that diffraction alone cannot cover shadow areas. This problem has some similarity to

the problem of camera placement for surveillance. However, our problem is simpler since we are only interested in line of sight coverage of all areas whereas camera placement has to do with identification and tracking of people.

5.1 OBSTRUCTIONS WITHOUT THICKNESS

For rectangular obstruction without thickness, we can imagine it is a straight line in a top down view of the room. It is easy to see that each such line (extended to the walls of the room) divides the room into two sub-areas. The first placement algorithm then is to place one antenna in each sub-area. Observe that each partition is a convex hull and therefore every point inside is visible from a central location. However, we can do better than using two antennas, one for each partition. For example, if we place one antenna on the top of the obstruction, it can still provide full coverage in the room.

Lemma 1. *For a single zero-thickness rectangular obstruction, the best antenna placement is on the top of the obstruction for full (100%) coverage.*

Proof. Consider one obstruction in a two dimensional space as shown in figure 5.1. The circle represents the antenna location. Let x be the distance between the antenna and the obstruction. Let h_a be the antenna height (this is the height from the ceiling to the floor) and h_o is the height of the obstruction. The triangular area shows the shadow caused by the obstruction which is the region of no signal coverage for this antenna placement.

Now we can use a simple calculation to find out the relation between x and the area without coverage.
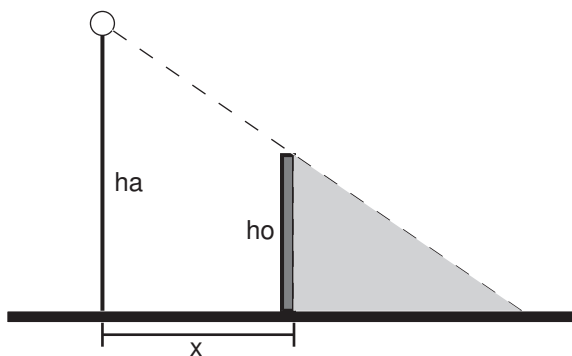
Figure 5.1: Relation between distance from antenna to obstruction and coverage

$$area\_without\_signal \quad = \quad \frac{h_o^2 \times x}{2(h_a - h_o)} \tag{5.1}$$

$$= \quad k \times x \tag{5.2}$$

In equation 5.2, $k = \frac{h_o^2}{2(h_a - h_o)}$. We want to find the minimum value of the $area\_without\_signal$. For full coverage, $area\_without\_signal = 0$. Since $h_a > h_o > 0$, $k > 0$. Therefore, to obtain yields $area\_without\_signal = 0$, we need $x = 0$. This proves the lemma.

An interesting observation we can make based on the above lemma is that the antenna can be placed *anywhere* on top of the obstruction and still provide complete coverage. Indeed, an antenna placed anywhere along the line extending the obstruction in either direction will also provide complete coverage, as shown in Figure 5.2. Note that in the figure we are seeing a top view of the obstruction. This leads us to the following corollary.

Corollary 2. *A single antenna placed at the intersection of two obstructions will provide complete coverage. If the obstructions do not intersect, an antenna placed at the intersection of the lines extending the obstructions in either direction will also provide complete coverage.*

28
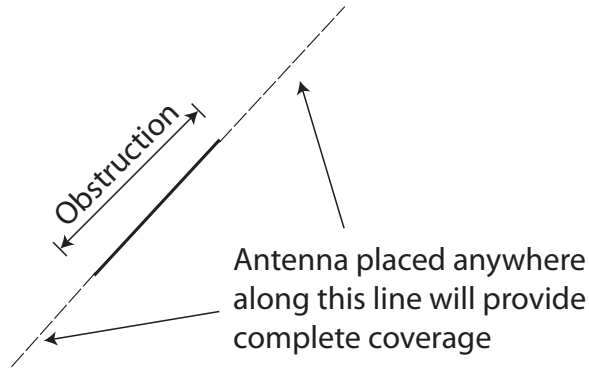
Figure 5.2: Generalization of Corollary 1.

Proof. Let us assume that the two obstructions are O_1 and O_2 and are not parallel to each other, as shown in Figure 5.3. By Lemma 1, placing an antenna anywhere along O_1 or along the line extending O_1 will provide complete coverage if O_1 is the only obstruction present. Similarly, if O_2 is the only obstruction present, complete coverage is provided by placing an antenna anywhere along the line extending O_2. Therefore, if we place the antenna at the *intersection* of these two obstructions, then that point satisfies the criteria for coverage for each of O_1 and O_2.

It follows from the corollary that if the two obstructions are parallel, then two antennas are required. Furthermore, if we also consider the walls of the room as obstructions then, if the point of intersection of two internal partitions lies *outside* the room, then we also need two antennas. This follows from the corollary by extending each obstruction to the walls and then placing an antenna at each of the two intersections. Using the corollary, we now have the following theorem.

Theorem 3. *If n rectangular obstructions are placed in a room, we can provide 100% coverage using no more than n antennas. In particular:*

1. *If none of the n obstructions intersect when extended within the room, then we require exactly n antennas.*

Placing antenna at
intersection provides
complete coverage

O_1

O_2
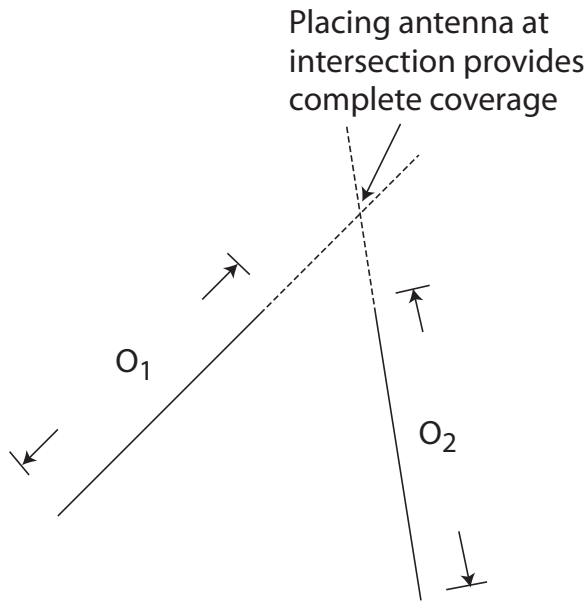
Figure 5.3: Antenna placement for two non-parallel obstructions.

2. *If m of the obstructions intersect within the room (when extended), then we need no more than $n - m + k$ antennas where $k < m$ is the number of subsets of m where each subset consists of partitions that meet at a single point when extended and all subsets have a null intersection with each other.*

Proof. The proof of (1) follows immediately from Lemma 1. For (2) take the m obstructions and extend them (staying in the room) till they meet another obstruction(s). Figure 5.3 shows this for the case when two obstructions meet at a point in the room. Next, form subsets of obstructions where obstructions that meet at a point are placed in the same subset. Further, after an obstruction is included in a subset, it can no longer be placed in another subset. For example, if O_1 and O_2 meet at a point and so do O_2 and O_3 (at a different point), we can form subsets $\{\{O_1, O_2\}, \{O_3\}\}$ or $\{\{O_1\}, \{O_2, O_3\}\}$. Assume that we form k such subsets. Then, from Corollary 1, placing one antenna at each of the k identified

intersections along with $n - m$ antennas placed atop each of the other obstructions will provide complete coverage in the room.

We must reiterate that if the point of intersection lies *outside* a room, then we need two antennas for two obstructions each placed atop each of the obstructions. Similarly, if the obstructions are parallel, then we will also need two antennas.

Now that we know that the best antenna placement for pairs of obstructions is at their intersection, we can develop an algorithm for antenna placement in a room with arbitrary collection of obstructions. Consider the two example rooms shown in Figure 5.4(a)(b) to demonstrate the methodology proposed.
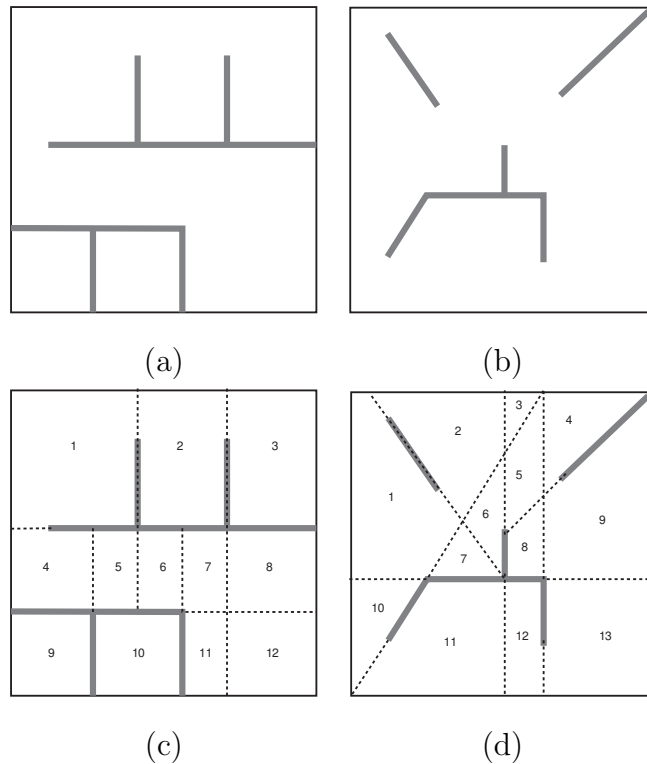
Figure 5.4: (a,b) Two different rooms with different locations for obstructions. (c,d) Extend the line on both sides of the obstructions

31

The first step is to extend both sides of the obstructions, which is shown as dotted lines in Figure 5.4(c)(d). When the lines hit the wall or any other obstruction, it stops. This process is used to identify all the possible intersections and the various sub-areas that are created. Let us represent each of the sub-areas in the room using a simple matrix representation. For example, figure 5.4 (c) has 12 sub-areas in total. We can create a three by four matrix to represent the entire room. Our goal is to determine the fewest antenna placements that will provide coverage in the entire room. Equivalently, we want to find the fewest number of antennas that can collectively cover all the identified sub-areas.

5.1.1 Exhaustive Search Algorithm

| (a) | (b) | (c) |
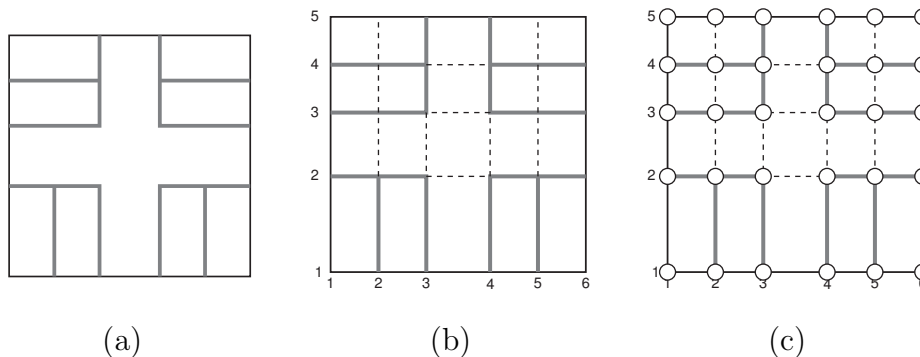
Figure 5.5: An office room space with 8 cubicles at four corner

In this section we provide an algorithm for finding the antenna placements for arbitrary rooms. As an illustrative example, we will use the room depicted in Figure 5.5 (a). Following the previously outlined procedure, we first obtain the set of all possible antenna placements which correspond to the intersections as in figure 5.5 (c). This process also splits the room into sub-areas that can be represented using a 5×4 matrix for our example. For each antenna placement we create one coverage matrix. Thus, for our example, since there are 30 possible antenna

placements (indicated by the circles), we get 30 coverage matrices. Initialize each of the matrix entries of each matrix to 0 indicating no coverage. Let a_{ij} be the coverage matrix corresponding to antenna placement (i, j). If placing an antenna at this position provides full coverage for some sub-area, we place a 1 in that position in the matrix a_{ij}. For example, consider matrix a_{23} corresponding to figure 5.5. By placing an antenna at location $(2, 3)$, we can cover subareas shown in figure 5.6 and the corresponding matrix is shown below. Note that the sub-area between antenna positions $(3, 1)$ and $(4, 1)$ is partially covered by placing the AP at $(2, 3)$. Therefore, the entry for this area is zero in the coverage matrix a_{23}.

Figure 5.6: Example of antenna a_{23} coverage area

The coverage matrices for all possible antenna placements are:

$$a_{11} = \begin{bmatrix} 0 & 0 & 0 & 0 & 0 \\ 0 & 0 & 0 & 0 & 0 \\ 0 & 0 & 0 & 0 & 0 \\ 1 & 0 & 0 & 0 & 0 \end{bmatrix} \; ; \quad a_{21} = \begin{bmatrix} 0 & 0 & 0 & 0 & 0 \\ 0 & 0 & 0 & 0 & 0 \\ 0 & 0 & 0 & 0 & 0 \\ 1 & 1 & 0 & 0 & 0 \end{bmatrix} \; ; \quad a_{31} = \begin{bmatrix} 0 & 0 & 1 & 0 & 0 \\ 0 & 0 & 1 & 0 & 0 \\ 0 & 0 & 1 & 0 & 0 \\ 0 & 1 & 1 & 0 & 0 \end{bmatrix} \; ;$$

$$a_{41} = \begin{bmatrix} 0 & 0 & 1 & 0 & 0 \\ 0 & 0 & 1 & 0 & 0 \\ 0 & 0 & 1 & 0 & 0 \\ 0 & 0 & 1 & 1 & 0 \end{bmatrix} \; ; \quad a_{51} = \begin{bmatrix} 0 & 0 & 0 & 0 & 0 \\ 0 & 0 & 0 & 0 & 0 \\ 0 & 0 & 0 & 0 & 0 \\ 0 & 0 & 0 & 1 & 1 \end{bmatrix} \; ; \quad a_{61} = \begin{bmatrix} 0 & 0 & 0 & 0 & 0 \\ 0 & 0 & 0 & 0 & 0 \\ 0 & 0 & 0 & 0 & 0 \\ 0 & 0 & 0 & 0 & 1 \end{bmatrix} \; ;$$

$$a_{12} = \begin{bmatrix} 0 & 0 & 0 & 0 & 0 \\ 0 & 0 & 0 & 0 & 0 \\ 1 & 1 & 1 & 1 & 1 \\ 1 & 0 & 0 & 0 & 0 \end{bmatrix} \; ; \quad a_{22} = \begin{bmatrix} 0 & 0 & 0 & 0 & 0 \\ 0 & 0 & 0 & 0 & 0 \\ 1 & 1 & 1 & 1 & 1 \\ 1 & 1 & 0 & 0 & 0 \end{bmatrix} \; ; \quad a_{32} = \begin{bmatrix} 0 & 0 & 1 & 0 & 0 \\ 0 & 0 & 1 & 0 & 0 \\ 1 & 1 & 1 & 1 & 1 \\ 0 & 1 & 1 & 0 & 0 \end{bmatrix} \; ;$$

$$a_{42} = \begin{bmatrix} 0 & 0 & 1 & 0 & 0 \\ 0 & 0 & 1 & 0 & 0 \\ 1 & 1 & 1 & 1 & 1 \\ 0 & 0 & 1 & 1 & 0 \end{bmatrix} \; ; \quad a_{52} = \begin{bmatrix} 0 & 0 & 0 & 0 & 0 \\ 0 & 0 & 0 & 0 & 0 \\ 1 & 1 & 1 & 1 & 1 \\ 0 & 0 & 0 & 1 & 1 \end{bmatrix} \; ; \quad a_{62} = \begin{bmatrix} 0 & 0 & 0 & 0 & 0 \\ 0 & 0 & 0 & 0 & 0 \\ 1 & 1 & 1 & 1 & 1 \\ 0 & 0 & 0 & 0 & 1 \end{bmatrix} \; ;$$

$$a_{13} = \begin{bmatrix} 0 & 0 & 0 & 0 & 0 \\ 1 & 1 & 0 & 0 & 0 \\ 1 & 1 & 1 & 1 & 1 \\ 0 & 0 & 0 & 0 & 0 \end{bmatrix} \; ; \quad a_{23} = \begin{bmatrix} 0 & 0 & 0 & 0 & 0 \\ 1 & 1 & 0 & 0 & 0 \\ 1 & 1 & 1 & 1 & 1 \\ 0 & 0 & 0 & 0 & 0 \end{bmatrix} \; ; \quad a_{33} = \begin{bmatrix} 0 & 0 & 1 & 0 & 0 \\ 1 & 1 & 1 & 0 & 0 \\ 1 & 1 & 1 & 1 & 1 \\ 0 & 0 & 1 & 0 & 0 \end{bmatrix} \; ;$$

$$a_{43} = \begin{bmatrix} 0 & 0 & 1 & 0 & 0 \\ 0 & 0 & 1 & 1 & 1 \\ 1 & 1 & 1 & 1 & 1 \\ 0 & 0 & 1 & 0 & 0 \end{bmatrix} \; ; \quad a_{53} = \begin{bmatrix} 0 & 0 & 0 & 0 & 0 \\ 0 & 0 & 0 & 1 & 1 \\ 1 & 1 & 1 & 1 & 1 \\ 0 & 0 & 0 & 0 & 0 \end{bmatrix} \; ; \quad a_{63} = \begin{bmatrix} 0 & 0 & 0 & 0 & 0 \\ 0 & 0 & 0 & 1 & 1 \\ 1 & 1 & 1 & 1 & 1 \\ 0 & 0 & 0 & 0 & 0 \end{bmatrix} \; ;$$

$$a_{14} = \begin{bmatrix} 1 & 1 & 0 & 0 & 0 \\ 1 & 1 & 0 & 0 & 0 \\ 0 & 0 & 0 & 0 & 0 \\ 0 & 0 & 0 & 0 & 0 \end{bmatrix} ; \quad a_{24} = \begin{bmatrix} 1 & 1 & 0 & 0 & 0 \\ 1 & 1 & 0 & 0 & 0 \\ 0 & 0 & 0 & 0 & 0 \\ 0 & 0 & 0 & 0 & 0 \end{bmatrix} ; \quad a_{34} = \begin{bmatrix} 1 & 1 & 1 & 0 & 0 \\ 1 & 1 & 1 & 0 & 0 \\ 0 & 0 & 1 & 0 & 0 \\ 0 & 0 & 1 & 0 & 0 \end{bmatrix} ;$$

$$a_{44} = \begin{bmatrix} 0 & 0 & 1 & 1 & 1 \\ 0 & 0 & 1 & 1 & 1 \\ 0 & 0 & 1 & 0 & 0 \\ 0 & 0 & 1 & 0 & 0 \end{bmatrix} ; \quad a_{54} = \begin{bmatrix} 0 & 0 & 0 & 1 & 1 \\ 0 & 0 & 0 & 1 & 1 \\ 0 & 0 & 0 & 0 & 0 \\ 0 & 0 & 0 & 0 & 0 \end{bmatrix} ; \quad a_{64} = \begin{bmatrix} 0 & 0 & 0 & 1 & 1 \\ 0 & 0 & 0 & 1 & 1 \\ 0 & 0 & 0 & 0 & 0 \\ 0 & 0 & 0 & 0 & 0 \end{bmatrix} ;$$

$$a_{15} = \begin{bmatrix} 1 & 1 & 0 & 0 & 0 \\ 0 & 0 & 0 & 0 & 0 \\ 0 & 0 & 0 & 0 & 0 \\ 0 & 0 & 0 & 0 & 0 \end{bmatrix} ; \quad a_{25} = \begin{bmatrix} 1 & 1 & 0 & 0 & 0 \\ 0 & 0 & 0 & 0 & 0 \\ 0 & 0 & 0 & 0 & 0 \\ 0 & 0 & 0 & 0 & 0 \end{bmatrix} ; \quad a_{35} = \begin{bmatrix} 1 & 1 & 1 & 0 & 0 \\ 0 & 0 & 1 & 0 & 0 \\ 0 & 0 & 1 & 0 & 0 \\ 0 & 0 & 1 & 0 & 0 \end{bmatrix} ;$$

$$a_{45} = \begin{bmatrix} 0 & 0 & 1 & 1 & 1 \\ 0 & 0 & 1 & 0 & 0 \\ 0 & 0 & 1 & 0 & 0 \\ 0 & 0 & 1 & 0 & 0 \end{bmatrix} ; \quad a_{55} = \begin{bmatrix} 0 & 0 & 0 & 1 & 1 \\ 0 & 0 & 0 & 0 & 0 \\ 0 & 0 & 0 & 0 & 0 \\ 0 & 0 & 0 & 0 & 0 \end{bmatrix} ; \quad a_{65} = \begin{bmatrix} 0 & 0 & 0 & 1 & 1 \\ 0 & 0 & 0 & 0 & 0 \\ 0 & 0 & 0 & 0 & 0 \\ 0 & 0 & 0 & 0 & 0 \end{bmatrix} ;$$

Lemma 4. *Let A and B denote sets of sub-areas that are covered with different antenna placements. Then, if $A \subset B$, we can eliminate A because B can cover all the positions A covers.*

This proposition follows from the definition of subset. Further, by the transitive property, if $A \subset B$ and $B \subset C$, $A \subset C$.

Lemma 5. *if $A = B$, then we can either eliminate A or B.*

In our example from figure 5.5, $a_{11} \subset a_{21}$ since placing an antenna at position $(2,1)$ covers all the areas covered by an antenna at position $(1,1)$, and more.

Therefore, in determining the minimal antennas needed, we can start by eliminating position $(1,1)$ from consideration. By a similar argument, we are eventually left with only seven antenna placements $a_{22}, a_{32}, a_{42}, a_{52}, a_{43}, a_{34}, a_{44}$ from which we need to find the fewest that can provide 100% coverage.

Given k such matrices, we need to find the fewest l that can provide complete coverage. The naive algorithm is to search through all subsets of k matrices and identify the smallest subset that satisfies the coverage requirement. In other words, we need to look at all $\binom{k}{1}$ sets, then at all $\binom{k}{2}$ sets, and so forth. While this process will identify the smallest set of antenna placements, its complexity can be easily seen to be $O(2^k)$.

5.1.2   Greedy Algorithm

Consider a more efficient algorithm for finding antenna placements. We start with the same process as above to eliminate redundant matrices. As noted above, for our example, this gives us matrices, $a_{22}, a_{32}, a_{42}, a_{52}, a_{43}, a_{34}, a_{44}$. The first step is to find the sum of these remaining matrices,

$$R_0 = \sum a_{ij} = \begin{bmatrix} 1 & 1 & 6 & 1 & 1 \\ 2 & 2 & 6 & 2 & 2 \\ 6 & 6 & 8 & 6 & 6 \\ 1 & 2 & 6 & 2 & 1 \end{bmatrix}$$

We now look at the value 1 in R_0, find the corresponding a_{ij} matrix (note: there will be exactly one matrix which has that value of 1). For example, if we look at the position$(1,4)$ which is the left top corner value, a_{34} was found. We keep a_{34} in our list of antenna positions that are required for full coverage and then we subtract a_{34} from R_0:

36

$$R_1 = R_0 - R_0 \otimes a_{34} = \begin{bmatrix} 0 & 0 & 0 & 1 & 1 \\ 0 & 0 & 0 & 2 & 2 \\ 6 & 6 & 0 & 6 & 6 \\ 1 & 2 & 0 & 2 & 1 \end{bmatrix}$$

Define $\otimes$ operation as follows:

$$A = \begin{bmatrix} a1 & a2 \\ a3 & a4 \end{bmatrix} ; B = \begin{bmatrix} b1 & b2 \\ b3 & b4 \end{bmatrix} ;$$

$$A \otimes B = \begin{bmatrix} a1 \times b1 & a2 \times b2 \\ a3 \times b3 & a4 \times b4 \end{bmatrix}$$

We repeat the process and choose another value of 1. Let's pick position(1,1) which is the left bottom corner value. a_{22} is found.

$$R_2 = R_1 - R_1 \otimes a_{22} = \begin{bmatrix} 0 & 0 & 0 & 1 & 1 \\ 0 & 0 & 0 & 2 & 2 \\ 0 & 0 & 0 & 0 & 0 \\ 0 & 0 & 0 & 2 & 1 \end{bmatrix}$$

We repeat the same process and find a_{44} and a_{52}. The resultant matrix becomes:

$$R_3 = R_2 - R2 \otimes a_{44} = \begin{bmatrix} 0 & 0 & 0 & 0 & 0 \\ 0 & 0 & 0 & 0 & 0 \\ 0 & 0 & 0 & 0 & 0 \\ 0 & 0 & 0 & 2 & 1 \end{bmatrix}$$

$$R_4 = R_3 - R3 \otimes a_{52} = \begin{bmatrix} 0 & 0 & 0 & 0 & 0 \\ 0 & 0 & 0 & 0 & 0 \\ 0 & 0 & 0 & 0 & 0 \\ 0 & 0 & 0 & 0 & 0 \end{bmatrix}$$

When the matrix becomes all zeros, it means that all sub-areas are covered by at least one antenna. In this example, the final chosen antenna positions are a_{34}, a_{22}, a_{44}, and a_{52} which is shown in figure 5.7.
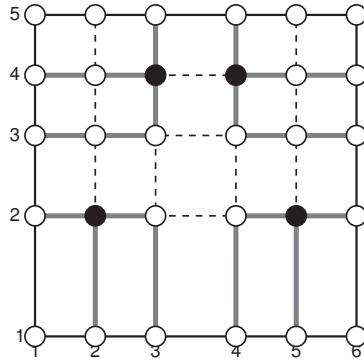

Figure 5.7: Antenna position found

This algorithm works well when the sum matrix R has a lot of one's and a variety of large and small numbers. Now let's consider a case when the sum matrix R has no one's or the above process stops at a stage that all one's are found and the remaining numbers are greater than or equal to two. At this point, we need to create a tree consisting of all the possible combinations by starting at the lowest number in the sum matrix. Here is an example to explain the algorithm and how to build the tree.

Let the coverage matrices be:

$$a_{11} = \begin{bmatrix} 1 & 1 & 1 \\ 0 & 0 & 1 \\ 1 & 0 & 0 \end{bmatrix} ; \quad a_{12} = \begin{bmatrix} 1 & 0 & 1 \\ 1 & 0 & 0 \\ 0 & 0 & 0 \end{bmatrix} ; \quad a_{13} = \begin{bmatrix} 1 & 1 & 1 \\ 0 & 0 & 1 \\ 0 & 1 & 1 \end{bmatrix} ;$$

$$a_{21} = \begin{bmatrix} 0 & 0 & 0 \\ 1 & 1 & 0 \\ 0 & 1 & 0 \end{bmatrix} ; \quad a_{22} = \begin{bmatrix} 0 & 0 & 0 \\ 1 & 0 & 0 \\ 1 & 1 & 1 \end{bmatrix} ; \quad a_{23} = \begin{bmatrix} 1 & 1 & 1 \\ 0 & 1 & 0 \\ 0 & 1 & 0 \end{bmatrix} ;$$

$$R_0 = \begin{bmatrix} 4 & 3 & 4 \\ 3 & 2 & 2 \\ 2 & 4 & 2 \end{bmatrix}$$

Name the array positions of R_0 as follows for ease of explanation:

$$R_0 = \begin{bmatrix} e1 & e2 & e3 \\ e4 & e5 & e6 \\ e7 & e8 & e9 \end{bmatrix}$$

Let $S(i)$ be a set which contains all the positions of the sum matrix which has value i. Thus, $s(2) = e_5, e_6, e_7, e_9$. The algorithm is as follows:

1. Set $i = 1$.

2. Check if $S(i)$ is an empty set. If yes, increment i. If no, go to the next step.

3. Start from the first element in the set $S(i)$.

4. Look up the matrix pool and there will be exactly i matrices that have value of 1 in the corresponding position.

5. Sum the matrix with the parent matrix. If the parent is root, then the resulting matrix is itself. If the resulting matrix is all one's, the algorithm

39

terminates. The path from the root to the leaf corresponds to the required antenna placements.

6. Otherwise, pick the next element from $S(i)$ if it is not empty. If it is empty, increment i and go to step 2.

7. Check if the position is already covered in the resulting matrix, if yes, do nothing. Otherwise, go to step 4.

Here is an example to work through the algorithm. The minimum number of R_0 is 2 and $S(2) = \{e5, e6, e7, e9\}$ Figure 5.8 shows the example tree structure. It starts with $e5$ (the first element in $S(2)$). Then we look up the matrices to see which two matrices have value of 1 in the $e5$ position. $a21$ and $a23$ are found. The square on the side of the node indicates the matrices where dark spot is 1 and white is 0. Since the parent is root, we go to the next element in $S(2)$ which is $e6$. We check both node $a21$ and $a23$ if position $e6$ has value of 1. However, both are zero. We need to look up which matrices have value of 1 in position of $e6$. $a11$ and $a13$ are found. We sum $a21$ and $a11$ and, the resulting matrix is shown at the bottom of the node $a11$. Likewise, we repeat and sum for the rest of other nodes. The next element in $S(2)$ is $e7$. However, all the resulting matrices show value 1 in position $e7$. Therefore, we take the last element in $S(2)$ which is $e9$. We again look up the matrix pool and find $a13$ and $a22$ have value of 1 at position $e9$. We sum the parent node with the current node and the result is all one's in three cases. Therefore, the optimal solution is not unique. The three choices are:

- a21, a11, a13; or

- a21, a11, a22; or

- a23, a11, a22

In this example, we have already found the solution to 100% coverage before we even got to go the the next set $S(3)$. If at the end of set $S(2)$, we still do not have all one's in the leaf matrices, we will need to go to the next set which is $S(3)$. And repeat the algorithm until a solution is found.
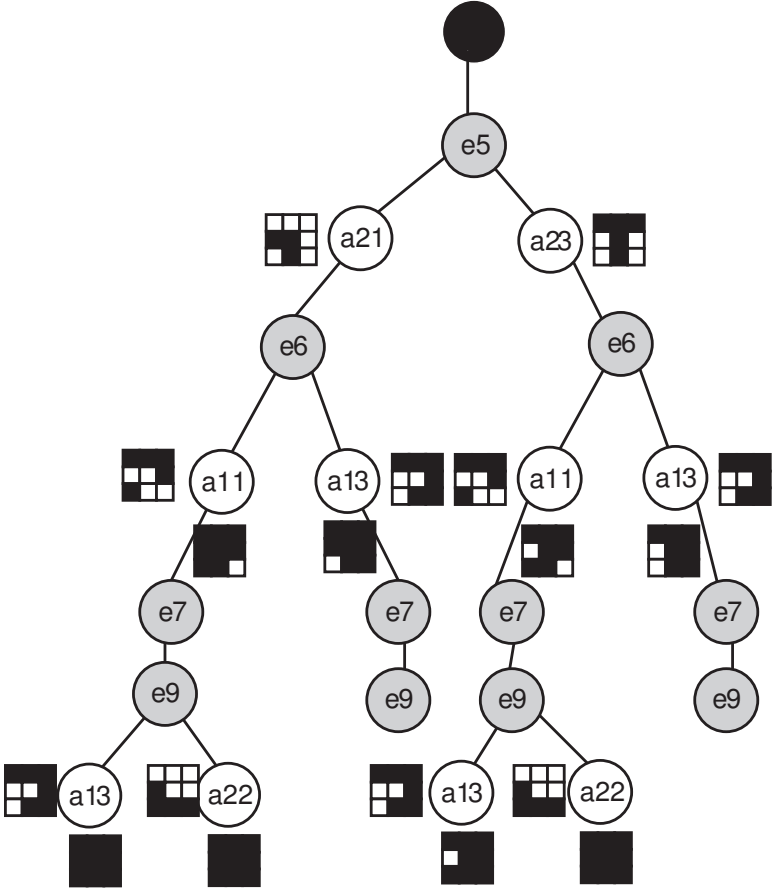

Figure 5.8: e5,e6,e7,e9 tree

Algorithmic Complexity and Optimality

The above greedy algorithm can be easily be seen to be optimal as follows. The first step of the algorithm selects those antennas that contribute to covering sub-areas that can only be covered by that antenna (the 1's in matrix R_0). Therefore,

these antennas have to belong to the optimal solution. The next step involves an exhaustive search as in Figure 5.8. Since this is an exhaustive breadth first search, we will stop when we cover the entire room with the fewest number of antennas. Hence the greedy algorithm is optimal.

Let n be the number of remaining matrices. m is the number of sub-areas (i.e., the matrix size, if it is a 3×3 matrix, $m = 9$). $n = C \times m$ where $C > 1$. We notice that in this algorithm, when the fanout increases, the height of the tree decreases. And the fanout is the number of values in the sum matrix and is less than n. The worst case is when the fanout is $\frac{n}{2}$. Then the complexity is $\left(\frac{n}{2}\right)^{\frac{2m}{n}+1} - 1$. Since $n = Cm$, the complexity can be rewritten as $\left(\frac{n}{2}\right)^{\frac{2}{C}+1} - 1 = O(n^3)$.
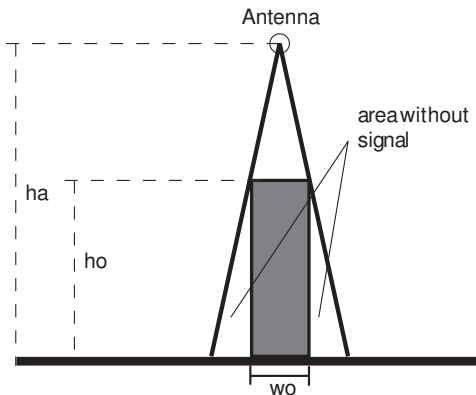
5.2   RECTANGULAR OBSTRUCTIONS WITH THICKNESS

Figure 5.9: Rectangular obstruction with thickness w_o and height h_o

If the obstruction has significant thickness, placing the antenna at the top of the obstruction will not give full coverage any more. For instance, as illustrated in Figure 5.9 when the antenna is placed at height h_a above a wall of thickness w_0 and height h_0, the wall's thickness casts a shadow on either side of the wall to a distance of $\frac{w_0 h_0}{2(h_a - h_0)}$. Thus, we can consider two alternative goals of antenna placement –

one goal is to provide complete coverage as before or we can aim for coverage that is almost complete. In the latter case, we may specify that the floor area not covered should be within γ of the wall. In practical situations, the latter approach is reasonable since, typically, the areas not covered lie immediately adjacent to walls or partitions and are generally not where we expect to use wireless laptops or other devices. Indeed, allowing some flexibility in coverage allows for simpler antenna placements. For a given obstruction, we find the antenna height required to satisfy the coverage goal is given by the inequality $h_a > h_0(1 + \frac{w_0}{2\gamma})$. Using this approximate approach, we can now determine antenna placements by putting one antenna atop each wall at the appropriate height.

5.2.1 Achieving Complete Coverage

While providing almost complete coverage is a reasonable goal, it is interesting to examine the question of what does it take to provide 100% coverage of the room in the presence of arbitrary thick obstructions. The first approach for doing this is a simple generalization of the algorithm presented in section 5.1.2. We think of each rectangular obstruction (of non-zero thickness) to be actually four zero-thickness rectangular obstructions. Then, we simply run the Greedy algorithm from section 5.1.2 with one change in initial conditions – we place a 1 in each matrix position that corresponds to the interior of any of the non zero-thickness obstructions. This ensures that the algorithm does not try to provide coverage "inside" an obstruction.

While the above approach does solve the problem, we note that the number of antennas used can be as many as $2n$. To see this note that by considering each obstruction as four zero thickness obstructions we end up with $4n$ obstructions. Using Theorem 1, we have $m = 4n$ (i.e., every obstruction intersects at least one

other obstruction) and we obtain $k = 2n$ subsets. This is because each of the four faces that form an obstruction yield two subsets (as per the construction in Theorem 1). Thus, we require $4n - 4n + 2n = 2n$ antennas in all. We can get by with fewer antennas as explained below.

Figure 5.10 shows a top view of a room with five rectangular obstructions labeled $R_1, \cdots, R_5$. As one can see, placing a single antenna anywhere in the room will create several shadows from each of the walls. The problem can be stated as determining the minimal number of antennas and antenna placements such that the entire room has coverage.
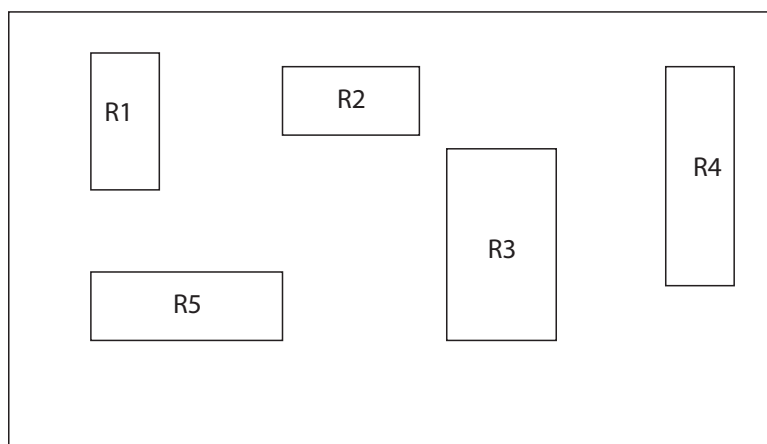

Figure 5.10: Room with five thick rectangular obstructions.

This problem is identical to a problem from Computer Vision called the *The Floodlight Illumination Problem.* The challenge there is to illuminate every surface of all the walls in a room in the museum using point sources of light. We note that if we can illuminate every wall surface, then we simultaneously illuminate every other part of the room since the shadow areas are always adjacent to walls. Thus, the solution to the floodlight problem can be directly applied to our antenna placement problem.
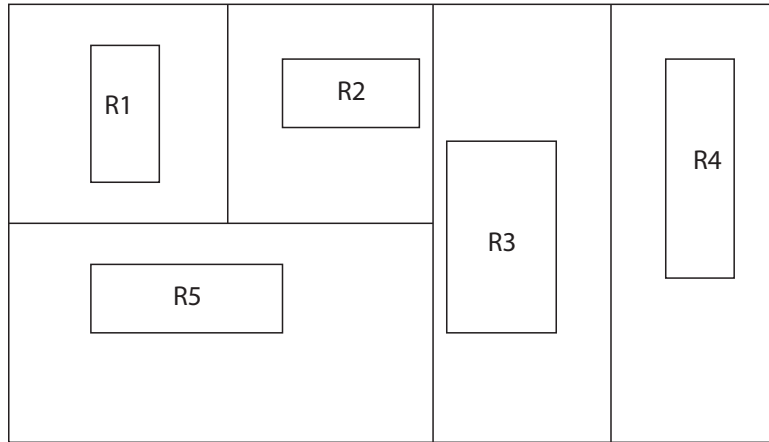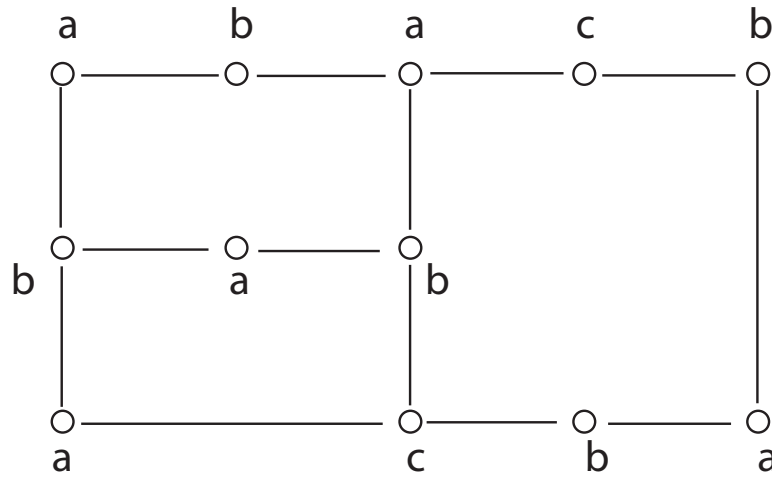
44

Figure 5.11: Maximal rectangles.

Figure 5.12: Reduction to graph coloring and then to antenna placement.

An early work [6] proves that for any room containing n isothetic rectangles, complete illumination of all walls can be provided using no more than $\lfloor (4n + 4)/3 \rfloor$ light sources placed at specific locations determined by the solution to a 3-coloring problem. Using Figure 5.10 as an illustrative example, the first step in the algorithm is to enclose each of the rectangular obstructions into maximal rectangles as shown in Figure 5.11. This construction then naturally gives us a

graphical representation (Figure 5.12) where each vertex of the graph corresponds to a corner of Figure 5.11. Finally, obtain a 3-vertex coloring of this graph. Of the three colors used, determine the most commonly used color. Then, place an antenna at each vertex that was colored using either of the two other colors. In Figure 5.12 we illustrate a 3-coloring using colors *a, b, c*. Since *a* is most commonly used, we place an antenna at each position labeled by *b* and c giving us 7 antennas.

5.2.2   Generalizing to Other Obstructions

In general, an obstruction may come in any shape including polygons and curvilinear. The above algorithm can be easily extended to these cases as well by converting the polygon into isothetic rectangles. For the case when the obstruction has curves, an approximate method would be to convert the smooth curve into a serious of short rectangles and then apply the same algorithm.

Chapter 6

ARCHITECTURE FOR 60GHZ DEPLOYMENTS: MULTIPLE DISTRIBUTED ANTENNAS

In this chapter and the next, we study different architectures for 60GHz WLANs. We explore two types of antennas placement: multiple distributed antenna architecture and multiple co-located antenna architecture. In the multiple distributed antenna architecture, we use multiple antennas in different locations to increase the coverage area. Each antenna may have multiple radio modules to support multiple simultaneous connections. In the multiple co-located antenna architecture, there is only one antenna (usually at the center of the room) connected to multiple antenna modules.

In the multiple distributed antenna architecture, we place the antennas using the description in session 6.1 to maximize the LoS coverage of the room. Then, we compare the cases when users are equipped with omni-directional antennas and directional antennas. In both cases, FDMA and TDMA are used for multiple access. Spatial reuse is employed in addition to FDMA/TDMA in the directional case at the user. Users equipped with directional antennas achieve 1-2Gbps/user data rate while users equipped with omni-directional antennas only, achieve 500Mbps/user on average when there are 10 users in the room.
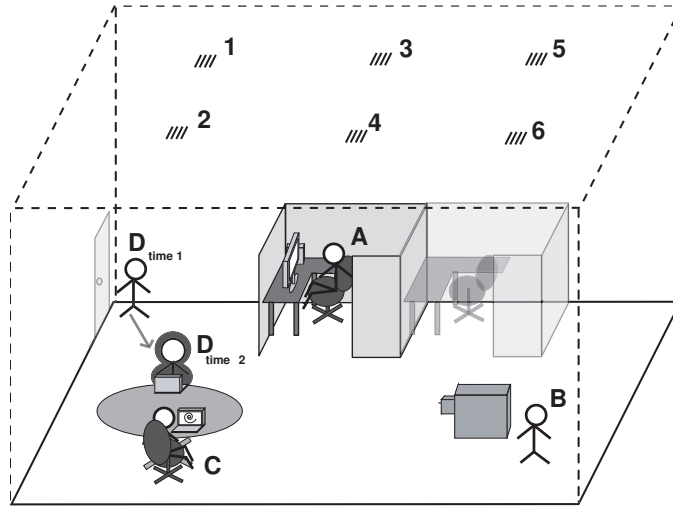
Figure 6.1: Multiple distributed smart antennas.

6.1 MULTIPLE DISTRIBUTED ANTENNAS

We study the key issue of providing coverage (ideally via LoS links) to users/devices who may be anywhere in the room. Given obstructions like furniture , partitions, other people, etc., as well as the unpredictable location of these obstructions, the only way to provide LoS paths is to have multiple antennas in the room. We therefore propose a spatially distributed version of a SDMA AP where the room has multiple smart antennas spread out such that coverage can be provided where needed. As a working example, consider Figure 6.1 where we have six smart antennas deployed in the ceiling. Note that these antennas may be deployed anywhere so long as coverage is provided. Figure 6.1 shows that not all users are visible from all antennas. Thus, user B is only visible from antennas 5 and 6, user A is only visible from antennas 3 and 4 whereas user C is visible from all antennas. The figure shows another constraint of this frequency band. C's LoS to antenna 1 is blocked by user D at time 2 (assuming D walks towards C, starting at time 1 and arriving at time 2). Thus, from the point of view of allocating links to users

(equivalently allocating antennas to users), we need to ensure that (1) the user is LoS and (2) the allocation may need to be changed dynamically as the demand changes and as some links are lost or others get created by movement.

We assume that each ceiling-mounted antenna is a smart antenna that allows it to beamform in any direction, place nulls in given directions to silence interferers or to reduce interference at other receivers, and find the direction of arrival of signals. This last capability is needed to track moving users as well as to find new users when they enter the space. However, we will not exploit this last capability in this thesis in order to keep a narrow focus on the resource allocation problem. While we assume that the AP has smart antenna capability allowing it to beamform in any direction, we do not make the same assumption for the user in this section (i.e. user uses an omni-directional antenna). We will study the case when user carries smart antenna in the next chapter.

6.2   RESOURCE ALLOCATION

The key problem addressed in this thesis is that of allocating resources to users such that we can provide very high data rates. The resources in our architecture consist of links between users and antennas as well as frequency channels (if multiple channels are available). In order to clearly explain the challenge, we introduce some notation first.

Let us assume that the room contains A smart antennas each with M beamforming modules. Each beamforming module is configured with array weights that allow the formation of a beam towards one user and nulls towards others. Thus, the signal received at the antenna elements are fed to each beamforming module in parallel which gives us M simultaneous channels for communication. Of course, the AP requires M radios to receive and transmit to M

49

users simultaneously. Since each beamforming module is connected to one radio, $a_{ij}, i = 1, 2, \cdots, A, j = 1, 2, \cdots, M$ denotes the jth module of antenna i. Note that from one antenna we can support two downlinks to two users simultaneously on the same channel so long as each user is separated in angular direction allowing each beamforming module to point the main beam at its user and place a null at the other user. However, user-to-user interference in uplink transmissions may be high when users use omni-directional antennas. This interference is greatly reduced with the use of upward pointing antennas.

We assume that there are $FC \geq 1$ frequency channels available within the room that can be allocated to different links. In the above example, if the user-to-user interference is very high, we may well decide to allocate a separate frequency channel to each user. Note that given the 5GHz bandwidth available in the 60GHz ISM band, and the poor propagation of the signal between rooms, it is reasonable to use multiple frequency channels simultaneously within each room. In this thesis we assume that the frequency channels are static (i.e., all have the same bandwidth) rather than dynamically defined (where channel bandwidth is defined based on demand). We denote a given frequency channel by $c_l, l = 1, 2, \cdots, C$. Finally, assume that there are N users $u_k, k = 1, \cdots, N$ in all. An *allocation* is a set of N tuples $< u_k, a_{ij}, c_l >$ such that each of the N users has an assignment. Note that multiple users may well be assigned to the same antenna/module/channel in which case they will all need to share the link using some protocol – in this thesis we assume TDMA.

Let us now consider some examples that better explain the constraints as well as novel features of this architecture. In Figure 6.2 let us assume that $FC = 1$ and $M = 1$. Then, because the two users are spatially close to one another, we assign them both to antenna a_2 where they share the channel (the allocation is $\{< u_1, a_{21}, c_1 >, < u_2, a_{21}, c_1 >\}$). On the other hand, if the users are separated
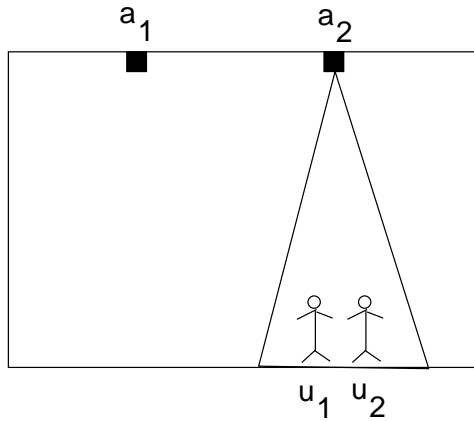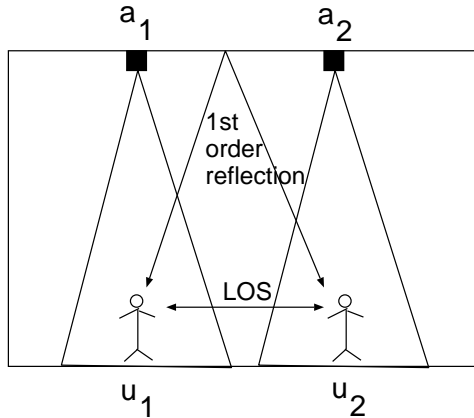
Figure 6.2: Two co-located users.

Figure 6.3: Two spatially separated users.

spatially as in Figure 6.3 then we can assign each to a different antenna albeit using the same channel (the allocation is $\{< u_1, a_{11}, c_1 >, < u_2, a_{21}, c_1 >\}$). This allocation will be reasonable if the interference between the two users (shown by the LoS and the reflected path) is small enough that the SNIR exceeds some threshold for uplink as well as downlink communication. Thus, if u_1 is transmitting to a_1 while u_2 is receiving from a_2, u_1's signal will interfere at u_2. Alternatively, when u_1 and u_2 both transmit, the received signal at a_1 from u_1 will see some

interference from u_2's transmission (and vice versa). Note that in Figure 6.3 if the interference is great enough then we will have to use some form of TDMA to separate communication between $u_1 - a_1$ and $u_2 - a_2$ in time. Alternatively, we can assign both users to the same antenna and again use TDMA. Finally, observe that if $FC = 2$ while $M = 1$, we can use the allocation shown in Figure 6.3 but using both channels as: $\{< u_1, a_{11}, c_1 >, < u_2, a_{21}, c_2 >\}$. The same allocation can also be used in Figure 6.2 since both users are visible from both antennas.

We define an *optimal* allocation as one which maximizes the total data rate achieved in the cell. In Figure 6.2 with the allocation $\{< u_1, a_{21}, c_1 >, < u_2, a_{21}, c_1 >\}$, we would compute the data rate under the assumption that the uplink as well as downlink channel is shared using TDMA. Therefore, we compute the SNIR at each user given TDMA and then determine the data rate we can achieve using appropriate modulation and coding for a given target BER (Bit Error Rate). Likewise we compute the SNIR at the antenna for uplink transmissions and do the same calculation. If $r_{ij,k}$ denotes the downlink data rate at user u_k from antenna i module j (i.e., a_{ij}) and $r_{k,ij}$ the uplink data rate, then we calculate the total data rate in the cell for this example as: $P = (r_{21,1} + r_{21,2} + r_{1,21} + r_{2,21})/4$. Similarly, for the allocation $\{< u_1, a_{11}, c_1 >, < u_2, a_{21}, c_1 >\}$, the data rate is $Q = (r_{12,1} + r_{1,12})/2 + (r_{21,2} + r_{2,21})/2$.

- In allocation P the channel is time shared and hence each directed communication gets one quarter of the channel. On the other hand, in allocation Q, we have spatial reuse of the channel and thus we can have two simultaneous transmissions ongoing at the same time. In other words, each of the two spatial channels are shared by only two entities – antenna and one user.

- It may appear that the second allocation Q will have a higher data rate. However this is not always true. Since there is only one frequency channel in

the cell, there will be interference at each user as well as antenna that will reduce the SNIR there by reducing the data rate. Indeed, in this situation it may sometimes be better to run TDMA in the entire cell to improve overall data rate.
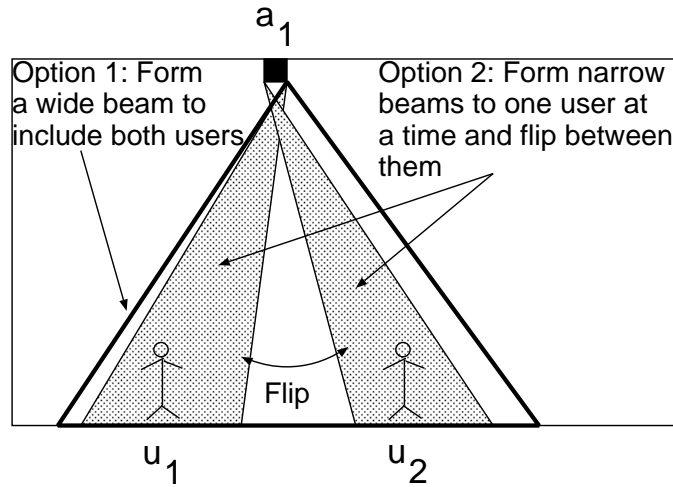

Figure 6.4: Flipping between separated users.

Consider one final example in Figure 6.4 where we have only one antenna with one module and two spatially separated users. The only allocation here is $\{< u_1, a_{11}, c_1 >, < u_2, a_{11}, c_1 >\}$. Since both users share the channel, we assume TDMA is used. Even with this allocation, we note that there are two possible data rates achievable. In the first case, we form a wide beam to accommodate both users (bold line in the figure). In this case, the transmitter's power is spread over a wider area resulting in lower SNIR. In the second case, we form a narrow beam towards the user who is presently communicating (by beamforming only to that user) resulting in a higher SNIR. Clearly, the second case gives us a much higher data rate overall and is the model we select in this thesis for the case when spatially separated users share a common antenna and module. We note that beamforming

is typically done in software by simply changing antenna weights and thus this *flipping* can be done very quickly, well within the guard time between slots of a TDMA schedule.
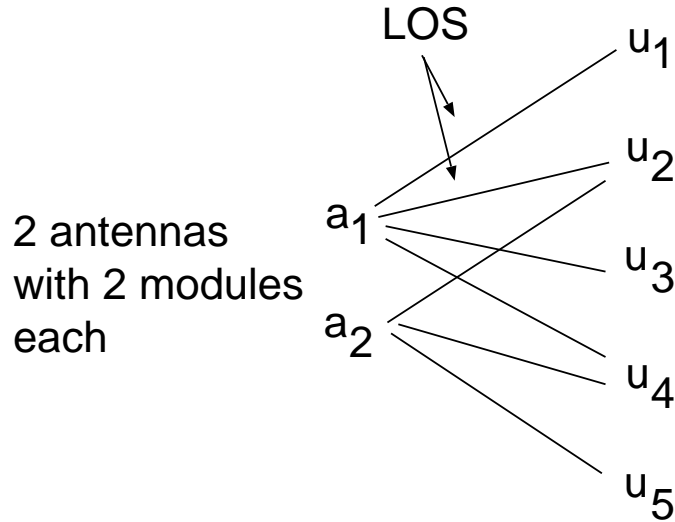

Figure 6.5: LoS graph between antennas and users.

The primary constraints we need to keep in mind when allocating frequency channels and modules to users is the limited number of modules per antenna as well as the limited number of channels. Therefore, we construct a graph that incorporates these constraints in its topology in a natural way. In order to explain this construction, we rely on an example where we have two antennas each with two modules and five users. The visibility of the antennas to each user is shown in Figure 6.5. Note that users u_1 and u_3 are not visible to a_2 while u_5 is not visible to a_1. Also, note that we have a total of four modules (2 per antenna) and five users which implies that at least two users will need to time share a common link. We maintain a LoS matrix c_{LOS} with one row per antenna and one column per user.

For our example the matrix is:

$$c_{LOS} = \begin{pmatrix} 1 & 1 & 1 & 1 & 0 \\ 0 & 1 & 0 & 1 & 1 \end{pmatrix}$$

Starting from Figure 6.5 we construct a new graph where each node consists of the pair $a_i u_j$ corresponding to each *edge* from the LoS graph in Figure 6.5. The edges in this new graph correspond to *interference*. We consider interference between two users as well as from an antenna to a user either via LoS paths or first order reflections.

To determine if a link exists between any pair of nodes in the graph we need to compute the interference. To do this assume that each transmitter transmits at a given power P dBm. Consider first the user-to-user interference between u_i and u_j. We construct the LoS path between these users and use free space propagation (since users are well above the ground) to determine the expected signal strength. If there is a cubicle or other partition between the users, then we decrease the signal strength by some amount that is determined by the material's properties. In addition to the LoS path, we find all the first-order reflections (i.e., we only look at signals that are reflected once) and compute the estimated signal strength of these paths – here, for the path loss we again assume free space but in addition, we attenuate the signal based on the attenuation suffered due to reflection. Summing up all these values, we get the signal power at u_i due to a transmission by u_j. This information is maintained in a $N \times N$ user-to-user interference matrix I_{u2u}.

If the value of interference between two users u_i and u_j exceeds some threshold γ dBm then we assume that interference exists between these two users (our simulations use $P = 10$ dBm, $\gamma = -70$ dBm). In this case we put an edge between all nodes $a_k u_i$ and $a_l u_j$ $\forall k$ and l. In a similar fashion, if a transmission from a_k to u_i interferes with user u_j, we put in an edge between $a_k u_i$ and $a_l u_j$ $\forall l$. We maintain

one $N \times N$ interference matrix I_{a_k} per antenna where row i corresponds to the case that antenna a_k is pointing to user u_i and the entry at (i,j) is the interference seen by user u_j due to a transmission on the downlink from a_k to u_i. Combining the various interference cases we obtain an interference graph and Figure 6.6 shows us one such interference graph for our example.
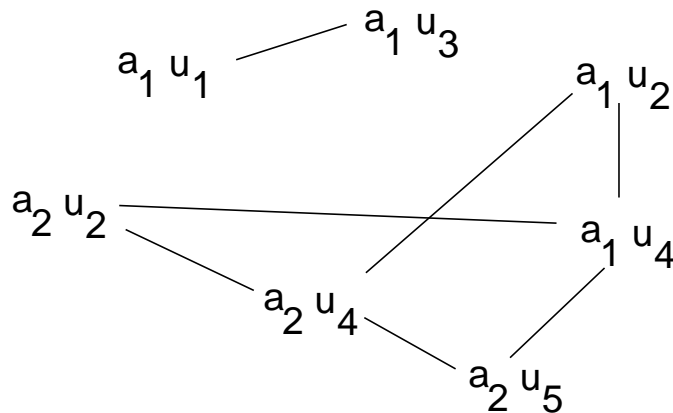

Figure 6.6: Interference graph derived from Figure 6.5.

Given the interference graph, we next prune nodes because we have to meet the constraint that each antenna has only M modules available. The algorithm for pruning is as follows:

1. For each antenna a_k count the number of nodes in the interference graph that include a_k in their label. In our example, a_1 has a count of 4 while a_2 has a count of 3. If the maximum count is greater than the number of modules at that antenna then proceed to step 2.

2. Select the antenna with the highest count. Of the nodes in the interference graph corresponding to this antenna, select the one with the highest degree. In this case say we pick $a_1 u_4$. We check to see if u_4 appears elsewhere in the graph. In this case the answer is *yes*, so we can delete this vertex. If the

answer is *no*, we go to Step 1 above and continue with the antenna with the second largest count.

3. Repeat Steps 1 and 2 until there are no more than N vertices (one per user).

4. At some point we will have pruned the graph down to exactly N vertices. If the total number of nodes with a_i in the label is less than or equal to M then we can assign each of the users u_j in the vertices $a_i u_j$ to a unique module at antenna a_i. If the number nodes with a_i in the label exceeds M, we have to combine nodes together. Intuitively, the idea is to combine two nodes $a_i u_j$ and $a_i u_k$ together if $u_j - u_k$ have the highest user-to-user interference and they share at least one common antenna. The specific algorithm we use proceeds as follows:

   (a) Consider matrix c_{LOS}. Initially, each column j corresponds to user u_j's visibility from all antennas. However, as we start combining nodes together, the columns are redefined. Thus, if we combine users u_i and u_j, the new c_{LOS} matrix will have one less column and the column i (if $i < j$) now corresponds to both u_i and u_j's LoS to all the antennas. In this matrix entry (k, i) is a 1 if a_k has LoS to both u_i and u_j. Otherwise the entry is 0.

   (b) For each pair of columns i and j from the latest c_{LOS} matrix, let U^i and U^j denote the set of all users that are represented by columns i and j respectively. Let X denote the maximum *user-to-user* interference between user's in sets U^i and U^j,

   $$X = \max_{u_p \in U^i, u_l \in U^j} I_{u2u}(p, l)$$

   We also compute the value of total *downlink* interference at U^i from

transmissions to U^j and vice versa,

$$Y = \sum_{k=1}^{A} \max_{u_p \in U^i, u_l \in U^j} I_{a_k}(p, l)$$
$$+ \sum_{k=1}^{A} \max_{u_p \in U^i, u_l \in U^j} I_{a_k}(l, p)$$

We then compute the "affinity" value,

$$T^{ij} = \frac{\#\text{shared antennas cols } i, j \times (X + Y - 1)}{|U^i| + |U^j|}$$

We compute the affinity value over all pairs i, j corresponding to the columns of c_{LOS} and take the maximum. Those two columns in c_{LOS} are combined together (and the corresponding nodes in the graph are combined together as well). The intuition here is to combine together nodes that have strong mutual interference with each other.

This combining process continues until the total number of nodes with a_i in the label is $\leq M$.

In our example, the first pruning step removes $a_1 u_4$ while the second time around we remove $a_1 u_2$. The graph we have is shown in Figure 6.7. We note that while a_1 only appears on the labels of two nodes, antenna a_2 appears on three labels. Therefore we now need to collapse nodes with a_2 in the label. In Figure 6.8 we show the final graph where we have collapsed $a_2 u_2$ and $a_2 u_4$ into one node. This means that u_2 and u_4 will need to time share the link to antenna a_2.
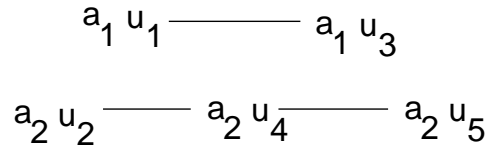

Figure 6.7: Pruned interference graph.

Finally, when we have the pruned and collapsed graph, we need to assign frequency channels to each connection (i.e., each node in Figure 6.8). We do this

by using a simple greedy algorithm where we color nodes (i.e., assign channels) in order of greatest to smallest degree. If we do not have enough colors then we go back and collapse additional nodes together and re-run the coloring algorithm.
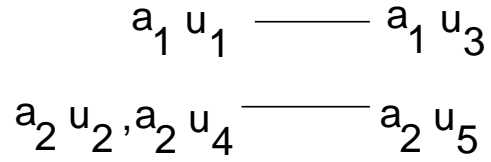
$$a_1\, u_1 \quad\text{——}\quad a_1\, u_3$$

$$a_2\, u_2\, , a_2\, u_4 \quad\overline{}\quad a_2\, u_5$$

Figure 6.8: Final collapsed graph.
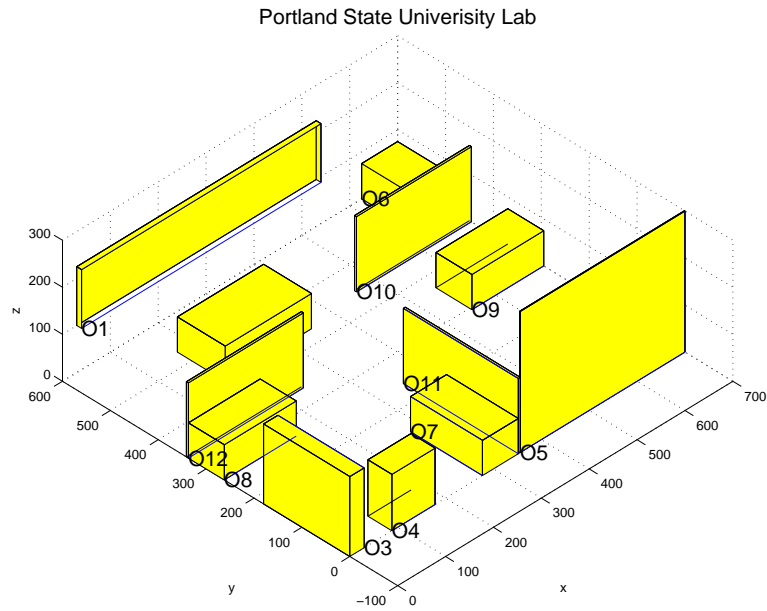
6.3 EXPERIMENTAL DESIGN

Figure 6.9: Laboratory setup used in the simulations (units are in cm).

In order to evaluate the allocation algorithm as well as to answer the larger

Transmit power	10dBm
Noise	-174 dBm/Hz
Channel Bandwidth	640MHz
Path loss	Freespace
Smart antenna gain of main lobe	21dBi
Sidelobe gain	-6.5dBi
Target BER	10^{-6}
γ (Interference threshold)	-70dBm

Table 6.1: Simulation parameters

question of whether gbps/user rates can be provided, we implemented a very detailed simulation in MATLAB. The simulator implements a detailed propagation model for 60GHz and is capable of providing signal strength at any location in the simulated indoor space. As input, we specify the architecture of the room we wish to study including the reflection and absorption properties of all the materials used in the room. For this simulation we used the layout shown in Figure 6.9. The attenuation data we used in the simulations is based on measurements reported in [27, 46] and is summarized in Table 6.2. We note that in the results reported here, we only use the one room described above. The reason is that since 60GHz signals do not propagate far therefore any large room can be split into smaller parts and each studied separately. Table 6.1 shows the fixed parameters we use in the simulations.

We use an ideal antenna model derived from [33] in our simulations. We used the following variable parameters:

- We vary the number of users between 2 and 10 to study the effect of load
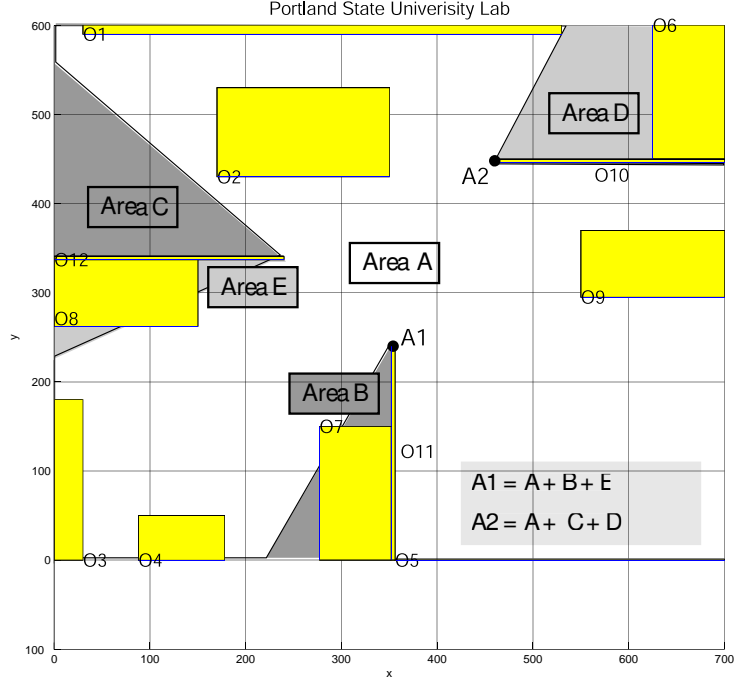
60

Figure 6.10: Location of two antennas.

on the system. For each run for a given number of users, we place users randomly uniformly in the room in meaningful locations (i.e., they cannot be under tables or inside filing cabinets). We also select a random height for each user between 0.5m and 1m above the ground.

- In one set of experiments we use 2 antennas with 3 modules each (shown in figure 6.10) while in another we use 3 antennas with 2 modules each. Thus the total number of beams we can form is kept at 6 for all experiments. Figure 6.11 shows the location selected for the three antennas and the coverage of each antenna.

- The number of available frequency channels (FC) used varies from 2 to 5.
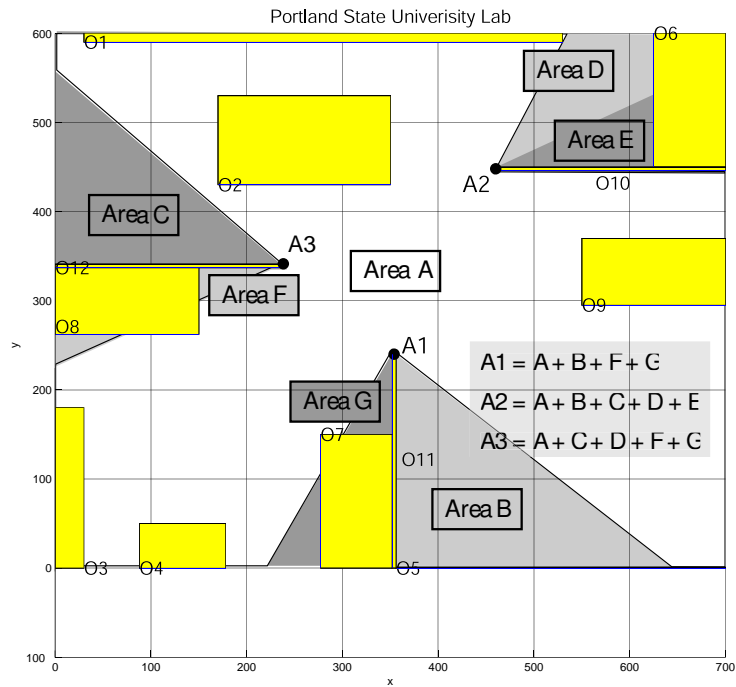
Figure 6.11: Location of three antennas.

- We assume that each user has an omni-directional antenna.

Each experiment is repeated 100 times giving us a total of $9 \times 2 \times 4 \times 2 \times 100 = 144,000$ individual runs.

At the end of a particular run we have an assignment of users to antenna/modules and a frequency. We now use this information and calculate the actual SNIR at each user and at each antenna. This information is then used to compute the data rate that can be achieved in the system for that run.

62

Object ID	Description/ Material	Attenuation [-dB] angle of incidence						
		10	20	30	40	50	60	70
O1	White Board/Acrylic Glass	6.2	5.5	5.5	5.5	6.0	7.6	13.1
O2	Table/Wooden Chipboard 1.3cm	13.4	10.7	9.5	11.7	7.9	5.5	5.3
O3	Book Self/Wooden Chipboard 1.3cm	13.4	10.7	9.5	11.7	7.9	5.5	5.3
O4	File Cabinet/Acrylic Glass	6.2	5.5	5.5	5.5	6.0	7.6	13.1
O5	Glass Door/Glass Smooth 0.8cm	8.8	9.8	12.1	9.1	5.5	3.4	2.6
O6-9	Desk/Wooden Chipboard 1.3cm	13.4	10.7	9.5	11.7	7.9	5.5	5.3
O10-12	Partition/Wooden Panels 1.9cm	22.0	21.7	18.4	18.2	15.2	9.3	6.5

Table 6.2: Attenuation values used from [27, 46].

6.4 RESULTS

Modulation	Code Rate	Min E_b/N_0 for $P_b \leq 10^{-6}$	Rate (Mbps)
64-QAM	3/4	22.65 dB	1080
64-QAM	1/2	22.65 dB	960
16-QAM	3/4	19.1 dB	720
16-QAM	1/2	19.1 dB	480
QPSK	3/4	16.7 dB	360
QPSK	1/2	16.7 dB	240
BPSK	3/4	11.45 dB	180
BPSK	1/2	11.45 dB	120

Table 6.3: Bit per second for different Modulation Schemes with block code rate used [14].

In order to determine the achievable data rate, we compute the SNIR values for each link formed after running the allocation algorithm. Then we assign the appropriate modulation and coding rates from Table 6.3 to each link and compute the total data rate in the room (these particular modulation and coding schemes are proposed in the draft 60GHz PHY standard [14]). This value is divided by the total number of users to obtain the average data rate per user. For each of the 1440 individual experimental set ups, we run the algorithm for 100 different user placements. The average data rate as well as the 95% confidence bounds are plotted in figure 6.12 and figure 6.13.

We note several interesting features of these figures. First, as the number of users increases, the average data rate per user drops from almost 1Gbps to between 300 and 600 Mbps. The drop is steeper when we have 2 frequency channels (FC=2 in the figure). Another interesting feature is that the drop is gradual (for FC =
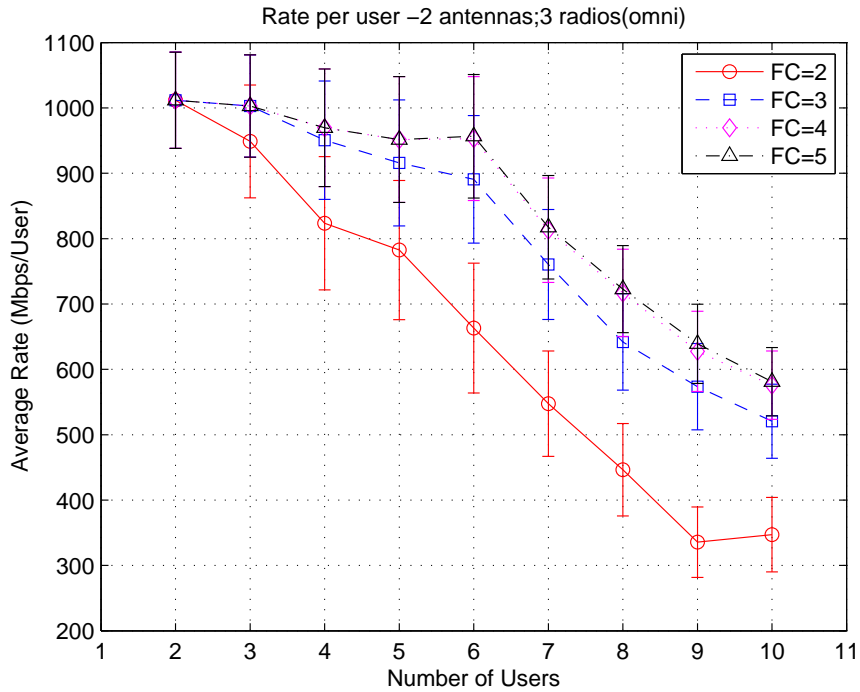
Figure 6.12: Average data rate per user for two antennas and three radios each case.

3,4,5) for upto 6 users after which the drop is faster. This happens because we have a total of six radios (either 2 antennas each with 3 radios or 3 antennas each with 2 radios) only and thus as the number of users continues to grow, more and more users end up sharing a link. Indeed, Figure 6.14 plots the average number of users sharing a beam for the case with three antennas. With the exception of the case with two channels, in all other cases, each user has its own beam when the number of users is ≤ 6. However, after that the users need to share since not enough radios are available. Indeed, for the case of 3, 4, 5 channels, the average number of users per beam from the figure (when the number of users is greater than 6) is very close to the actual number of users divided by 6.

The case when we have only 2 channels is an interesting one since it illustrates
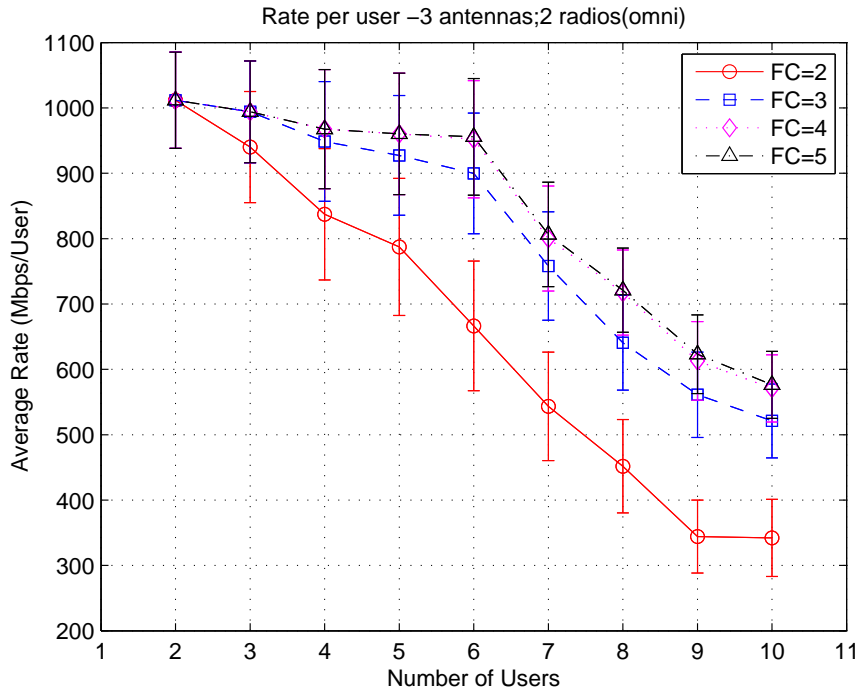
Figure 6.13: Average data rate per user for three antennas and two radios each case

the problem with interference even in the case when we have enough antennas and modules to form spatially separate beams. Consider 6.15 where we plot the total number of beams formed. In the case with 2 channels, the number of beams formed reaches a maximum at around 4 implying that several users share the beams resulting in a lowered data rate per user. Interestingly, when we have 3 or more channels, we form 5-6 beams (where 6 is the maximum that can be formed) because we have enough frequency channels to ensure less interference between users. Indeed, recall that after we form a collapsed graph (Figure 6.8) we run a greedy coloring algorithm to assign channels to each link. However, if not enough channels are available we collapse more nodes together. This is what happens when we only have 2 frequency channels that then results in lowered data rate.
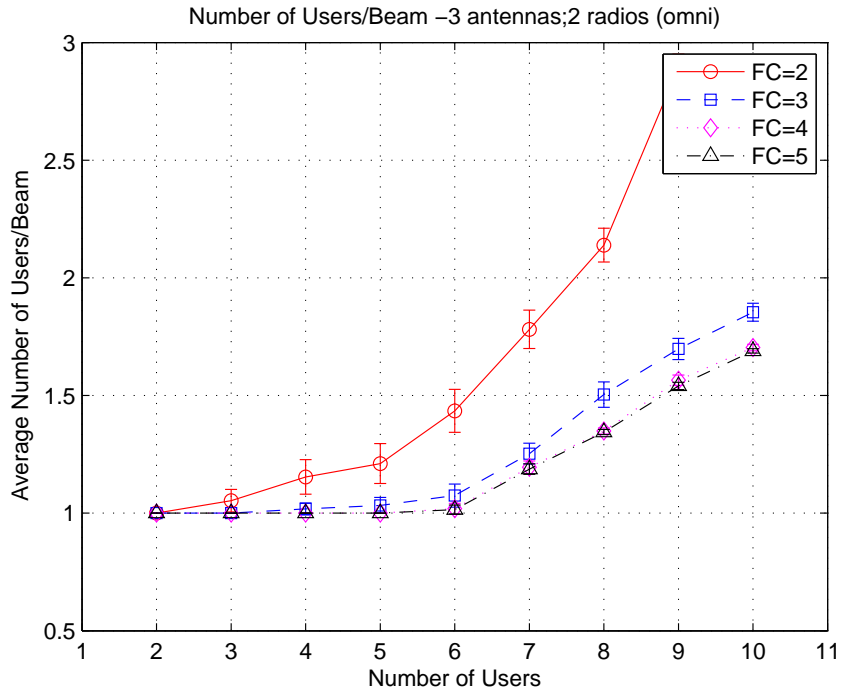
Figure 6.14: Average number of users sharing a beam for the omni case.

Finally, let us look at the SNIR scatter plot for the case when FC=2 on the downlink at the user (after channel allocation is done), Figure 6.16. We observe that in most cases the values range between 20 and 60 dB while in some cases we see a 0 dB. The 0 dB case happens when the user is in a dead spot. Otherwise we see the other range of values. The theoretical data rate that we then see is derived from Table 6.3. It is interesting to observe that the SNIR is quite large in many instances thus attesting to the fact that the 60GHz signal attenuates significantly with distance and with reflection/transmission through materials. Indeed, this figure best illustrates why this frequency band can provide high data rates.
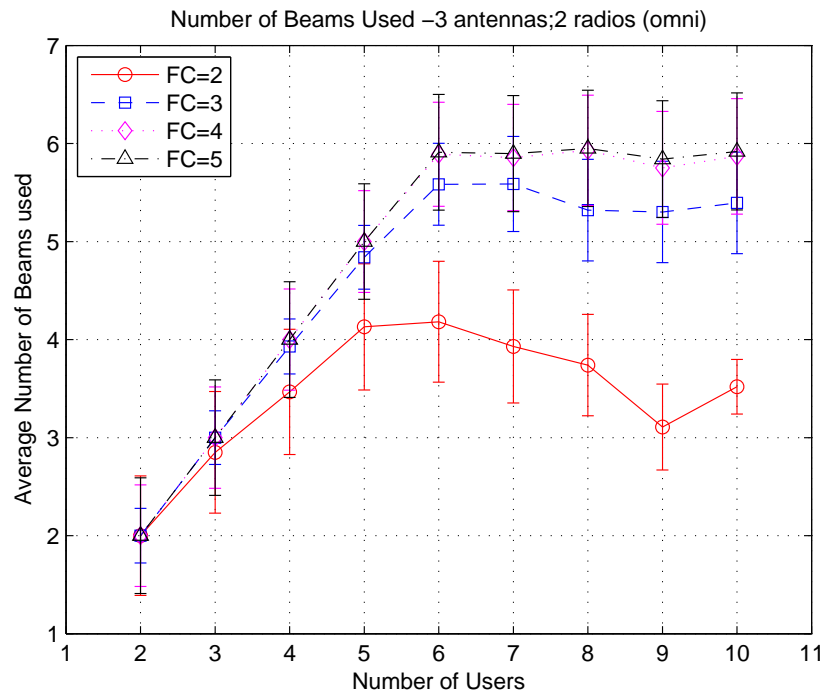
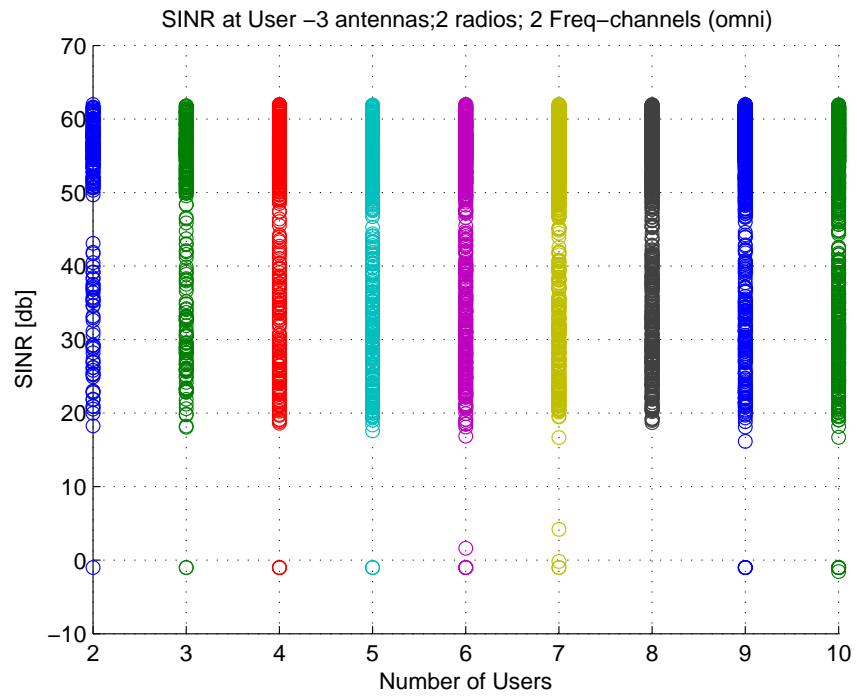Figure 6.15: Average number of beams formed for the omni case.

Figure 6.16: SNIR per link when we have two channels for the omni case.

Chapter 7

ARCHITECTURE FOR 60GHZ DEPLOYMENTS: MULTIPLE CO-LOCATED ANTENNAS

Multiple Co-located Antennas associated with multiple beamforming modules at a single AP allows multiple links to operate simultaneously such that the aggregate data rate is maximized. Each beamforming module has highly directional gain gives us the opportunity to exploit the spatial locality of a beam. In this chapter, we look at the problem of determining the protocol-independent maximum and average throughput of a 60GHz system when the AP as well as users are equipped with identical smart antennas.

The array elements of an antenna can be arranged in many ways. In this thesis, we study two of them: linear and circular array. We choose these two type of antenna arrays because they are geometrically very different. This will give us an idea of how the geometry of array elements affect the performance. The other important design choice is how to allocate users given limited resources. In chapter 6, a dynamic allocation is used to allocate user. This means access points beamform at the user where the user is located. Therefore, the user always receives the maximum signal power of the beam. Another allocation alternative is to statically partition the room and allocate a frequency channel to each partition (similar to cell phone networks). This may, unfortunately, cause the signal strength at the user to be well below the maximum. However, this approach is simpler and results in less computational complexity.

70

Below, we first study the capacity of the two antenna types (linear and circular array) using static allocation. As we will see, the results show that a linear array achieves higher capacity than a circular array because of lower interference between partitions.

Secondly, a comparsion of static allocation and dynamic allocation is given in section 7.2. An important result is that, due to interference in dynamic allocation, this scheme can not scale with the number of users even when using multiple channels. In contrast, static allocation is a better choice because, in addition to the performance gain, static allocation also gives us a simpler system design over all.

Finally, we develop an analytical model for static allocation and show a close match with simulation. In this study, we assume perfect channel sharing (e.g., using TDMA) in each beam.

7.1 STATIC ALLOCATION: LINEAR VS CIRCULAR

The idea of static allocation is to first partition the room into fixed regions and then assign frequency channels to each region. Within the same region, TDMA is used to support multiple users. For example, Figure 7.1 illustrates three users(A,B,C) in a room which has N regions (the shape of the region depends on the array arrangement, this example is independent of the region shape). B and C are in region 2 while A is in region N. Therefore, B and C have to share the frequency channel using TDMA.

The shape of the region depends on how the array elements are arranged. In section 7.1.1, we see that a linear array forms a long strip while circular array forms an irregular shape. Each region may have different shapes even though the same type of antenna array is used. The shape also depends on the angle at which
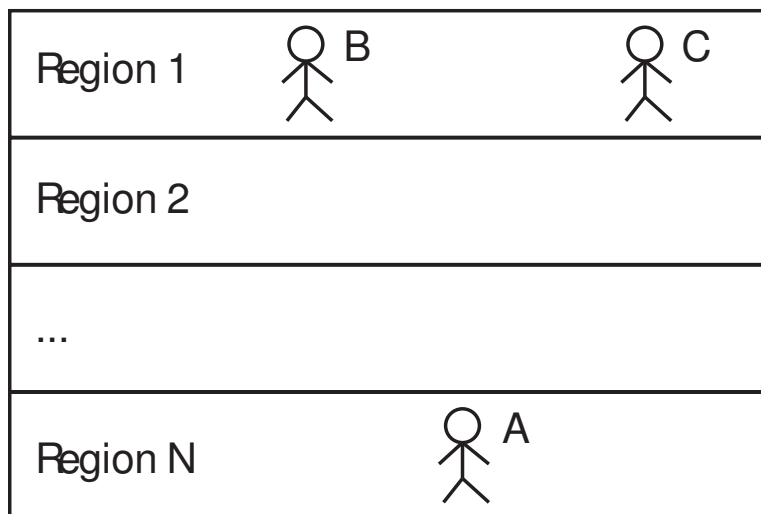
Figure 7.1: Example of a partition room with N regions.

the beam intersects the floor. We determine the region based on the following rules:

- Each region's coverage area is defined to be the locations that have a signal strength within 3dB of the main beam boresight. This provides a strong enough signal to have good connectivity for the entire region.

- Interference should be minimized between regions.

After each region is identified, each module beamforms at the center of its region while using nulls to minimize the interference from other simultaneous transmissions in other regions (the reader can find the nulling technology in detail in Chapter 4). To improve the signal to interference ratio, we introduce a novel nulling method to greatly reduce interference to almost noise level. Details of the nulling method for each type of antenna array will be given in the two sections below.

7.1.1 Linear Array: Constructing Regions

Elements of a linear array lie on a straight line. Figure 7.2 shows the antenna gain in dBi from the AP to the user. The AP is located at the center of the room on the ceiling and the user is located at coordinate (150,150,50). As is evident, the rotational symmetry (about the array axis) causes the region of highest gain to be spread in a narrow strip across the floor of the room (when viewed on the x-y plane). Indeed, if we sweep the beam across all the angles, we will see this strip move in the direction of the y-axis. This behavior gives us a natural way to think about constructing multiple regions.
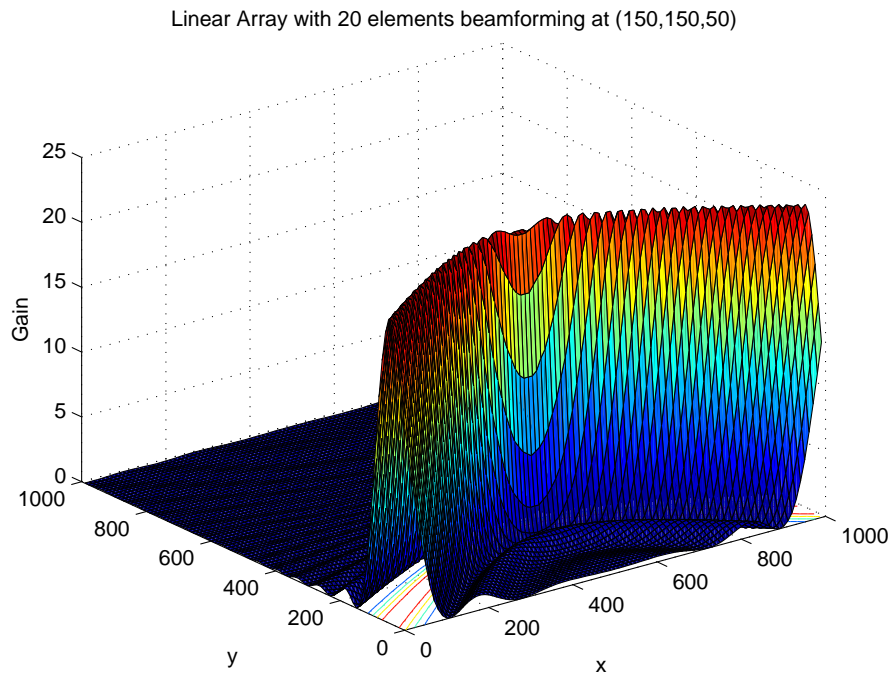

Figure 7.2: Gain with 20-element linear array pointing to (150,150,50) and the axis of the antenna aligned along the y-axis (units are in cm).

It is evident that there are large number of possible solutions (given the continuous nature of the variables such as angle) to the problem of where to point each beam and then sweeping the beams to cover the room. One important consideration we need to keep in mind is that the entire room needs to be covered. Therefore, our approach is to sweep the beams across the room in discrete time steps to identify regions of coverage and using these as the resource to be allocated to different beamforming modules. To explain the idea, let us consider a room of dimensions 10m X 10m X 3m. The linear array is located in the center of the ceiling at (5m, 5m, 3m) and aligned parallel to the x-axis. We begin by forming a beam to a user located at (0.1m, 5m, 0.5m). We define region 1 as all the locations that are within 3 dB of the maximum gain. Region 2 is now formed by aiming the beam at another point (x m, 5m, 0.5m) and including all locations that are within 3 dB of the maximum gain of this beam. The value of x is such that the overlap between region 1 and region 2 is very small and these two regions are right next to one another. This process is continued until we cover the entire room.
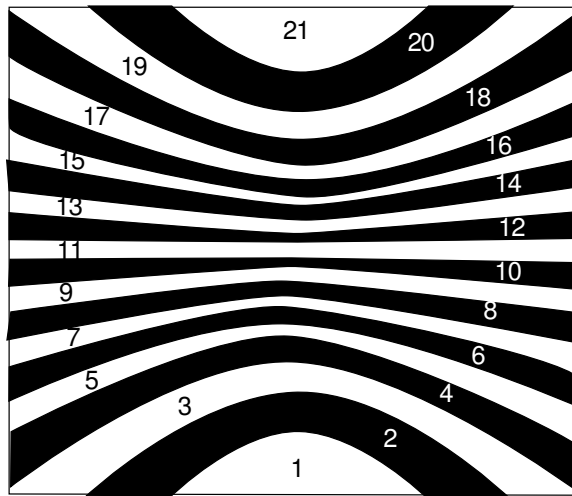

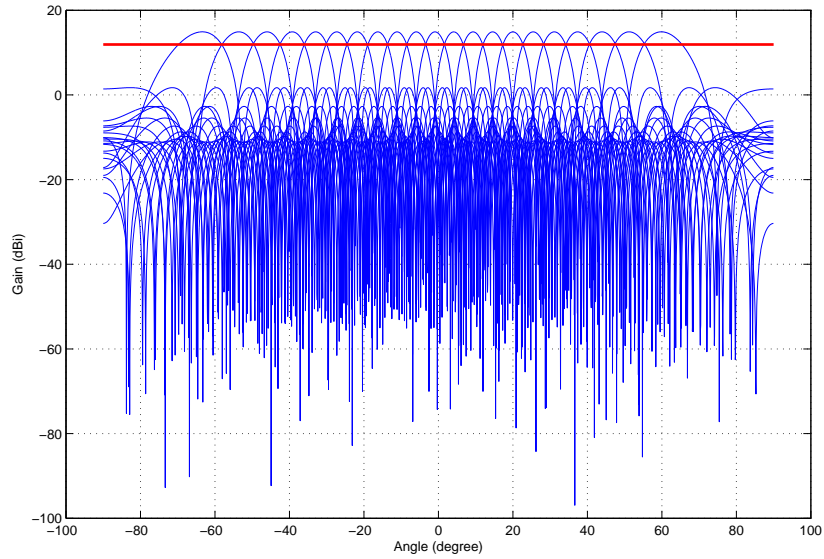Figure 7.3: The 21 regions formed with a linear array.

Figure 7.4: The gain seen at the 21 regions formed with a linear array.

Figure 7.3 shows the 21 regions obtained for the example room we are considering. As we can see, the shape of each region is slightly different from one another. Figure 7.4 plots the corresponding antenna gain when we point the beam at the center of each region. The gain shown in the 2D plot corresponds to the gain seen along the line connecting points (0m, 5m, 0.5m) and (10m, 5m, 0.5m) the line running along the center of the room parallel to the x-axis and 0.5m above the floor. Note that the gain seen in region i from a beam formed towards region $i + 1$ (or $i - 1$) is less than 3 dB (in Figure 7.4 this is shown via the intersection of the horizontal line with the gain plot).

7.1.2 Linear Array: Constructing STDMA Schedule

Assume the AP has multiple beamforming modules (so it can support multiple simultaneous transmissions). Regions can then be used to form spatial channels

such that users located in different regions can transmit simultaneously. Users that are not spatially separable can be assigned resources using TDMA resulting in a STDMA (Spatial Time Division Multiple Access) schedule.

As an example, given two modules, we can form one beam at some angle θ_1 and the other at θ_2 such that the interference between these two beams is low enough to maximize throughput. In other words, the gain of the transmission at angle θ_1 *in the direction* of θ_2 should be very small, and vice versa. This constraint can be naturally extended to the case when we have k modules available at the AP allowing us to form up to k links.

For a given STDMA schedule, we compute the *maximum* and *average* obtainable throughput as follows. The maximum throughput is the mean of the maximum throughput seen in each region. The maximum throughput in a region will typically only occur at a few points. This is the value used for that region. The average throughput for the WLAN is the mean of the average throughput's seen in each region. The average throughput in a region is computed by randomly uniformly placing a user in the region and finding the mean data rate. To compute the data rates, we use system parameters from Tables 7.1 and 6.3.

The STDMA schedule is found simply as follows. For k modules, we can simultaneously form k beams. To ensure that interference between beams is minimized, we maximize the angular separation between the beams. Figure 7.5 shows the example of $k = 7$. Therefore, we have the following schedule: {(1,4,7,10,13,16,19), (2,5,8,11,14,17,20), (3,6,9,12,15,18,21)}. Thus we use 3 time slots and in each we simultaneously have 7 links. In the figure, the regions that have the same color are assigned to the same time slot. The schedule for $k = 8$ is: {(1, 4, 7, 10, 13, 16, 19, 21), (2, 5, 8, 11, 14, 17, 20), (1, 3, 6, 9, 12, 15, 18, 21)}. As we can see, when the number of regions is not perfectly divisible by k, the separation of regions in the same time slot is not uniform. Given r regions and k modules, the separation

Room dimensions	10m x 10m x 3m
AP location	Center of ceiling
Transmit power	10 dBm
Bandwidth	640 MHz
Modulation	Table 6.3
No. antenna elements AP and user	$M = 20$
No. Modules k at AP	$1 - 21$ (Linear)
	$1 - 49$ (Circular)

Table 7.1: Experimental Parameters.

between regions in the same time slot is either $\lfloor \frac{r}{k} \rfloor$ or $\lceil \frac{r}{k} \rceil$.
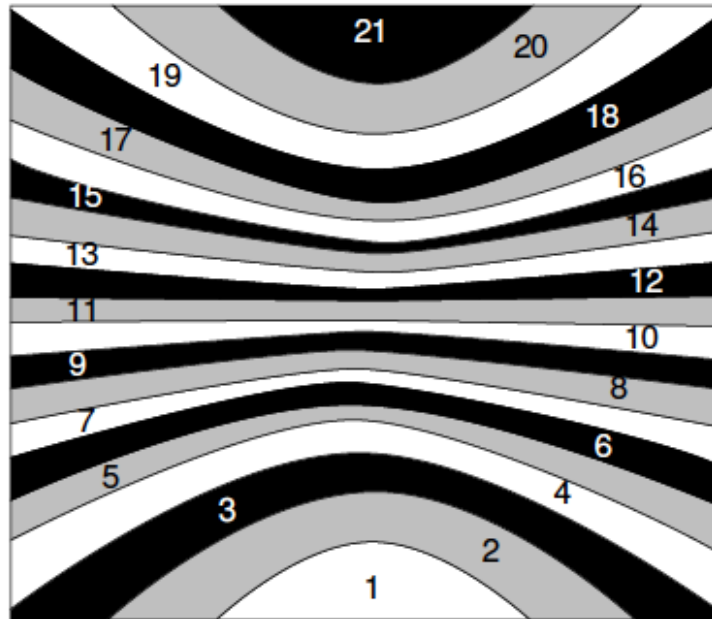

Figure 7.5: Example of linear array schedule for k=3

7.1.3 Linear Array: M-1 Nulling Method

In our experiments, we also use the nulling capability of smart antennas. Thus, given k modules, we form k simultaneous beams – each module beamforms in one direction and nulls the remaining $k-1$ directions. For instance, if $k=3$ and regions (1,8,15) are active simultaneously, the module that beamforms towards region 1 also nulls the center point of regions 8 and 15, and so on. An interesting observation we can make is that since our antennas have $M=20$ elements, we can potentially form 19 nulls per module. Thus, if $k < M$ and we form $k-1$ nulls as described, we still have the capability to form an additional $M-k$ nulls per module. The question is where to form the additional nulls, and whether this is a useful thing to do.

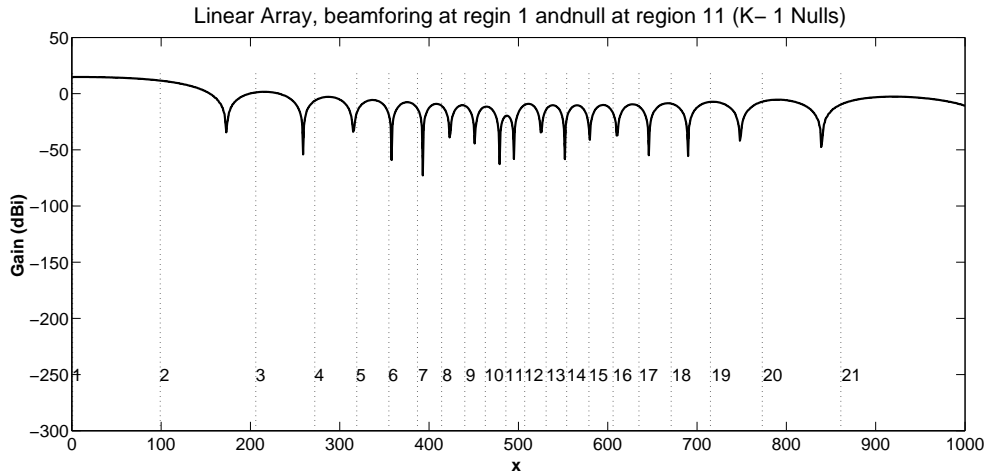Figure 7.6: Beamform to region 1, place a single null in region 11 (x-axis is in cm).

We research this question in some detail. Consider Figure 7.6 where we beamform towards region 1 and null the center of region 11 and we only use $k=2$ beamforming modules. If we look at the gain at areas close to the null, we see a steep increase in gain – the center of region 11 is at -48 dBi while the edges are

at -30 dBi. This means that even if we null the center of any region from Figure 7.3, it is likely that there will be significant gain as we go to the boundaries of that region, which will result in more interference. This observation means that given the opportunity to form additional nulls, we should form more than one null per region at different angular locations such that interference in that region is reduced overall. In Figure 7.7 we plot the case when we form $M-1$ nulls in region 11 (each null is incrementally located a small fraction of a radian off center) while beamforming to region 1 and vice versa. We see that the interference from beamforming at region 1 towards region 11 is now well below -100 dBi across the entire span of region 11 (and vice versa). This clearly indicates that forming multiple nulls within a region is a beneficial thing to do.
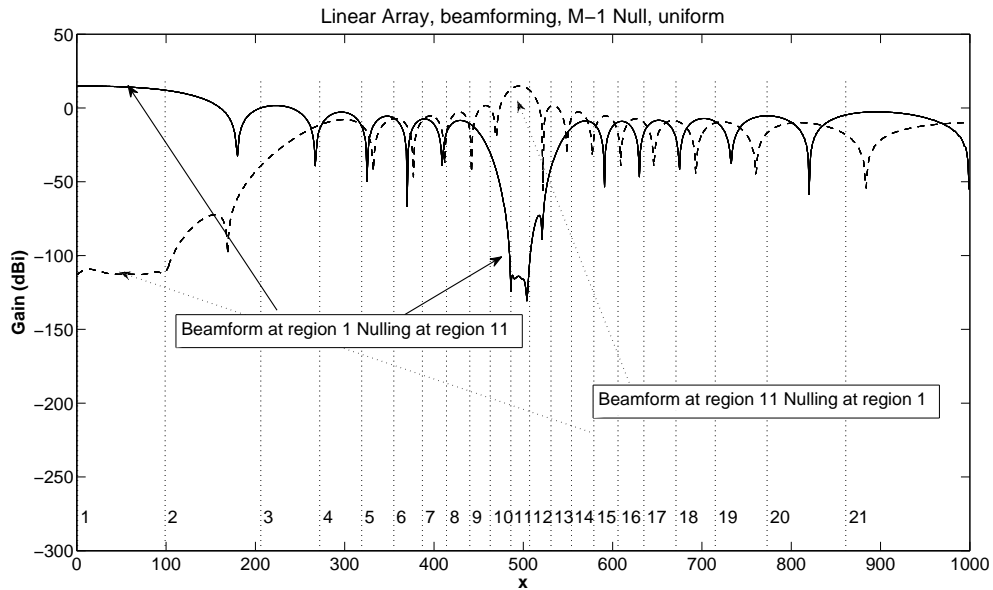

Figure 7.7: Forming 19 nulls in each region (x-axis is in cm).

We compared the cases when modules only form $k-1$ nulls and when modules form $M-1$ nulls. The algorithm we used to allocate the additional $M-k$ nulls is

as follows. For each of the $k-1$ nulling directions, we allocate $\lfloor \frac{M-k}{k-1} \rfloor$ additional nulls. These nulls are then formed at angles $\pm\epsilon, \pm 2\epsilon, \cdots$ about the center of the region until we form all the allocated nulls. The performance of the algorithm for different values of ϵ are somewhat different and in our plots we report on only two extreme values, $\epsilon = 0.0005, 0.03$ radians. Another method we consider is called *uniform* where we first find the beamwidth of a region (i.e., the 3 dB boundary) and then distribute the $\lfloor \frac{M-1}{k-1} \rfloor$ nulls equally spaced (in an angular sense) in the region. Note that in all experiments the user also beamforms towards the AP using an identical antenna array. However, the user does not form nulls since interference from uplink transmissions from other users is negligible.
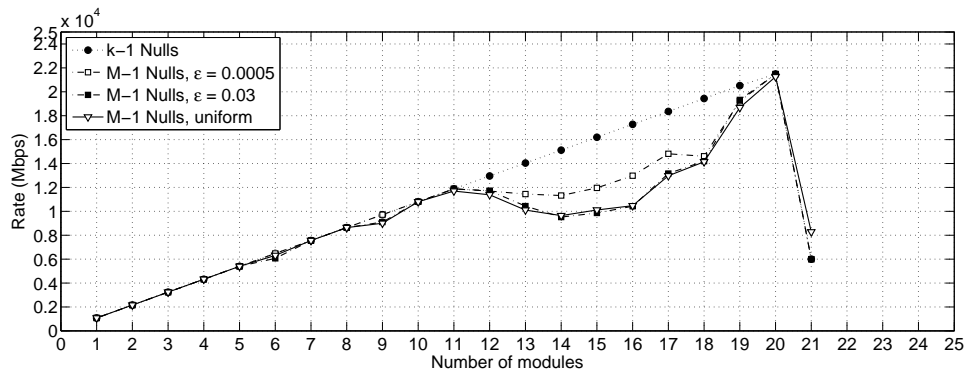
Figure 7.8: Maximum throughput for the linear array.

Figure 7.8 plots the maximum throughput obtained for the room we are considering as a function of the number of beamforming modules available, k. Figure 7.9 plots the average throughput. Initially, as we increase the number of modules, the throughput (maximum and average) also increases linearly as seen in the two figures. This is because the mutual interference is very low and thus we are simply gaining throughput as we add modules. Let us now look at Figure 7.8 in more detail. It is interesting to note that the maximum throughput of 22 Gbps is obtained when using 20 modules and forming $k-1 = 19$ nulls. Indeed, the maximum

80

Figure 7.9: Average throughput for the linear array.

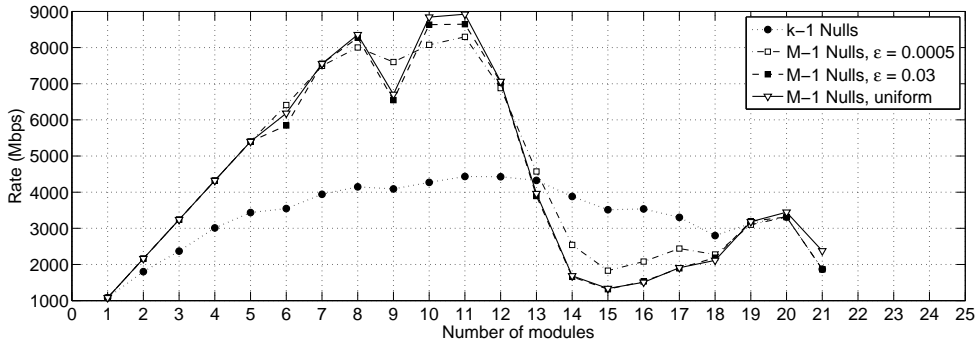data rate is equal to the number of modules multiplied by 1.08Gbps. Furthermore, forming $k-1$ nulls is the best choice rather than forming $M-1$ nulls! The reason for this is that since we are only finding the best SINR per region (a single point), when we form $M-1$ nulls per region, the main beam shifts and flattens slightly resulting in lower desired signal levels. There appears to be little difference in maximum throughout for the two values of ϵ selected.

If we look at the average throughput in Figure 7.9, however, the story is quite different. The maximum throughput of 9 Gbps is obtained at 10 and 11 modules when we form $M-1 = 19$ nulls. Indeed, forming only $k-1$ nulls causes the average throughput to reduce in half. The reason that forming more nulls is better is simply that we reduce interference levels in the *region as a whole* from other beams. Since the average is computed by assuming a uniform random user placement over the entire region, more nulls provide a greater overall benefit. Increasing the number of modules beyond 13 appears to be detrimental as we increase the total interference seen and thus lower the data rate. In Figure 7.10 we plot the signal levels at each region when using $k = 14$ modules and beamforming at region 1. There is one plot for the case when forming $M-1$ nulls using the uniform algorithm and for the case when forming $k-1$ nulls. As is clear, the desired signal in region 1 is

81

much higher when we only form $k - 1$ nulls. The reason is that as we form more and more nulls, the main beam flattens out and spreads more. Therefore, there is an optimal number of nulls one can form that trades off the benefits of reducing interference with the cost of reducing the desired signal strength.
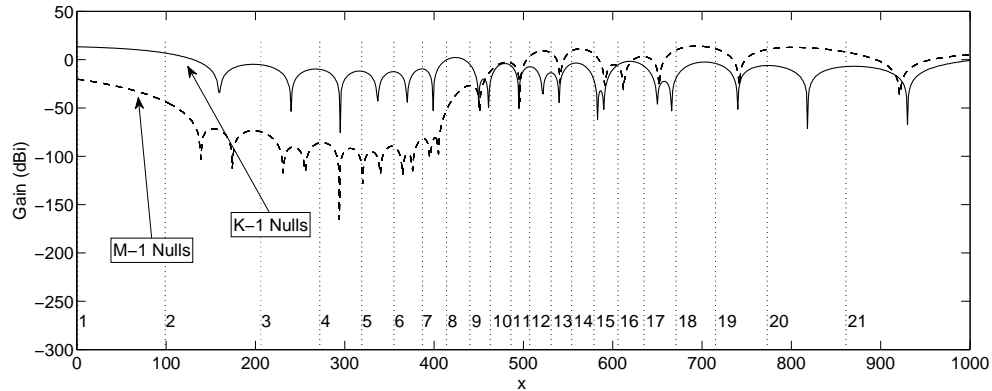

Figure 7.10: Comparison of the desired signal levels when using 14 modules.

7.1.4   Circular Array: Constructing Regions

The array elements of a circular array form a circular shape. Figure 4.6 shows the antenna gain beamforming from the AP to the user. The AP is located at the center of the room on the ceiling and the user is located at coordinate (150,150,50). In order to illustrate the effect of interference from the sidelobe(i.e. unintended signal created in other direction), the figure on the right shows the exact same antenna gain but the unit is recalculated in dB. As we can see, there is significant signal power in the area beside the main beam.

We use similar methodology to construct the regions for the circular array as we did for the linear array. However, there are two angles of freedom in the circular array (there is only one angle of freedom for the linear array). Therefore, we have

to sweep the room in both x-axis and y-axis. Here are the steps to construct the regions (assume the AP is located in the center of the ceiling at (5m,5m,3m)):

- We overlay a grid on the room floor with grid squares of size 10cm x 10cm.

- Beamform at (0.1m,0.1m,0.5m) and calculate the corresponding boresight angle. For every grid that sees a signal strength within 3dB of the maximum, assign it to region 1.

- Next, sweep the boresight along the y-axis and beamform at (0.1m, y m, 0.5m) where y is such that the overlap of the first beam and second beam is minimized and the covered area remains within 3dB from the maximum. Assign all of these grid locations to region 2. Note that some of the grid locations in the first coverage region will also belong to the second coverage region. As a result, these grid locations are now assigned to region 2. Continue this process along the y-axis.

- Return to region 1 and sweep along the x-axis to find the grid locations not covered. Now repeat the previous step sweeping along the y-axis but starting at this new position.

- Repeat the above two sweeps until the entire room is covered.

Figure 7.11 shows the regions for a circular array with 20 elements. As we can see, the regions formed are not uniform and are of different sizes. The reason for this is two fold: first, we use 10cm x 10cm grids and as a result the boundaries are not smooth. Second, after grid locations are assigned to one region, some of them may be reassigned to another region. Both of these factors together cause the observed asymmetry. For the $10m \times 10m$ room, we get 49 distinct regions. Observe that as we get further away from the center of the room, the regions get elongated. This happens because the beam hits the floor obliquely.
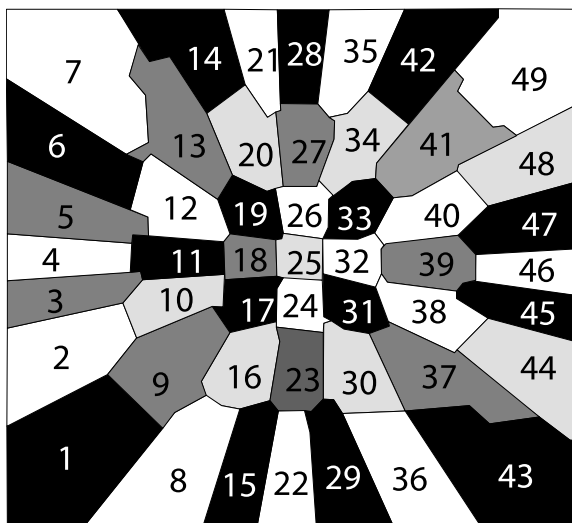
Figure 7.11: The 49 regions formed with a circular array.

7.1.5 Circular Array: Constructing STDMA Schedules

Again, multiple beamforming modules at the AP is assumed. As in the case of the linear array, the problem of computing the maximum and average throughput relies on constructing appropriate STDMA schedules with k modules such that the room is completely covered. There are many different approaches one can take to find the best possible throughput (indeed, the problem of finding the optimal throughput can be shown to be NP-complete). However, we instead use the following algorithm for its computational simplicity. Given k modules, we compute $d = \lfloor \frac{49}{k} \rfloor$. The schedule then is: $\{(1, d+1, 2d+1, \ldots, (k1)d+1), (2, d+2, 2d+2, \ldots, (k-1)d+2), \ldots, (d, 2d, 3d, \ldots, kd)\}$. If the number of regions is not perfectly divisible by k then we will need an additional time slot to accommodate the remaining regions.

Figure 7.12 shows the example of k = 17. The schedule looks like $\{(1, 4, 7, 10, 13, 16, 19, 22, 25, 28, 31, 37, 43, 46, 49), (2, 5, 8, 11, 14, 17, 20, 23, 26, 29, 32, 35, 38, 41, 44, 47), (3,6, 9, 12, 15, 18, 21, 24, 27, 30, 33, 36, 39, 42, 45, 48)\}$. The regions colored in blue is assigned to time slot 1, white is assigned to time slot 2 and black is assigned

to time slot 3. From the figure, observe that the number of neighbouring regions for circular array is more than linear array. This means that regions introduce more interference in the case of circular array. We use the same methodology to compute data rate using system parameters from Table 9.1 and 9.2.
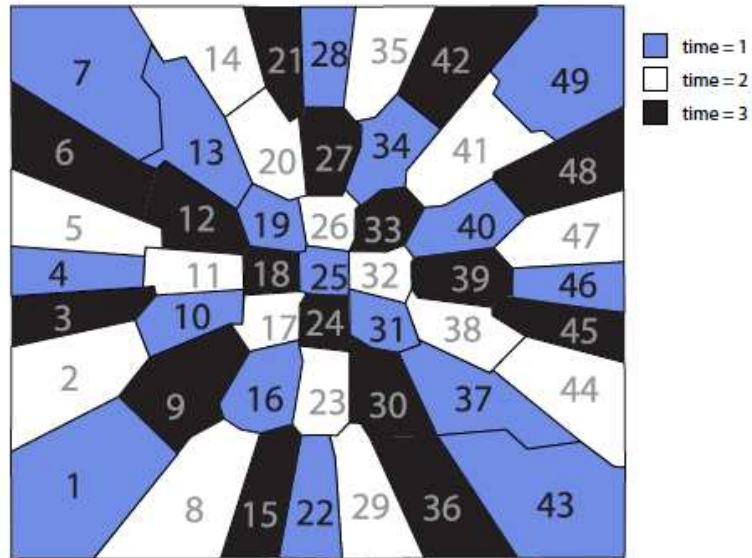
Figure 7.12: Example of circular array schedule.

7.1.6 Circular Array: M-1 Nulls

The problem of forming nulls is similar to the discussion we had previously. Thus, we consider the case when we form only k-1 nulls given k modules and when we form M-1 nulls. Because of the two angles of freedom in a circular array, we need different algorithms for forming $\lfloor \frac{M-1}{K-1} \rfloor$ nulls per region. The challenge of forming nulls in the circular array is that each region has an irregular shape and it is hard to find the best way to find the optimal M-1 nulls. Therefore, we compare two different algorithms.

The first algorithm, called ϵ-walk is illustrated in Figure 7.13. The idea is that

we walk along a grid of side ϵ around the center of a region and use the vertices as locations for the additional nulls. In our experiment, we try different values of ϵ and find the one that gives us maximum throughput. The second algorithm is illustrated in Figure 7.14. Here, we take the region to be nulled and uniformly distribute $\lfloor \frac{M-1}{K-1} \rfloor$ nulls within it. The difference between the ϵ-walk and the uniform case is that in the ϵ-walk algorithm, the nulls will tend to be clustered about the center of the region while the nulls are uniformly distributed about a region in the other case. From the experience of M-1 nullings in linear array, we know that the more uniform the nulls placement, the lower the interference. However, the later method requires manually picking the nulling points while the ϵ-walk tries to automate the process.
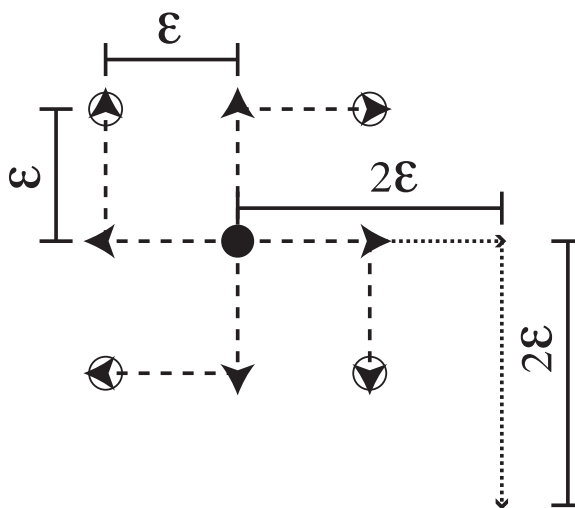
Figure 7.13: ϵ-walk algorithm.
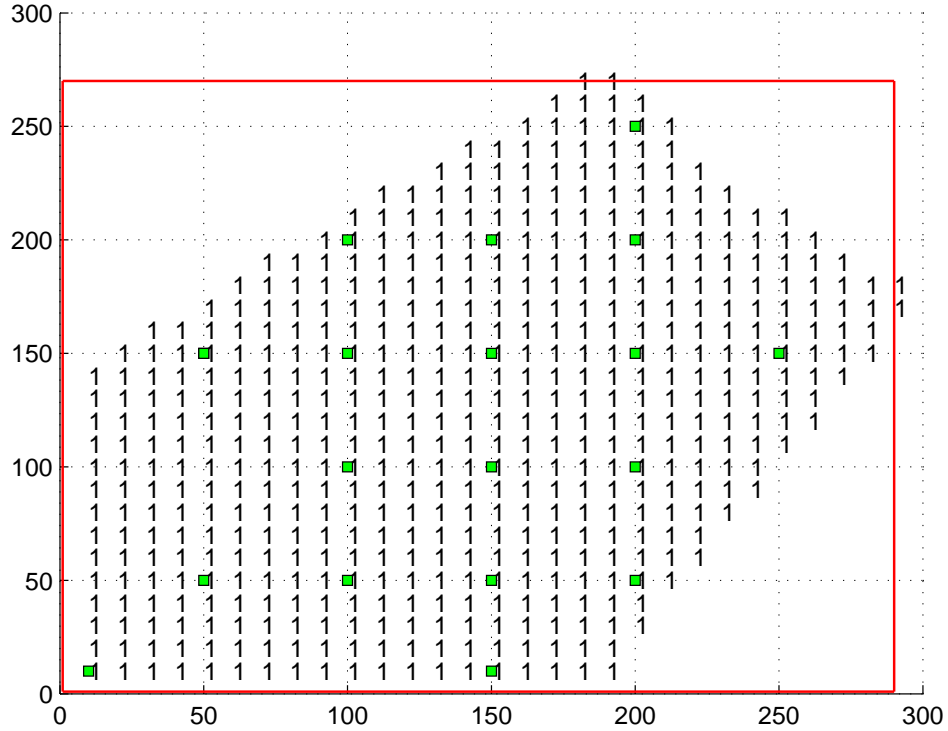
Figure 7.14: Uniform placement of 16 nulls.

7.1.7 Circular Array: Results

Figure 7.15 plots the maximum throughput for the circular array. We note that the maximum throughput of 8 Gbps is obtained when we have 11 modules. Interestingly, forming more than $k - 1$ nulls does not have much of an impact. The reason is the same as in the linear case where forming more nulls does not improve maximum throughput as it is computed at one point per region (the point that has the highest SINR). However, in comparing these results with those in Figure 7.8, observe that the maximum throughput for the circular array is far below the linear case, even though we expect the circular array to provide a narrower beam.

The reason for this difference is made clear if we look at Figures 7.2 and 4.6. The SIR for a link can be shown to be proportional to the ratio G_t/G_I where G_t is the gain of the transmitter in the direction of the receiver and G_I is the gain of the interferer in the direction of the receiver. Note that in our case, the desired transmitter as well as the interferer are co-located (we simply use different modules for beamforming and nulling). In the case of the linear array from Figure 7.2, $G_t = 13.72$ dBi and $G_I = -3.09$ dBi (on average). Thus the SIR is proportional to $G_t/G_I = G_t$ (dBi)$-G_I$ (dBi)$= 16.81$ dBi. In case of the circular array the values we have are $G_t - G_I = 14 - 1.68 = 12.32$ dBi. The difference in SIR between the linear array and the circular array is thus more than double (3 dBi) and this explains why the linear array shows greater maximum throughput.
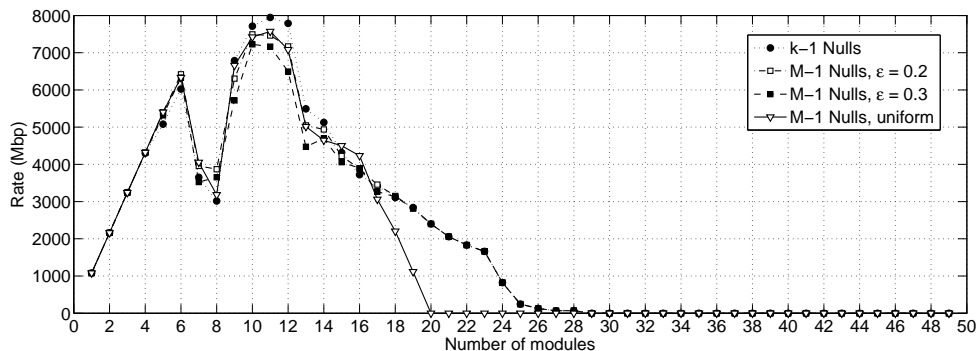
Figure 7.15: Maximum throughput with a circular array.

Figure 7.16 plots the average throughput for the circular array. We obtain a maximum of 3.25 Gbps when using 4 modules and forming $M - 1$ nulls uniformly spaced in the regions being nulled. The ϵ-walk algorithm does not perform as well since the nulls are being clustered about the center of the region which leaves the remaining parts of the region to have non-trivial gain values. The difference between forming only $k - 1$ nulls and $M - 1$ nulls is more than double, as in the linear case.

Figure 7.16: Average throughput with a circular array.

The wavy behavior of the maximum throughput plot and the average throughput plot is an artifact of the manner in which the STDMA schedules are constructed. When $k = 8$, with 49 regions, we get $\lfloor 49/8 \rfloor = 6$. Thus, regions (1, 7, 13, 19, 25, 31, 37, 43) are assigned to the same time slot. As we can see in Figure 7.11, all regions with the exception of 1 lie next to one another along a diagonal. Thus, even though we perform nulling, the SIR is going to be poor.
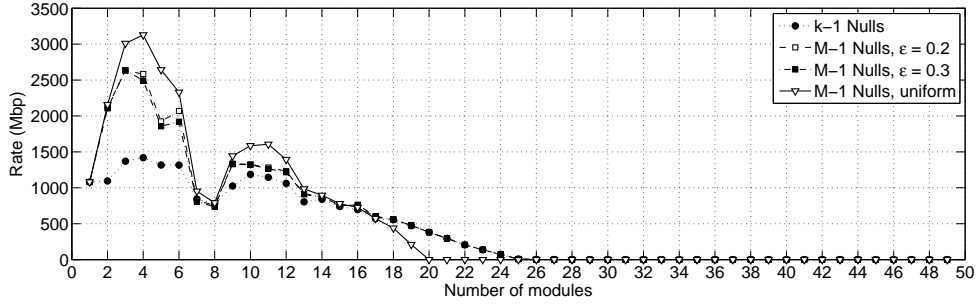
In *summary*, our detailed analysis indicates that a linear array provides higher average and maximum throughput. Further, given the symmetry of the beam formed by the linear array, statically dividing the room into regions enables efficient spatial channel allocation. Finally, forming multiple nulls in a direction (with a small angular separation between the nulls) doubles average throughput.

7.2 STATIC VS DYNAMIC ALLOCATION

The results in Section 7.1, which showed the obtainable average and maximum throughput, was based on a static STDMA schedule where the assumption (for the average case) was that users were uniformly randomly located all over the room. In reality, this is a rare situation that may only occur when we are considering rooms that have a great many users (e.g., lecture halls). What happens if the

89

users are clustered in some discrete locations? Clearly, allocating the channel to parts of the room that are empty is meaningless. How, then can we construct an efficient STDMA schedule?

The simplest approach is to continue using the static regions identified in Figure 7.3 and 7.11. However, we create a transmission schedule that only covers those regions that contain users. The only constraint in constructing the schedule will be to meet the user QoS needs. For example, if one region has 5 users while another has only one user, then the STDMA schedule should give five times as much time to the region with more users. Similarly, given data rate requirements, the STDMA schedule can be trivially adapted to satisfy those needs as well.

Unfortunately, we can easily create situations where using the statically identified regions as in Figures 7.3 and 7.11 will not be efficient. For example, if users are located on the boundaries between regions, then the signals they will receive will be 3 dB less than the signal they would receive if they were located in the middle of the region. In these cases, therefore, it makes sense to redefine the regions and create STDMA schedules around those regions. The algorithm for identifying the regions is simple. For the linear antenna array case where the elements are parallel to the x-axis we order users using the x-coordinate and begin beamforming to each starting with the leftmost (lowest x-coordinate). Users who fall within the 3 dB beamwidth of an already formed beam are allocated to that beam. For the circular array case, we can run a similar algorithm by systematically sorting through the user locations.

What is the data rate we would get if we use dynamic STDMA? It is clear that the maximum rate can be no better than what we saw when using static allocation in Figures 7.8 and 7.15 because these rates are calculated by finding the maximum rate per region (at a single point). Indeed, for large enough number of dispersed users, the average rate we get will also be close to what we saw for the static case.

7.2.1 Static STDMA

Recall the static allocation in section 7.1 as follow:

- Let N be the number of users. Find the region that each user falls into. Sort the users according to region number.

- Let ρ take positive integer values.

- A schedule may consist of one or more time slots. In the first time slot, the user in the lowest numbered region is allocated a channel (and a module). If the user is in region number x then a user from region numbers $x + \rho$ is also allocated a channel in the same time slot.

- If some users have not yet been allocated a time slot, we remove the users already allocated a slot and run the above algorithm for the remaining set.

- If all users have been allocated a time slot, we are done and the schedule repeats.

We explore the performance of the algorithm for $\rho = 1, 2, 3$. When $\rho = 1$ we allow neighboring regions to be active simultaneously. This results in higher interference and thus lower data rates. If $\rho = 3$ we get the lowest interference but the schedules will be longer since fewer users are packed into one time slot.

7.2.2 Dynamic STDMA

The dynamic algorithm performs channel allocation by first sorting users according to their angular locations with respect to the AP. The schedule is then constructed as follows:

- In the first time slot, the leftmost user (smallest θ) is allocated a module. The first user outside the 3 dB of the beam formed towards the first user is then allocated a module, and so on. In other words, all users who do not lie within the 3 dB beamwidth of each others beams are allocated the channel in the first time slot. Each of these users then forms nulls in the direction of the other users in the same slot.

- Of the remaining users who have not been allocated the channel, we perform the above step again. This process is continued until all users have been allocated the channel.

The primary difference between the dynamic and static cases is best illustrated by considering a single user. In the static case, this user will be allocated a static beam in some region. However, if the user is not in the center of the region, the gain will be smaller than if the beam was formed directly at that user, as in the dynamic case. Thus, we expect that the signal strength of the desired signal in the dynamic case will be better than in the static case.

7.2.3 Comparsion of Static and Dynamic STDMA for Single Channel

For our experiments we used the system parameters given in Tables 7.1 and 6.3. The simulations were conducted in MATLAB using a detailed propagation model developed for 60GHz utilizing measurement studies described in section 2. The metrics we studied are:

1. The *average* total (or aggregate) throughput in one WLAN. This is calculated by randomly placing N users in the room and running the two SDMA algorithms. After finding the SNIR for each user, we find the data rate achieved using Table 6.3. The throughput per slot in the schedule is the sum of the

data rates per user in that slot. The data rate is summed over all slots in the schedule and averaged by the number of time slots.

2. The average number of *modules or radios* used at the AP. As we mentioned previously, the number of modules we use is a function of the room geometry and not N since interference is the limiting factor on achievable throughput. We plot the number of modules used as a function of N to show this behavior.

3. The average *delay* is the average number of slots per schedule.

Figure 7.17 plots the average total throughput in the room as a function of N for the static and dynamic algorithms (all figures show the 95% confidence intervals). As the number of users increases, the total throughput in the WLAN also increases, as is to be expected since more users are active. However, after peaking at 8 gbps at 25 users, the throughput falls somewhat for the dynamic case because of increased interference as more users are allocated in the same time slot. The throughput for the static case (for $\rho = 1, 2, 3$) is much smaller than the dynamic case for $N \leq 35$. The reason is that in the static case we may have two users at the opposite ends of a region's boundary but they will be allocated to the same region (and hence to different time slots in the schedule). In the dynamic case, however, it is likely that these two users will be allocated to the same time slot because they lie outside each other's 3 dB beamwidth. As N increases, however, the static case and dynamic case become similar in performance because the schedule lengths are similar. Figure 7.18 plots the average length of a transmission schedule for the various schemes.

The performance of the static algorithm for different ρ values is quite different. The reason $\rho = 1$ is the poorest performing algorithm is that by allowing neighboring static regions to be active simultaneously, we are increasing interference. When $\rho = 3$, however, interference is minimized allowing higher data rates.
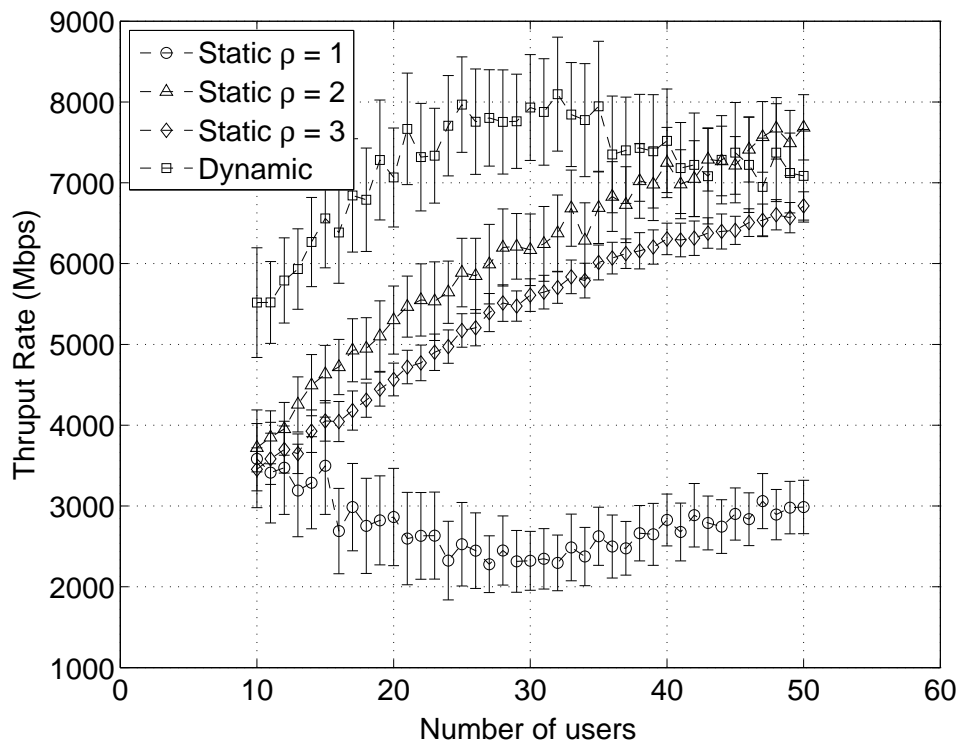
Figure 7.17: Average throughput.

Figure 7.18 shows the schedule lengths for different schemes. As we can see, the schedule length for $\rho = 1$ is 1 while it is 50% greater for other values of ρ and for the dynamic case. Indeed, while shortening the schedule length helps increase the throughput for the $\rho = 1$ case, the increased interference causes a far greater reduction in throughput.

Figure 7.19 plots the number of modules at which maximum throughput is obtained for each value of N for each algorithm. As expected, the number of modules used by the static case when $\rho = 1$ is by far the largest. However, for the dynamic case (which has the highest throughput for all values of N), the number of modules used is no greater than 10. This indicates a good separation of beams between nodes assigned to the same time slot.
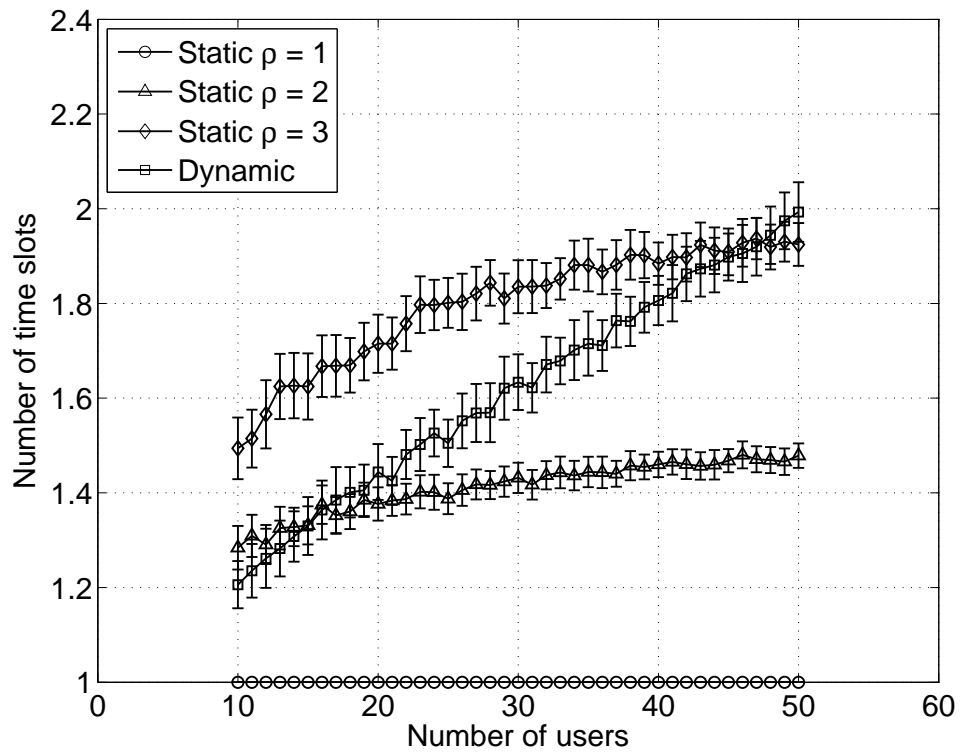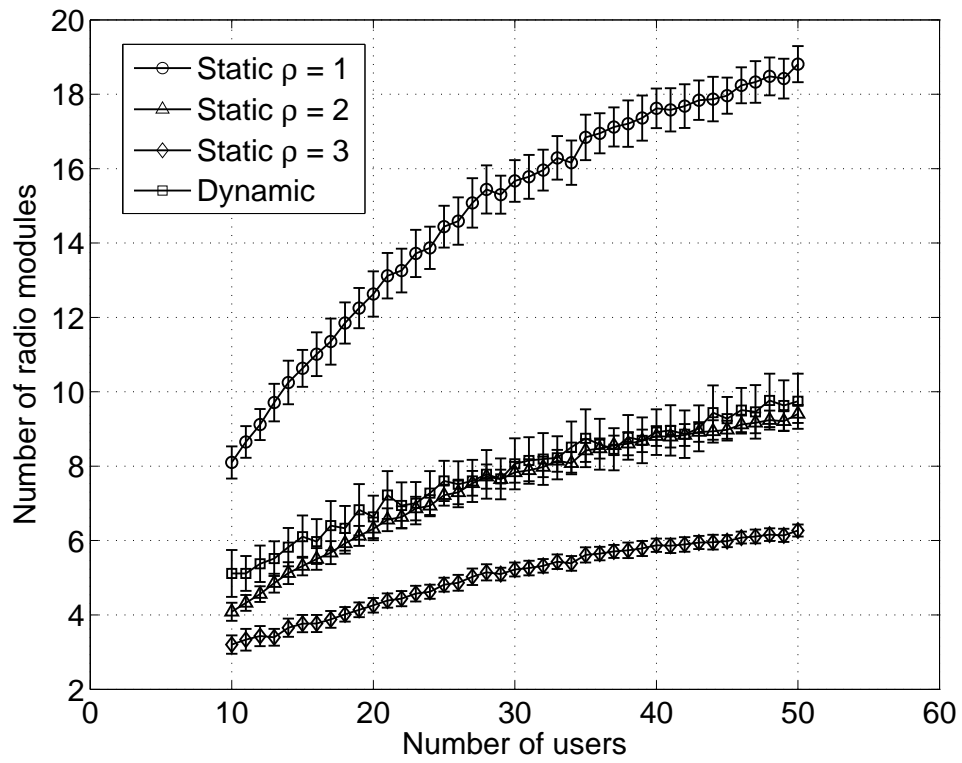
94

Figure 7.18: Average schedule lengths.

Figure 7.19: Number of modules used to maximize average throughput.

7.2.4   Static and Dynamic STDMA in Multiple Channels

The 60GHz ISM band has over 5GHz of available bandwidth allowing us to utilize multiple channels simultaneously within a cell. We therefore modified the static and dynamic SDMA algorithms to examine the potential benefits of doing so. The modification made in each case is the same:

- Start with a transmission schedule constructed for the single channel case. If this schedule has m slots and $m \leq 7$ (with 5GHz of bandwidth we can get a total of 7 channels of 640MHz with 80MHz spacing), we shrink the schedule down to one time slot and assign users from each slot of the static schedule to a different channel. Frequently, m is of the order of 2-3 time slots. This means that we will be left with 4-5 free channels. We divide these channels among the users as follows. Take the channel with the largest number of users and split the set in two with one subset retaining the original channel and the other subset being assigned to a new channel. This process is repeated until no channels remain.

  In the unusual case that $m > 7$, we shrink the first 7 slots into one slot as above, and repeat the algorithm for the remaining $m - 7$ slots yielding a multi-slot schedule.

A point to note is that the number of radio modules used in this case will equal the *total* number of users in the slot. Therefore, unlike in the single-channel case, the total number of radio modules will be much greater.

Figure 7.18 plots the average number of time slots as a function of N. As we can see, $m \leq 2$ in most cases. Thus, as per the algorithm above, we will first reduce the schedule length to one slot by assigning separate channels to users in each time slot from the single-channel schedule and then we allocate the remaining 5 channels.
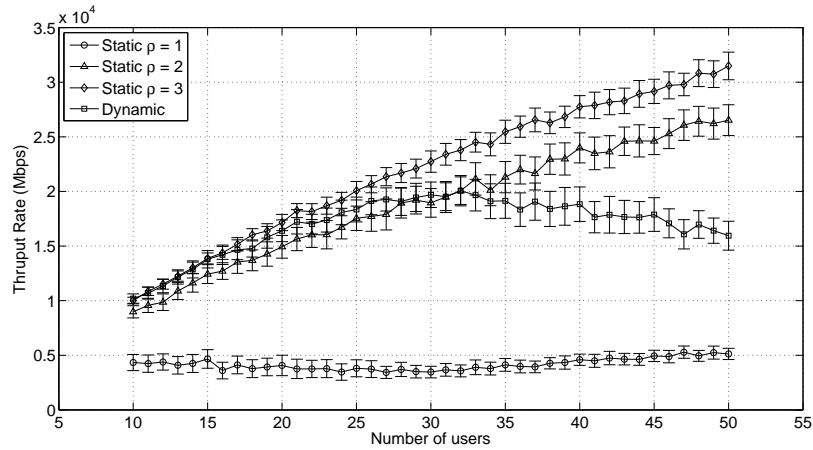
Figure 7.20: Average throughput utilizing multiple channels.
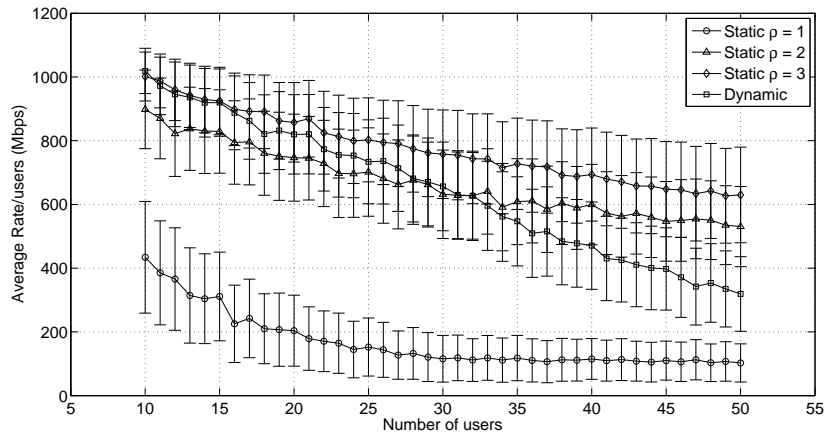
Figure 7.21: Data rate per user utilizing multiple channels.

7.2.5 Analytical Model

Figure 7.20 plots the average aggregate throughput in the room as a function of N. Note the almost linear scaling of the static algorithm ($\rho = 3$) with N. Indeed, the maximum throughput of 31 gbps is obtained at $N = 50$ users. To understand this performance, consider the following approximate mathematical model. Recall

that the static algorithm uses the $k = 21$ statically defined regions to allocate the channels. Let n denote the number of users in the system. These users are randomly uniformly distributed among the k regions. If a region has no users in it, we do not allocate a channel to that region. On the other hand, if a region has two or more users, we allocate two channels to that region and distribute users equally between the two channels. In the static algorithm with $\rho = 3$, we can reuse the channels every fourth region. Thus, channels used in region 1 can be reused in region 4 and so on. The schedule for this model of the static algorithm has a length of one slot. In order to compute the aggregate data rate, we need to find the number of regions r_1 with exactly one user and the number r_2 with more than one user. The aggregate throughput is then written as:

$$S = 7/6 \, (r_1 + r_2 \times 2) \ \text{gbps}$$

Note that we multiply r_2 with 2 since we allocate two channels and the aggregate rate per channel can be as high as 1 gbps. We multiple the expression on the right by 7/6 since we are using only 6 out of the 7 possible channels (that are used in the simulation).

In order to compute r_1 let us first find the probability $p_1(i)$ of the event when i regions out of k have at least one user. We can write this as,

$$p_1(i) = \frac{\binom{k}{i} \binom{n-1}{i-1}}{\binom{n+k-1}{n}}$$

Out of these i regions some number j will have more than one user. The conditional probability $p_2(j|i)$ of this happening can be calculated using the above formula but
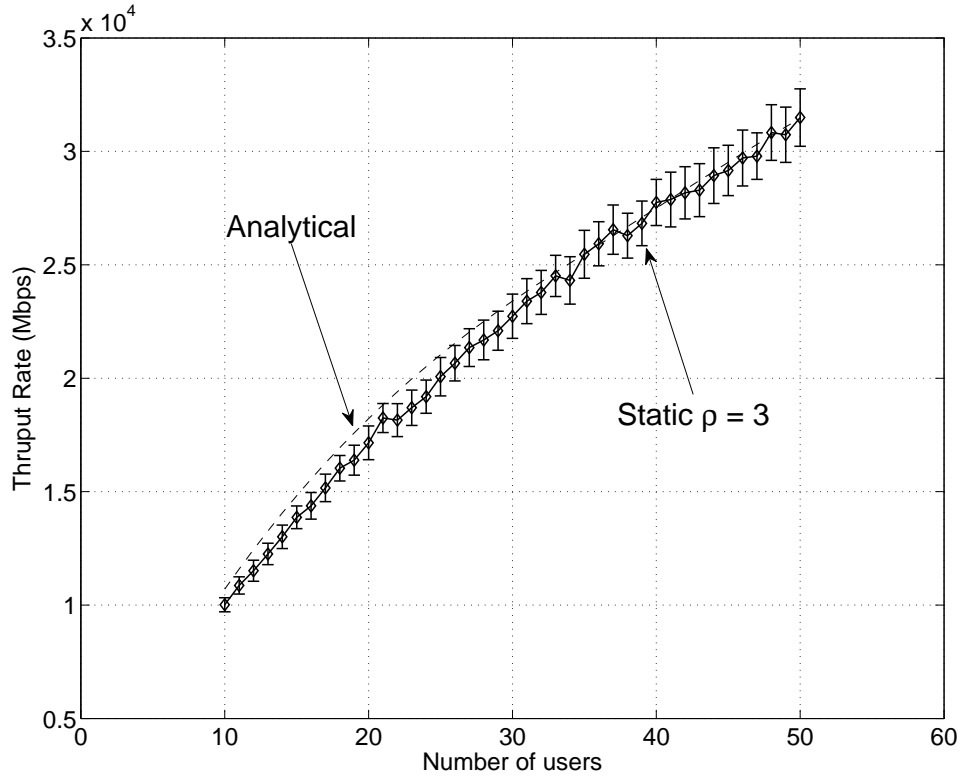
Figure 7.22: Analytical model for the static algorithm with $\rho = 3$.

substituting k with i, n with $n - i$, and i with j. Then,

$$r_2 = \sum_{i=1}^{k} p_1(i) \sum_{j=1}^{i} j p_2(j|i)$$

We can then obtain r_1 as,

$$r_1 = \sum_{i=1}^{k} i p_1(i) - r_2$$

Figure 7.22 plots the analytical model versus the simulation for the static algorithm. As we can see, the correspondence is very good. We observe that the above analysis can be carried forward for other values of ρ as well.

A second item of note is that the throughput of the dynamic algorithm is much

worse than that of the static algorithm ($\rho = 3$) unlike the case with a single-channel. The reason for this is that in the dynamic algorithm, spatial channels are separated by 3 dB only whereas the separation is much greater with the static algorithm when $\rho = 3$. The impact of this difference in channel spacing in the single-channel case is that we get a shorter schedule for the dynamic algorithm as opposed to the static algorithm, Figure 7.18. The immediate impact of a shorter schedule is greater aggregate throughput. In the multiple-channel case, all schedules end up being of length one slot and thus the dynamic algorithm loses that advantage. On the other hand, because the dynamic algorithm separates simultaneous spatial channels by only 3 dB, the interference in each channel is significant and starts playing a dominant role. This is why the dynamic algorithm performs poorly compared to the static algorithm.

Chapter 8

LINK REPAIR FOR MOBILE USERS

60GHz is well-suited for device-to-device communication and for general in-home applications due to its huge available bandwidth. However, links at this frequency are easily degraded by environmental conditions. Indeed, the poor multi-path makes it necessary to maintain good LoS (Line of Sight) paths between communicating pairs of nodes. In this chapter we analyze the problem of link breakage and degradation in point-to-point 60GHz networks. We propose two techniques to provide alternate paths between communicating nodes when the direct path degrades. The first technique uses static reflectors. This is a simple approach in which we add reflective material to the walls to provide an alternative path. The second technique uses repeaters. The decision on which path to use is driven by the goal of maximizing data rate per connection as well as overall throughput in the network.

Using extensive simulations we show that that by using static reflectors, we can maintain the connectivity at a cost of a reduction of 200Mbps in throughput. On the other hand, by carefully using repeaters, we can maintain Gbps rates for each pair of communicating nodes in indoor spaces.

8.1 PASSIVE/STATIC REFLECTORS

The 60GHz spectrum is susceptible to oxygen absorption and higher attenuation when encountering different materials in its path. The implications of this poor

signal propagation for WLAN design means that the connectivity of users may be poor. Thus, a user may be blocked by a wall or partition from the AP resulting in poor signal quality causing in very low data rates. Similarly, a user's link may be intermittently broken by the movement of other people in the room. Finally, as a user with an open connection moves about the room, the link may again be subject to obstructions. The challenge is how to mitigate these various types of connectivity problems.

The approach we study in this thesis is to use strategically placed *reflectors* to provide alternate paths for the signal to reach such disadvantaged users. Materials such as wire mesh glass [46] have excellent reflective properties at 60GHz and only attenuate the signal by 3dB for most angles of incidence. Thus, by placing sections of this material strategically on the walls of the room, the AP can provide better coverage.

Let us examine the problem of integrating reflectors into the STDMA schedules developed for the linear and circular antenna arrays respectively. In the case of a linear array, say we were to place a reflector on one wall (assume the array axis is parallel to the x-axis and we place the reflector on the wall parallel to the x-z plane). This has the effect of reflecting some regions back into the room. Consider Figure 8.1 where we assume that two walls parallel to the x-z plane are covered by a reflector over the bottom 1.5m. As we can see, each region is reflected back into the room.

In reality, we will only place small reflectors at specific locations to provide coverage in dead spots. So, for example, if we have a dead area in a part of region 4, we can cover it with a reflection of either region 4, 5, 6, 7, or 8 (depending on where the dead spot is located). Let us assume that the location of the dead spot is such that it is covered by the reflection of region 5. In that case, from the point of view of constructing a STDMA schedule, we need make no changes – this part of
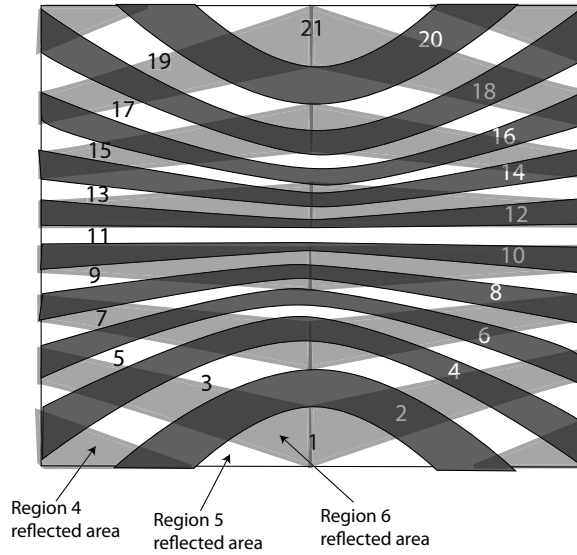
Figure 8.1: Reflected regions assume two walls are reflective at the bottom 1.5m.

region 4 is simply assigned to region 5 and users in the dead spot share bandwidth with the users located in region 5.

While the scheduling issue is simple to deal with, we do have to be aware of interference that is caused by reflected signals. Thus, assume that the dead spot in region 4 is covered by the reflection of region 7 and further assume that region 4 and 7 are scheduled in the same STDMA slot. In this case, there will be some interference caused at parts of region 4 from the reflected signal of region 7. Thus users need to place a null in the direction of the reflector. Since users are equipped with 20-element antenna arrays, this is not a problem.

We evaluate the data rate achieved with a linear array for three different cases when entire regions are a dead spot. The three cases considered are that either region 1 or region 4 or region 13 are dead spots. We use 7 modules and form $M - 1$ nulls from each module to maximize average throughput. For the regions covered by reflections, we use a 10dBm transmit power. Figure 8.2 plots the average data rate in each region. As expected, average throughput in all LOS regions remains

high while the regions that are dead spots show lower average throughput. The reason the throughput is lower is that the signal path length is longer when going via the reflector and because of attenuation of 3dB at the reflector. The throughput of region 13 is much lower than that of regions 1 and 4 because the total interference in region 13 is higher – region 13 is in the center of the room and is thus susceptible to more interference from direct as well as reflected paths. However, in general, the data rates achieved are still in the Gbps range for all cases.
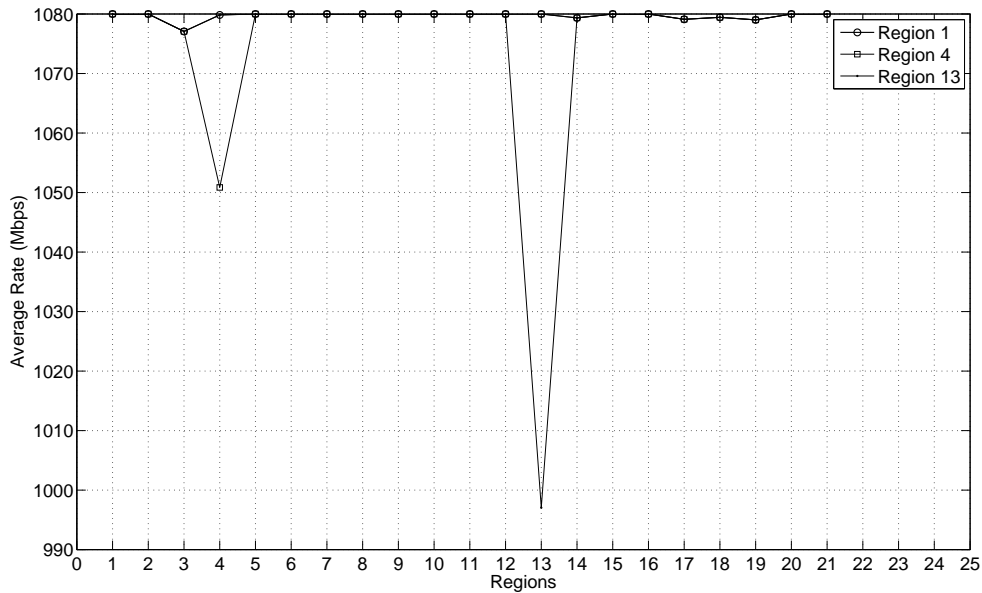
Figure 8.2: Data rate for three dead spot scenarios (Linear Array).

Next, let us consider the use of reflectors when the antenna array is circular. Unlike the linear case, the regions are smaller and better contained. Therefore, it is simpler to deploy reflectors and schedule transmissions. For example, if a dead spot occurs in region 15, then during the STDMA slot when region 15 is scheduled, rather than transmitting directly to region 15, the AP forms its beam at an appropriately placed reflector that covers region 15. Thus, the schedule will
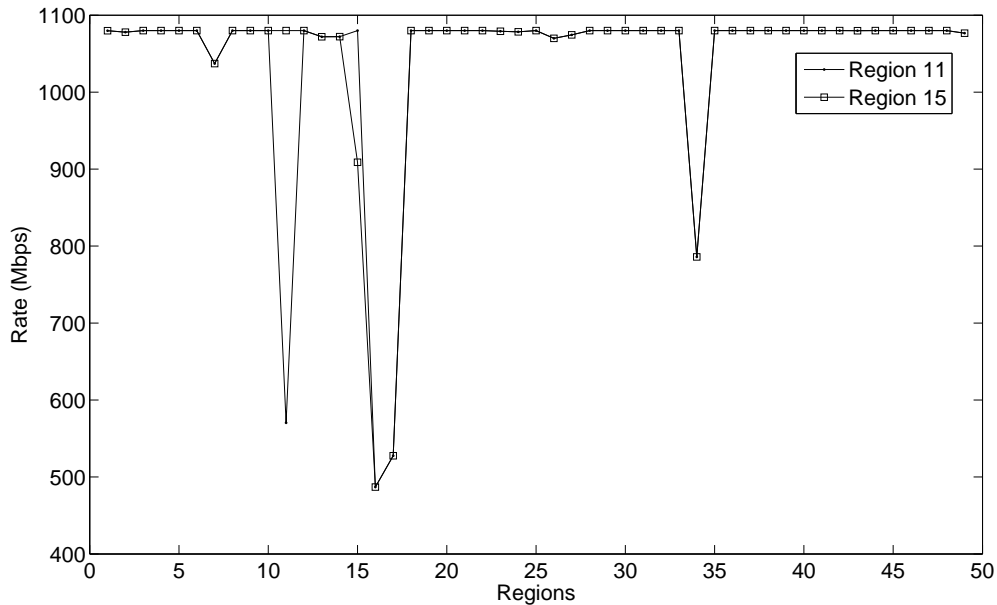
Figure 8.3: Data rate for two dead spot scenarios (Circular Array).

not change. The drawback is the added interference at neighboring regions since the reflected beam will spread out more as it travels a longer distance (AP to reflector to region 15). Figure 8.3 shows the data rate for the circular array case when the regions 11 and 15 are in dead spots. The data rate at these regions when using reflectors is 600 Mbps and 500 Mbps respectively.

8.2 ACTIVE REFLECTORS

In Figure 8.4 we show a typical room with several communicating pairs of devices. The wall-mounted display is showing a home movie that is streamed from a camera while a pair of users has set up a separate link to communicate and a third link connects a media server to a user's music headset. In the context of this network model, we note that there exists a problem with link breakage or degradation

106

because of interference. For instance, consider Figure 8.5 where a person has walked into the room. In this position, the presence of the user can break or severely degrade link 2 between the video camera and the display. Figure 8.6 shows a case where a new user enters the room and sets up a link with another device. This causes link 3 to degrade due to interference. In both of these cases, the existing links need to be repaired so as to maintain the needed data rate. This chapter studies the problem of selecting links that meet the needed data rate for pairwise communication in such indoor environments.
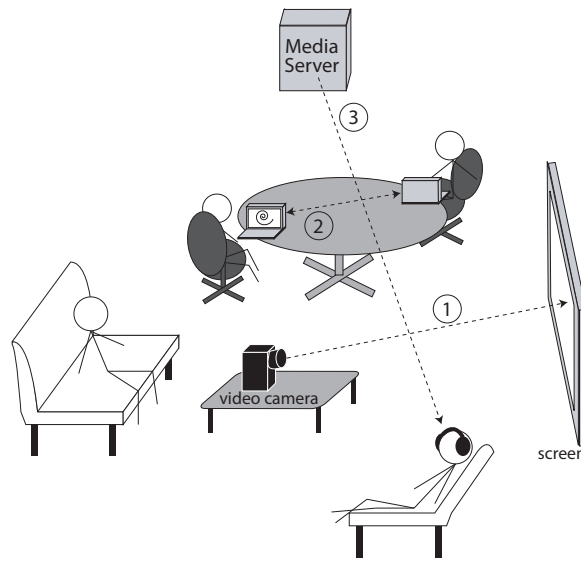
Figure 8.4: A typical use environment showing 3 pairs of communicating pairs.

The approach we investigate relies on the existence of one or more repeaters strategically placed about the room. These devices provide alternative routes between communicating pairs. For the case illustrated in Figure 8.5, a new 2-hop link can be established between the video camera and display that is obstruction free as shown in Figure 8.7. Likewise, when the quality of link 3 in Figure 8.6 degrades due to LoS interference, the link can be recreated via another repeater, also as shown in Figure 8.7. These examples illustrate the benefits of repeaters
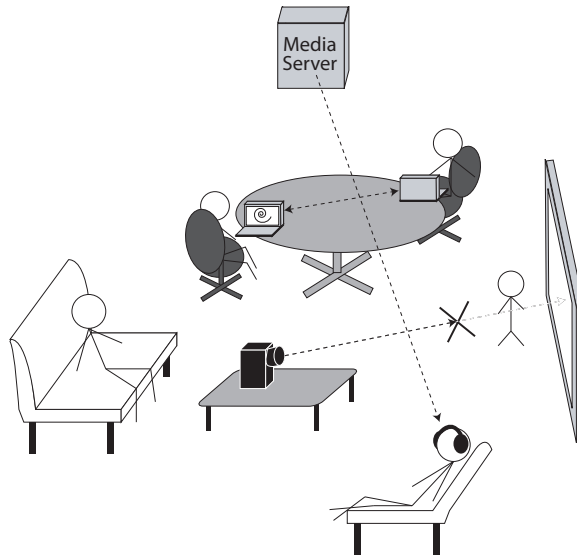
Figure 8.5: Link 1 between video camera and screen degrades due to obstruction (person).
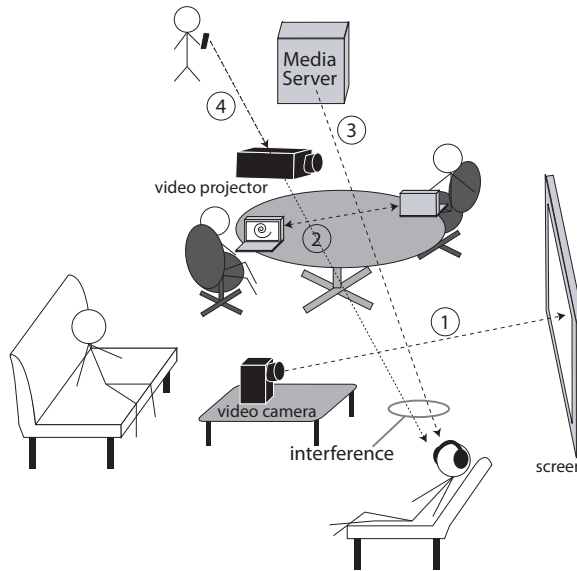
Figure 8.6: Interference caused at the user of link 3 by the appearance of new link 4.
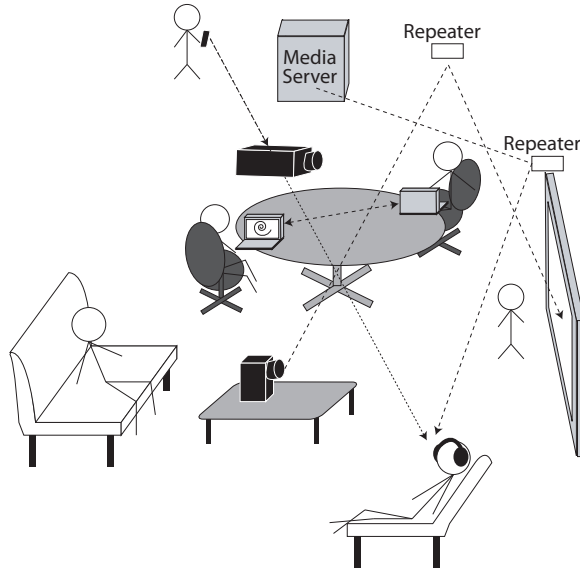
Figure 8.7: Repairing links using repeaters.

but it should be clear that in more complex environments, the placement and selection of repeaters is a non-trivial problem. Indeed, it is quite possible that using a repeater to fix one link may well degrade another existing link. Also, if several repeaters are needed simultaneously, the assignment of repeaters to links is key to reaching the required data rate per pair-wise connection as well as system throughput. In this chapter we study the problem of repairing links via repeaters and propose an algorithm for the assignment problem. We conduct a detailed analysis of the solution and study how it scales with increasing numbers of links.

8.3 SYSTEM MODEL

Figure 8.4 illustrates the usage model we consider. In general, we assume there are n pairs of communicating nodes and some number k of repeaters deployed about the room (the repeaters may well be other idle nodes that are tasked to aid active connections). All the nodes and repeaters are assumed to be equipped

109

with smart antennas, each with M antenna elements. The nodes and repeaters can beamform in any direction. Further, since a repeater serves to connect a communicating pair of nodes, we assume that it can simultaneously communicate with both the nodes that form the end-points of the link. Thus, the repeaters may be implemented either as store and forward nodes that receive packets on one link and then forward them on the other or as cut-through devices where the incoming signal is not decoded but simply forwarded on the outgoing link. We note that the analysis in this thesis is valid for either model.
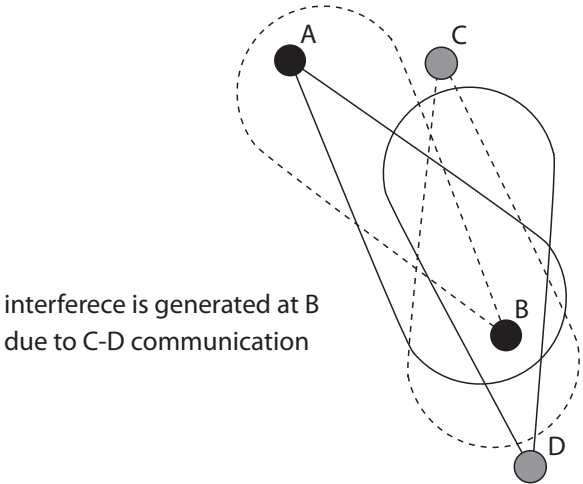
Figure 8.8: Degradation of a link due to interference from another.

The problem we consider can be summarized as follows: given n communicating node pairs and k repeaters, how can we establish n connections such that data rates are maximized for each pair? The problem is non-trivial because of interference and the existence of obstructions in the LoS path between pairs of communicating nodes. Figure 8.8 illustrates a simple case where one link interferes with another, thus reducing the data rate for that link[1]. As we can see, the transmissions from

---

[1]We emphasize that our focus in this thesis is on the data rates achievable using appropriate

node A to B will generate an interfering signal at node D thus degrading the SINR (Signal to Interference and Noise Ratio) and the data rate at D.

One can argue that with narrow enough beams, the amount of such interference can be eliminated or made negligible. In order to study this assertion further, we ran MATLAB simulations for random node placements and measured the interference. For a given n, we randomly uniformly place each node of that link somewhere within a room of size 10mx10m. Each node is assumed to have a *linear array* with $M = 20$ antenna elements. We use standard expressions for computing the array factor (AF) [17],

$$AF = \sum_{i=1}^{M} e^{j(i-1)kd(\sin\theta - \sin\theta_0)} \tag{8.1}$$

where $k = 2\pi/\lambda$ and d is the antenna element spacing. θ_0 is the angle at which we are forming the main beam and θ is the angle at which we are computing the array factor. λ is the wavelength at 60 GHz.

Each transmitter beamforms towards its receiver and each receiver beamforms towards its transmitter. At each receiver we calculate the *total interference* generated from each of the other $n-1$ transmitters. To do this accurately, we use a detailed 60GHz propagation model (described in [55]) that we have built in MAT-LAB. The model uses measured attenuation data for transmissions through and reflections off surfaces to predict the signal strength at each point in the room. Thus, at each receiver, we measure the sum total of direct as well as reflected signal components that act as interference. The path loss exponent is assumed to be 2.1 following [40]. The simulation model also accounts for inter-symbol interference due to multi-path between a communicating pair. We use a symbol time of

---

resource allocation algorithms at the Physical layer. We assume that collision events (i.e., where two or more transmissions collide at a receiver) are handled by a MAC layer.

Room dimensions	10m x 10m x 3m
Transmit power	10 dBm
Bandwidth	640 MHz
Modulation	Table 8.2
No. antenna elements	$M = 20$

Table 8.1: Experimental Parameters.

1.5625ns for the 640MHz channel considered. Other system parameters used are given in Tables 8.1 and 8.2.

Modulation	Code Rate	Min E_b/N_0 for $P_b \leq 10^{-6}$	Rate (Mbps)
64-QAM	3/4, 1/2	22.65 dB	1080, 960
16-QAM	3/4, 1/2	19.1 dB	720, 480
QPSK	3/4, 1/2	16.7 dB	360, 240
BPSK	3/4, 1/2	11.45 dB	180, 120

Table 8.2: Bit per second for different modulation schemes [39].

Figure 8.9 plots the number of links that break due to interference as a function of n. A link breaks if the SINR at the receiver is low enough that none of the 60 GHz rates can be supported. We see that when there are 10 links, on average 2 break and as many as 5 can break depending on the actual positions of the communicating nodes. This is despite the fact that we use highly directional beams for communication. The effect of interference is better illustrated when we look at Figure 8.10 where we plot the per-link throughput (max and average). Here, as the number of links increases, the average throughput starts falling linearly reaching a low of 600Mbps with 20 links. The inescapable conclusion is that, despite narrow beams and the constrained propagation behavior of 60 GHz signals, there is sufficient interference between simultaneous links to cause communication
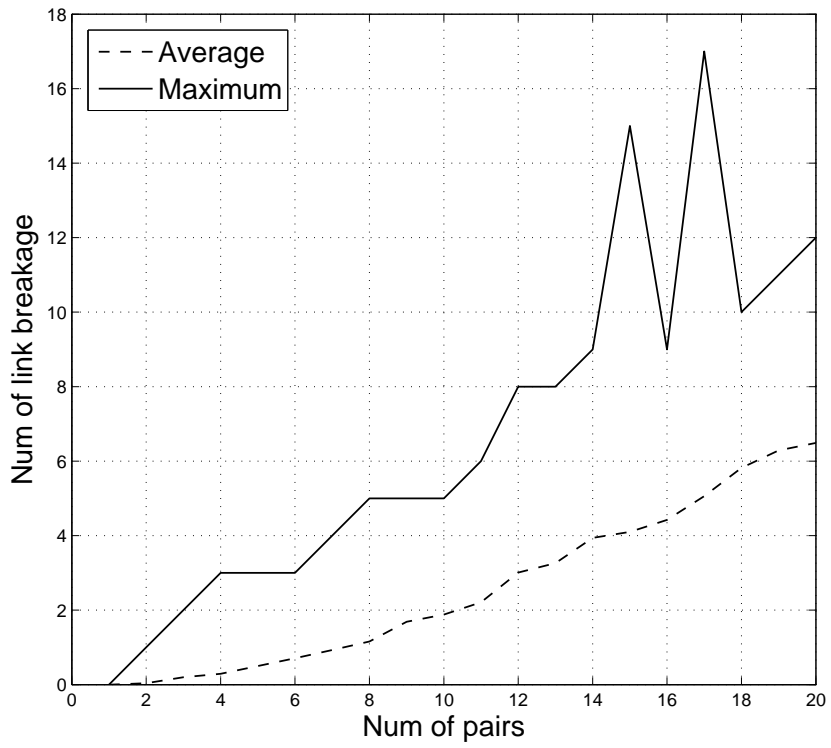
Figure 8.9: Impact of interference in number of broken links

failure. Hence the case for repeaters is well-justified.
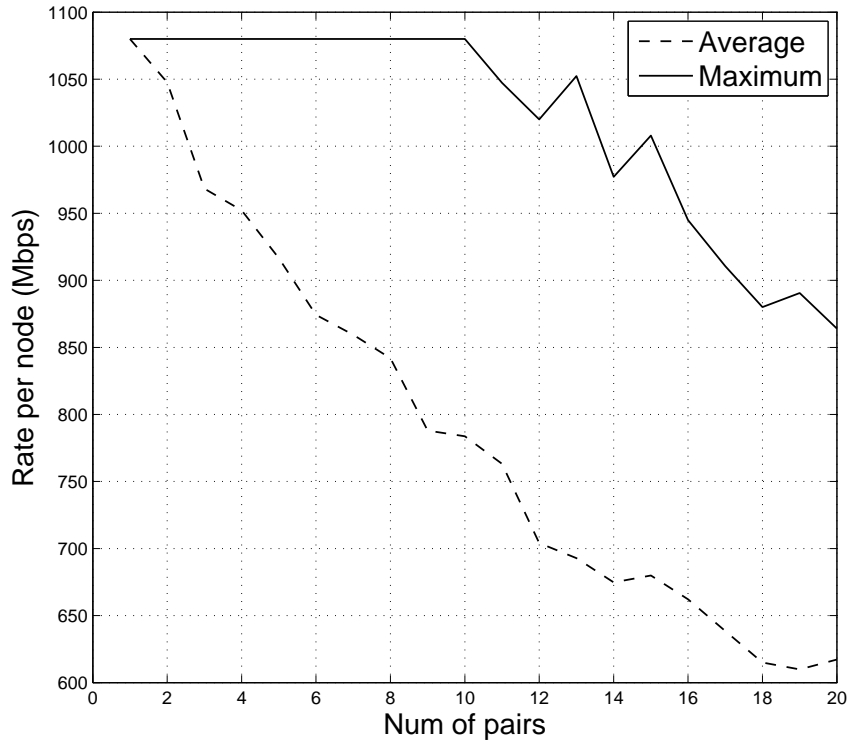
Figure 8.10: Impact of interference in throughput

8.4 ANALYTICAL MODEL

Let $p_1, p_2, \cdots, p_n$ denote the n communicating pairs of nodes and let k be the number of available repeaters. An allocation $\vec{a}$ is a n-tuple $(a_1, a_2, \cdots, a_n)$ where, $0 \leq a_i \leq k$ such that, $\forall a_i, a_j > 0, i \neq j, a_i \neq a_j$. The interpretation is that if $a_i = 0$ then the pair p_i communicates directly. If $a_i = l$ then the pair sets up a connection via repeater l. For a given allocation $\vec{a}$ let $\{r_1, r_2, \cdots, r_n\}$ be the data rates achieved by each pair of communicating nodes (after considering interference, attenuation, etc.) and let $r(\vec{a}) = \min\{r_1, r_2, \cdots, r_n\}$. Define $\vec{a}*$ to be the optimal

114

allocation if,

$$r(\vec{a}*) \geq r(\vec{a}), \forall \vec{a} \in \mathcal{A}$$

where $\mathcal{A}$ is the set of all possible allocations. The number of allocations can be written as,

$$|\mathcal{A}| = \sum_{i=0}^{k} \binom{k}{i} \binom{n}{i}$$

Observe that the optimal solution may only use $k' \leq k$ repeaters. We note that the problem of finding $\vec{a}*$ can be shown to be NP-hard (equivalent to integer programming).

The more realistic version of the problem is one where *each pair* of communicating nodes tries to optimize its performance independently of the other pairs. In this *distributed* version of the problem, the definition of optimum remains unchanged but the problem of finding the optimal solution is harder. In the next section we focus on this distributed problem and develop a simple solution to it.

8.5   GREEDY ALGORITHM

We develop a distributed greedy algorithm for finding an allocation that, in most cases, achieves the optimal link allocation. The algorithm is iterative and works as follows:

1. Initially each link is set up directly between the two end-points.

2. Each pair computes the best achievable rate for each direction of communication.

3. If a link does not achieve 800Mbps rate (in either direction), it will randomly uniformly choose a free repeater.

4. The link is now set up via this repeater, and this is done by all the links that fall below 800 Mbps.

5. After this step, each link recomputes the achievable data rate. It is possible that a previously good link now shows degraded performance due to interference from a newly rerouted link. As previously, every link that falls below the 800 Mbps threshold selects a new free repeater.

6. The algorithm iterates until no further improvement is seen in two consecutive steps. It is possible that the algorithm terminates with some pairs seeing data rates that are below the 800Mbps threshold.

Figure 8.11 illustrates the workings of this algorithm for a case when we have $n = 6$ and k is unrestricted (this is a screenshot of a visualization tool built on top of our MATLAB simulator). The room is 10mx10m and all nodes as well as repeaters are at a height of 1m. In the figure, each of the six pairs is labeled 1– 6 and the repeaters that get used are numbered R1, R2, etc. Initially, each of the pairs sets up a direct connection between the two end-points using their smart antennas. The bottom two bar charts in the figure correspond to the *four* iterations of the algorithm where the SINR and Rate is shown at the end of each iteration for each of the six pairs of nodes. Each bar (in a set of four bars) is one iteration of the algorithm for a given node.

In the figure, we plot the minimum observed SINR for each pair as the first bar (of the four bars) and is labeled by 'D'. The achieved data rate for each of the pairs is shown in the bottom most plot. Pairs 3 and 4 have a low data rate of 600Mbps and they each re-route the connection via repeaters in the next step – pair 3 goes via R8 and pair 4 goes via R1. The new SINRs and data rates for the five pairs are shown as the second bar in each group of bars in the bottom two plots. As a result of this re-routing (pair 3 via R8 and pair 4 via R1), the SINR for

116
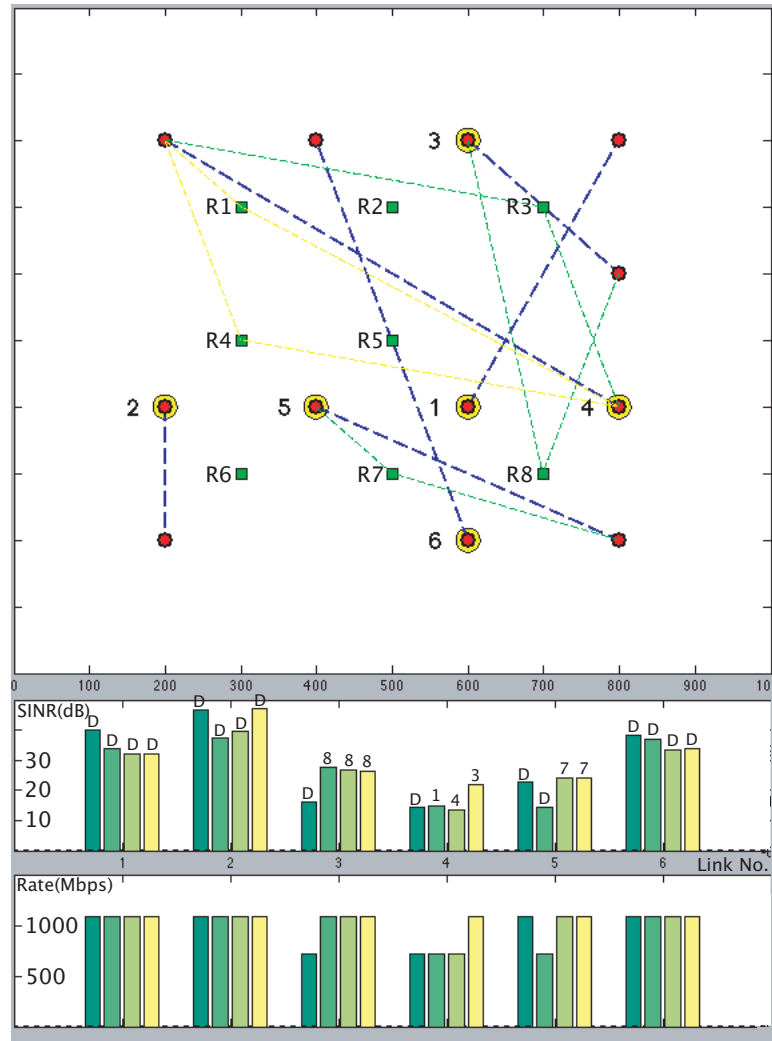
Figure 8.11: Illustration of the greedy algorithm (R-repeaters, node pairs are numbered from 1-6).

pair 5 drops, as does its data rate. Pairs 1 and 2 also see a small degradation in SINR but the data rate remains high. In the next iteration, pair 4 switches from R1 to R4 and pair 5 now chooses to go via a repeater R7. This improves pair 5's data rate but pair 4 is still below threshold. Finally, pair 4 changes the repeater yet again and selects R3. At this point, all the pairs have a data rate greater than

the threshold of 800 Mbps and the algorithm terminates.

8.6 EXPERIMENTAL EVALUATION

The goal of the simulations is to understand the effectiveness of repeaters in mitigating link failure. The *metrics* we used to study this question are:

- Data rate achieved per user,

- Number of repeaters used to fix *all* link breakages,

- Percentage improvement in throughput when using repeaters.

In order to get a comprehensive understanding of how repeaters may help, we used a large number of node placements in our study. Specifically, we use a room of size 10mx10m within which we placed $2n$ nodes randomly uniformly giving us n links. We considered $n = 4, 5, 6, 7, 8$. For each value of n we randomly generated 1000 different configurations and studied the performance of our algorithm in each case. Repeaters are placed at grid locations within the room and we use 16 repeaters in all. Note that no more than n repeaters will be used for a given n since we only consider cases when a link is routed through at most one repeater. The case when the number of repeaters $k < n$ is a subset of the case when k is unrestricted. For instance, if the number of repeaters used for a n is l then we know that using $k < l$ will result in $(k - l)$ broken links.

Finally, we place the nodes and repeaters all at a height of 1m above the floor. There are two reasons for this choice. First, in real deployments, the repeaters may actually be other idle nodes rather than special purpose devices. And second, as compared to the case when repeaters are deployed on the ceiling, the interference from repeaters towards the receivers will be significant in this case. This gives us a good lower bound on the benefits of using repeaters.
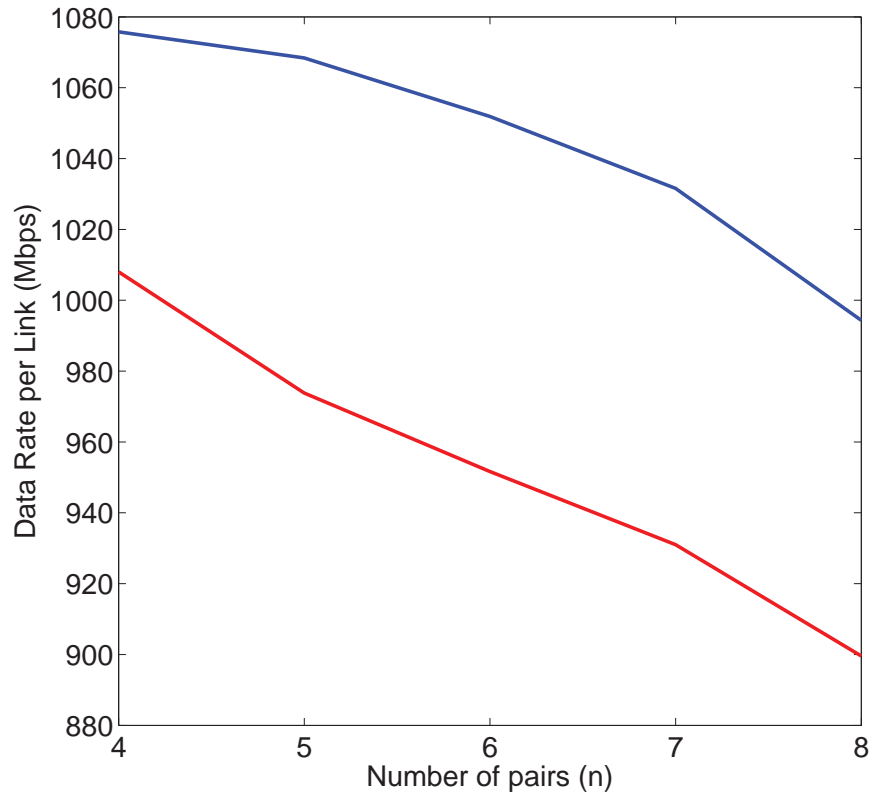
Figure 8.12: Overall improvement in data rates with repeaters.

In Figure 8.12 we plot the average per link data rate achieved as a function of the number of links with and without repeaters. We see that when using repeaters, the average per link data rate continues to be above 1Gbps whereas the data rate is much lower when we do not allow repeaters. Also, the average data rate per link falls with increasing number of links because there is greater interference, even when using repeaters. Figure 8.13 plots the average number of repeaters used as a function of n (averaged over 1,000 runs). It is interesting to see that even with $n = 8$ pairs, we use an average of only 2 repeaters. But the benefits of adding these two (on average) repeaters is enormous - the average data rate jumps from

less than 900Mbps to over 1Gbps/user.
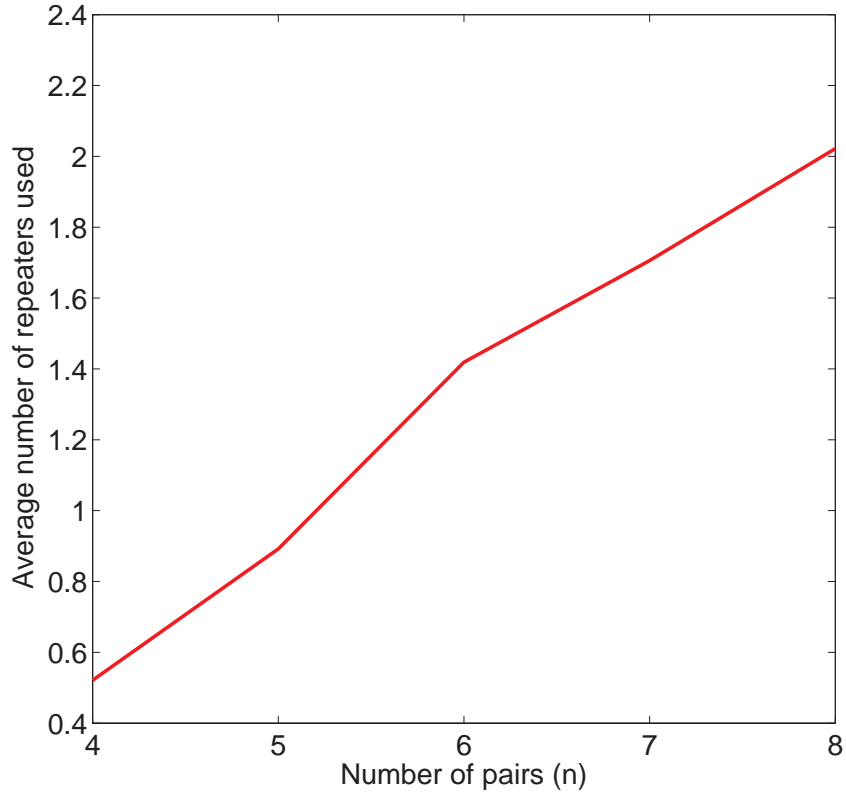
Figure 8.13: Average number of repeaters used.

In order to study the application of repeaters in more detail, let us consider the case when there are $n = 6$ pairs. The plot for the data rate in Figure 8.14 shows the expected improvement in data rate per link when using repeaters. The x-axis reports on the number of degraded links (when all pairs use the direct LoS link). When no link is degraded the data rate seen by each pair is over 1Gbps. When one pair's link is subject to interference, the average data rate without repeaters falls to 930Mbps. But when repaired using a repeater, the data rate climbs to over 1Gbps. When 4 or 5 of the six pairs see link degradation due to interference, the

average data rate is at about 500Mbps only but jumps up to 1Gbps with repeaters.
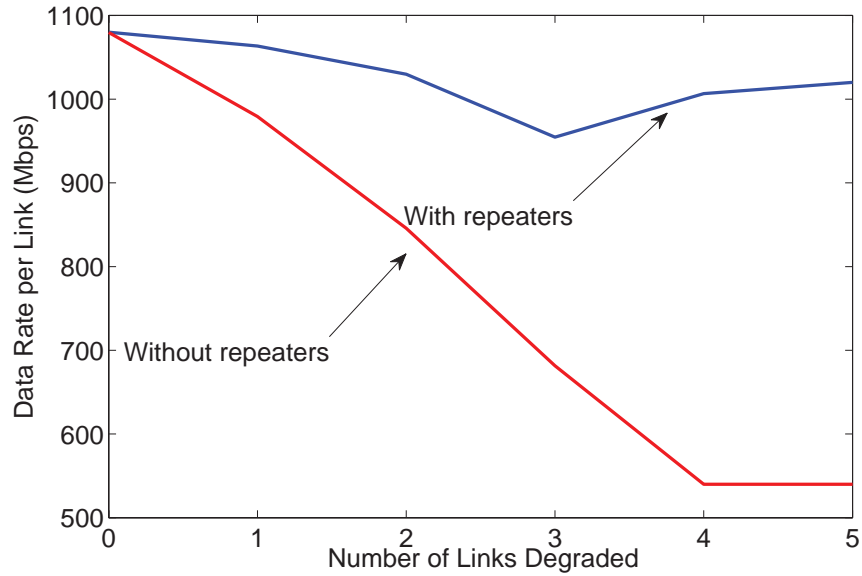
Figure 8.14: Improvement in data rate for $n = 6$ links.

In order to understand how often links degrade, Figure 8.15 plots the pdf (probability density function) of the number of links that fall below threshold when repeaters are not used. 30% of the time we see that repeaters are not required since no pair sees degraded link quality. However, about 35% of the time one pair does see poor quality of its direct link. Interestingly, there are cases when 5 out of 6 links fall below threshold. This clearly underscores the impact of interference and the need for repeaters. Figure 8.16 plots the number of repeaters used as a function of the number of links that degrade. The interesting observation is that the number of repeaters used scales linearly with the number of degraded links – this means that in most cases, repairing one link does little to improve another link's performance and thus each degraded link needs its own repeater. In some cases, for instance when 4 links are broken, the average number of repeaters used
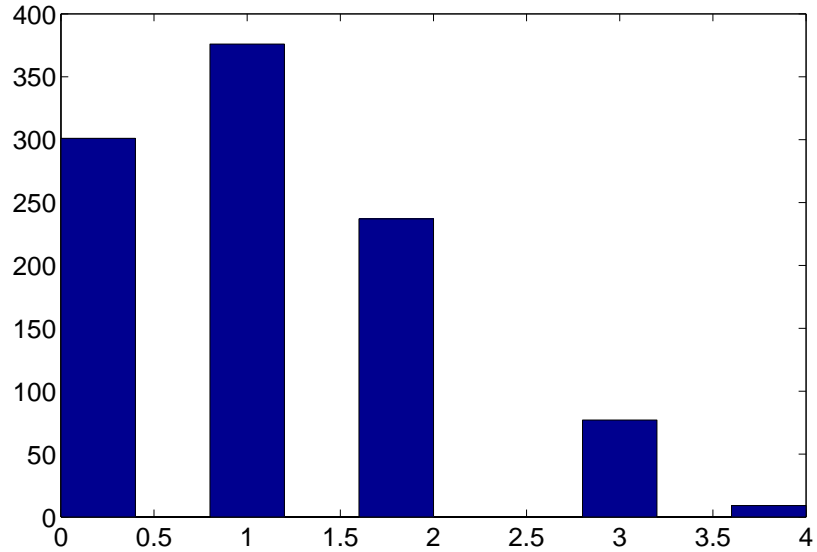
Figure 8.15: Probability density function of number of links broken for $n = 6$ links.

is 4.5. The reason for this is that re-routing a broken link via a repeater tends to break a previously good link (as we see in Figure 8.11 where link 5 was originally in good condition but then gets degraded due to link 4 being rerouted). Therefore, the total number of repeaters we may use could exceed the number of broken links without repeaters. Figure 8.17 plots the percentage improvement in data rate when using repeaters. We see that in all cases, the improvement is over 50% thus, again, showing the benefits and need to use repeaters.

8.7 DISCUSSION

We consider the problem of maintaining high data rate connectivity between pairs of communicating nodes in a 60GHz network. The challenge in maintaining these good connections is link breakage due to interference or mobile obstructions. We solve the problem by using repeaters that are randomly deployed about the room.
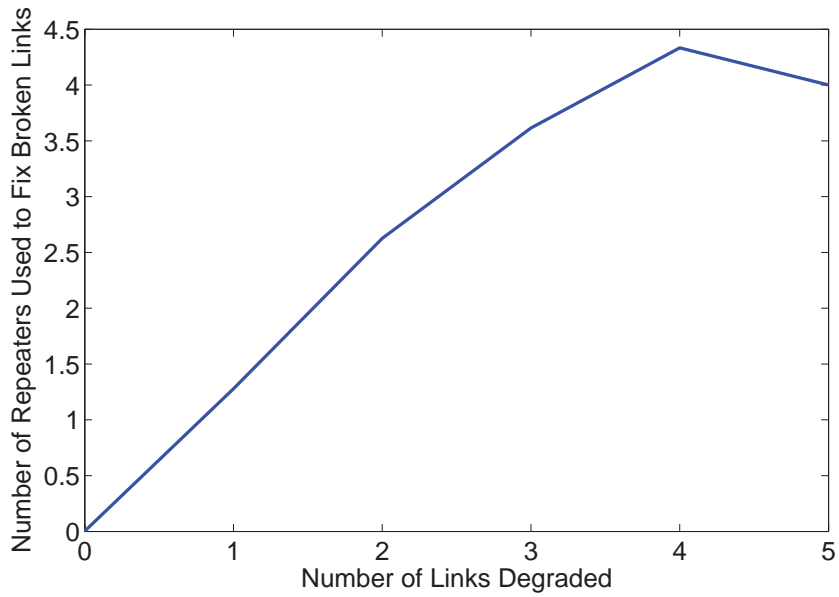
Figure 8.16: Number of repeaters used for $n = 6$ links.

If a pair of communicating nodes sees their data rate drop, they re-route their connection via a repeater. We show that a distributed greedy algorithm suffices to bring the system to a stable operating point in most cases with all pairs achieving over 1Gbps data rates.
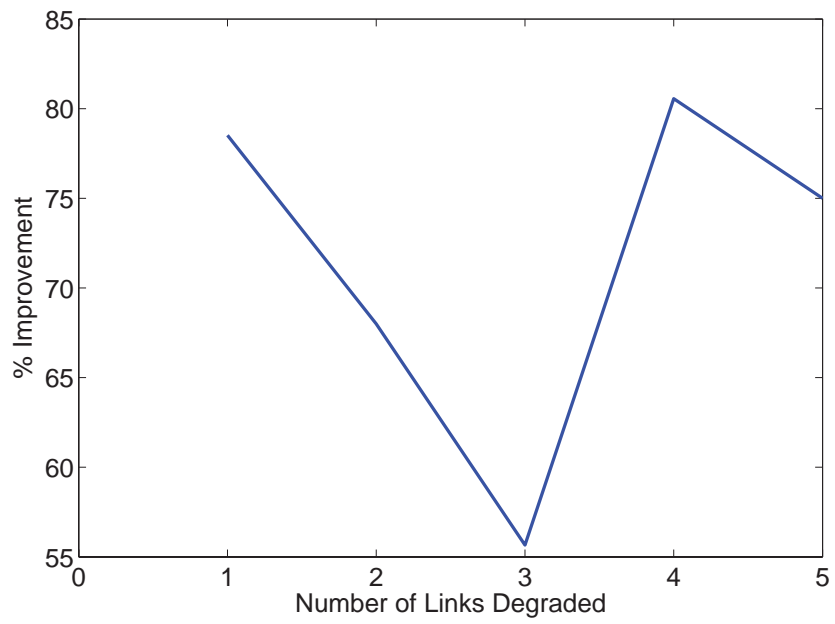
Figure 8.17: Improvement in data rate when using repeaters for $n = 6$ links.

Chapter 9

CONCLUSIONS AND FUTURE WORK

In this dissertation we have exploited the unique propagation properties of 60 GHz signals to provide gigabit/second rates to individual users in typical office settings. The research explored various challenges in using smart antennas for achieving this goal while simultaneously dealing with problems posed by frequent link breakages caused by mobile obstructions.

The following are the unique contributions of this research:

- Algorithms for antenna and/or access point placement in the room for 100% coverage in the presence of different obstacles were developed. Given n obstructions (partitions or isothetic rectangles) we show that fewer than n antennas are needed for full coverage. Indeed, if obstructions intersect in the room, we show that we require one less antenna for each such intersection.

- An examination of signal coverage within rooms using different smart antenna configurations revealed interesting ways to spatially partition the room to maximize frequency re-use. This fact was exploited to achieve gigabit/sec/user throughput. Thus, linear antenna arrays partition the room in long narrow strips (perpendicular to the antenna axis) whereas a circular antenna array partitions the room in more convex shapes. In both cases, the same frequency band can be used in partitions that are two partitions apart. Thus, the 5 GHz frequency band can be split into three giving us well over

1 GHz of spectrum for use in each narrow portion of a room. This, in turn, enables us to provide very high data rates to each user.

- In addition to WLANs, 60 GHz can be used for device-to-device communication in a room. We developed efficient link assignment algorithms (with repeaters located in the ceiling) to maximize throughput between each communicating pair. The algorithm is dynamic and adapts to changing configurations in the room as well as changing interference.

- Given that links break easily when there are mobile obstructions (such as people), we developed link repair algorithms that use passive reflectors located strategically about the room to extend coverage into these blocked areas. The passive reflectors degrade the signal by at least 3 dB but despite this we show that aggregate throughput in these areas is still well above 600 Mbps. The approach of using passive reflectors works naturally with the resource allocation algorithms developed.

- A great deal of work relied on detailed MATLAB simulations for validation. To this end we developed one of the earliest indoor propagation models for 60 GHz based on measurement studies and geometric algorithms for modeling signal propagation. This MATLAB code can be used for any room configuration and is thus of general interest to the research community.

9.1 FUTURE WORK

When this research was undertakes, there were few 60 GHz radios available for experimentation. Indeed, this part of the spectrum poses many design challenges including antenna design to cover over 5 GHz of spectrum. However, since then, some radios have been developed that cover portions of this spectrum. Therefore,

126

a possible future research direction is implementation of the developed resource allocation algorithms and experimentation using the available hardware. Another research direction is the development of MAC protocols that are specific to this frequency. Thus, CSMA protocols may not be a good choice because of the huge bandwidth (and hence small packet sizes). Alternative MAC protocols that use TDMA/FDMA/CDMA jointly appear to be a better choice. A detailed study of these protocols using 60 GHz hardware is another avenue of research. A third research direction is to develop MAC protocols closely tied with multi-media applications for specific application scenarios such as HDTV to Internet connections, etc. These protocols have a specific mode of operation and can be made very efficient by using cross-layer design techniques where application needs drive MAC and physical layer protocol design.

References

[1] A. T. Alastalo and M. Kahola. Smart-antenna operation for indoor wireless local-area networks using ofdm. *IEEE Transactions on Wireless Communications*, 2003.

[2] C. R. Anderson and T. S. Rappaport. In-building wideband partition loss measurements at 2.5 and 60 ghz. *IEEE Trans. on Wireless Communications*, 3(3):922 – 928, May 2004.

[3] F. Babich, M. Comisso, M. D'Orlando, and L. Mania. Interference mitigation on wlans using smart antennas. *Wireless Personal Communications*, 36(4), 2006.

[4] M. Bengtsson, D. Bartolome, J. L. Vicario, and C. Anton-Haro. Beamforming and bit-loading strategies for multi-user sdma with admission control. In *IEEE PIMRC*, 2005.

[5] W. Choi and J. Andrews. Downlink performance and capacity of distributed antenna systems in multicell environments. *IEEE Transactions on Wireless Communications*, Under Submission.

[6] Jurek Czyzowicz, Eduardo Rivera-Campo, and Jorge Urrutia. Illuminating rectangles and triangles in the plane. *J. Comb. Theory Ser. B*, 57:1–17, January 1993.

[7] C. Degan and L. Bruhl. Linear and successive predistortion in the frequency domain: performance evaluation in sdma systems. In *IEEE WCNC*, 2005.

[8] S. Diggavi, N. Al-Dhair, A. Stamoulis, and A. Calderbank. Great expectations: the value of spatial diversity in wireless networks. *Proceedings of the IEEE*, 92(2):219 – 270, Feb 2004.

[9] Richard Draves, Jitendra Padhye, and Brian Zill. Routing in multi-radio, multi-hop wireless mesh networks. In *Proceedings of the 10th annual international conference on Mobile computing and networking*, MobiCom '04, pages 114–128, New York, NY, USA, 2004. ACM.

[10] J-P. Ebert et. al. Paving the way for gigabit networking. In *Global Communications Newsletter*, April 2005.

[11] G. Fettweis and R. Irmer. Wigwam: system concept development for 1 gbit/s air interface. Wireless OWrld, Rsearch Forum, 2005.

[12] D. Gesbert, M. Shafi, D s. Shiu, P. Smith, and A. Naguib. From theory to practice: An overview of mimo space-time coded wireles systems. *IEEE-JSAC*, 21(3):281 – 302, April 2003.

[13] L. Godara. Application of antenna arrays to mobile communications, part ii: beamforming and direction-of-arrival considerations. *Proceedings of the IEEE*, 85(8):1195 – 1245, Aug 1997.

[14] E. Grass, M. Piz, F. Herzel, and R. Kraemer. Draft phy proposal for 60 ghz wpan. IEEE 802.15-05/0634r1, November 2005.

[15] E. Grass, M. Piz, F. Herzel, and R. Kraemer. Draft phy proposal for 60ghz wpan: Ieee p802.15 wg on wpans, November 2005.

[16] F. B. Gross and D. H. Schmidt. A new approach to sdma using spreading sequences as array weights. In *Wireless and Microwave Technology, 2005. WAMICON 2005. The 2005 IEEE Annual Conference*, 2005.

[17] Frank Gross. *Smart Antennas for Wireless Communications*. McGraw Hill, 2005.

[18] B. Hassibi. Multiple-antenna systems and wireless networks. In *IEEE Radio and Wireless Conference*, pages 63 – 66, 2006.

[19] C. Hoymann. Mac layer concepts to support space division multiple access in ofdm based ieee 802.16. *Wireless Personal Communications*, 36(4), March 2006.

[20] O. Kagami, I. Toyoda, and M. Umehira. Technologies for next-generation wireless lans. *NTT Technical Review*, 3(1):31 – 36, Jan 2005.

[21] M. Kobayashi, G. Caire, and D. Gesbert. Impact of multiple transmit antennas in a queued sdma/tdma downlink. In *6th IEEE Workshop on Signal Processing*, 2005.

[22] I. Koutsopoulos, T. Ren, and L. Tassiulas. The impact of space division multiplexing on resource allocation: a unified approach. In *IEEE INFOCOM*, 2003.

[23] I. Koutsopoulos and L. Tassiulas. Adaptive resource allocation in sdma-based wireless broadband networks with ofdm signalling. In *IEEE INFOCOM*, pages 1376 – 1385, 2002.

[24] I. Koutsopoulos and L. Tassiulas. Adaptive channel assignment in sdma-based wireless lans with transceiver resource limitations. *Signal Processing*, 2006.

[25] A. M. Kuzminskiy, H. R. Karimi, and C. B. Papadias. Downlink sdma for legacy ieee 802.11a/g mobile stations: acknowledgement recovery and channel estimation. In *Signal Processing Advances in Wireless Communications, 2005 IEEE 6th Workshop on*, 2005.

[26] A.M. Kuzminskiy, H.R. Karimi, D.R. Morgan, and C.B. Papadias. Downlink throughput enhancement of ieee 802.11a/g using sdma with a multi-antenna access point. *Signal Processing*, 86(8), 2006.

[27] B. Langen, G. Lober, and W. Herzig. Reflection and transmission behavior of building materials at 60ghz. In *IEEE PIMRC'94*, pages 505–509, 1994.

[28] C. P. Lim, R. J. Burkholder, J. L. Volakis, and R. J. Marhefka. Propagation modeling of indoor wireless communications at 60 ghz. In *IEEE Antennas and Propagation Society International Symposium*, pages 2149 – 2152, 2006.

[29] M. Marcus and B. Pattan. Millimeter wave propagation: spectrum management implications. *IEEE Microwave Magazine*, June 2005.

[30] V. Nikolopoulos, M. Fiacco, S. Stavrou, and S. R. Saunders. Narrowband fading analysis of indoor distributed antenna systems. *IEEE Antennas and Propagation Letters*, 2:89 – 93, 2003.

[31] J. Noreus, M. Flament, A. Alping, and H. Zirath. System considerations for hardware parameters in a 60 ghz wlan. In *Proceedings 60 GHz 2000 Symposium*, pages 267 – 270, March 2000.

[32] A. J. Paulraj, D. A. Gore, R. U. Nabar, and H. Bolcskei. An overview of mimo communications: A key to gigabit wireless. *Proceedings of the IEEE*, 92(2):198 – 218, Feb 2004.

[33] Ram Ramanathan. On the performance of ad hoc networks with beamforming antennas. In *ACM MOBIHOC*, pages 22 – 32, 2001.

[34] M. Schubert and H. Boche. Solution of the multiuser downlink beamforming problem with individual snir constraints. *IEEE Transactions on Vehicular Technology*, 53, 2004.

[35] F. Shad, T. Todd, V. Kezys, and J. Litva. Dynamic slot allocation (dsa) in indoor sdma/tdma using a smart antenna basestation. *IEEE/ACM Transactions on Networking*, 9(1):69 – 81, Feb 2001.

[36] W. Shen, Z. Fang, and Z. Wang. Multi-user mimo sdma system in broadband wlan. In *Broadband Networks, 2005 2nd International Conference on*, 3 – 7 Oct 2005.

[37] Harkirat Singh and Suresh Singh. Smart-aloha for multi-hop wireless networks. *Mob. Netw. Appl.*, 10:651–662, October 2005.

[38] Bernard Sklar. *Digital Communications Fundamentals and Applications*. Prentice Hall, 2000.

[39] Bernard Sklar. *Digital Communications*. Prentice Hall, 2005.

[40] P. Smulders. Exploiting the 60ghz band for local wireless multimedia access: prospects and future directions. *IEEE Communications Magazine*, pages 140 – 147, January 2002.

[41] P. Vandenameele, S. Thoen, M. Engels, and H. De Man. A combined ofdm/sdma approach for wlan. In *Proceedings IEEE VTC*, pages 1712 – 1716, 1999.

[42] Vieri Vanghi, Aleksandar Damnjanovic, and Branimir Vojcic. *CDMA: Principles of Spread Spectrum CommunicationCDMA: Principles of Spread Spectrum Communication*. Prentice Hall, 2004.

[43] A. wittneben and B. Rankov. Distributed antenna systems and linear relaying for gigabit mimo wireless. In *IEEE VTC-Fall*, volume 5, 2004.

[44] P. Wolniansky, G. Foschini, G. Golden, and R. Valenzuela. V-blast: an architecture for realizing very high data rates over the rich-scattering wireless channel. In *Proceedings URSI International Symposium on Signals, Systems, and Electronics., (IEEE, New York, NY, USA)*, pages 295 – 300, 1998.

[45] K.H. Wu, W.H. Fang, and J.T. Chen. Joint doa-frequency offset estimation and data detection in uplink mimo-ofdm networks with sdma techniques. In *IEEE VTC-Spring*, volume 6, 2006.

[46] H. Xu, V. kukshya, and T. Rappaport. Spatial and temporal characteristics of 60ghz indoor channels. *IEEE Journal in Selected Areas in Communications*, 20(3):620 – 630, April 2002.

[47] H. Yin and H. Liu. Performance of space-division multiple access (sdma) with scheduling. *IEEE Transactions on Wireless Communications*, 1(4):611 – 618, October 2002.

[48] C. Yiu and S. Singh. Tracking people in indoor environments. In *5th International Conference on Smart homes and health Telematics (ICOST'07)*, 2007.

[49] C. Yiu and S. Singh. Empirical capacity of mmwave wlans. *Selected Areas in Communications, IEEE Journal on*, 27(8):1479 –1487, october 2009.

[50] C. Yiu and S. Singh. Sdma for 60ghz gigabit wireless networks. In *Communications, 2009. ICC '09. IEEE International Conference on*, pages 1 –6, june 2009.

[51] C. Yiu and S. Singh. Link selection for point-to-point 60ghz networks. In *Communications (ICC), 2010 IEEE International Conference on*, pages 1 –6, may 2010.

[52] C. Yiu and S. Singh. Coverage problem for 60ghz wireless networks. In *Proceedings IEEE International Communications Conference (ICC) 2012*, 2012 (under submission).

[53] Candy Yiu and S. Singh. High data rate wlan. In *Vehicular Technology Conference, 2008. VTC Spring 2008. IEEE*, pages 1821 –1825, may 2008.

[54] Candy Yiu and S. Singh. Architecture considerations for 60 ghz wireless networks. In *Ultra-Wideband, 2009. ICUWB 2009. IEEE International Conference on*, pages 6 –11, sept. 2009.

[55] Candy Yiu and Suresh Singh. Impirical capacity of mmwave wlans. *IEEE Journal on Selected Areas in Communications*, 2009.

Appendices

Appendix A

PATH LOSS IN MATLAB

```
% This function return path loss in free spce from point p1 to point
% p2 and return path loss in db
% Input parameters:
%        p1 - point 1 in pair
%        p2 - point 2 in pair
%        alpha - path loss exponent


function [loss] = PathLoss(p1,p2,alpha)


n = alpha;              %path loss exponent
C = 0;                  %System Constant
d = points_dist_nd (3,p1,p2)/100;
loss = 10*n*log10(d)+C;



%This function returns the distance between point p1 and point p2


function dist = points_dist_nd ( dim_num, p1, p2 )
```

```
dist = sqrt ( sum ( ( p1(1:dim_num) - p2(1:dim_num) ).^2 ) );
```

Appendix B

LINEAR ARRAY IN MATLAB

```
%This function is to calculate the antenna gain of a linear array
%given the following parameters:
%xx - x coordinate of the antenna
%yy - y coordinate of the antenna
%zz - z coordinate of the antenna
%Rx - x coordinate of the angle of interest
%Ry - y coordinate of the angle of interest
%Rz - z coordinate of the angle of interest
%W - room size in width
%L - room size in length
%step - resolution of how accuracy the output should be
%nTheta - nulling direction
% M - number of array elements
%debug mode on = 1/off = 0
% weightM = 1 use exact weight

function G_est = linearGain4A_NULL(xx,yy,zz,Rx,Ry,Rz,...
                W,L,step,nTheta,M,debug,weightM)
```

```matlab
% Assign the desired angle (DOA)
theta(1) = getMapAngle(xx,yy,zz,Rx,Ry,Rz);


% Follow by all interference angle
for q=1:length(nTheta)
    theta(q+1) = nTheta(q);
end


if(Rz == 300)
    GmaxArray = ones(50,50)*14;
else
    GmaxArray = ones(50,50)*14;
end


Gmax = 14;


d = 0.5;                              % element spacing in wavelengths
u = [1;zeros(length(theta)-1,1)];
x = [1:step:W];
y = [1:step:L];


%----- Determine steering vectors and matrix of steering vectors -----%
i = -(M/2-.5):(M/2-.5);


for n = 1:length(theta)
    A(:,n) = exp(1j*i*2*pi*d*(sin(theta(n) )-sin(theta(1)))).';
end
```

```
%----- Determine Array Weights -----%
if(length(theta)==M)
    if(weightM == 1)
        w = u.'*inv(A);
    else
        w = u.'*A'*inv(A*A'+1e-9*eye(M));
    end
else
    w = u.'*A'*inv(A*A'+1e-9*eye(M));
end


th = -pi/2:.001:pi/2;


AF = 0;


for l = -(M/2-.5):M/2-.5
    AF = AF + w(l+(M/2+.5)).*exp(1j*l*2*pi*d*(sin(th)-sin(theta(1))));
end


AFn = abs(AF).^2/max(abs(AF).^2);
G_est = 10*log10(AFn.*10^(Gmax/10));


if(debug == 1)
    figure1 = figure;
    plot(th*180/pi,AFn,'b');
    hold on;
```

```matlab
    plot(th*180/pi,AFno,'k');

    grid on;

    plot([theta(1)*180/pi theta(1)*180/pi],[0 1],'r');

    hold on;

    for i=1:length(nTheta)

        plot([nTheta(i)*180/pi nTheta(i)*180/pi],[0 1],'g');

        hold on;

    end

    title(strcat('Beamforming at ',int2str(theta(1)*180/pi)));

    legend1 = legend('Exact weight','Estimated weight',...

            'DOA','Nulling SNOI');

    set(legend1,'Position',[0.4142 0.5487 0.1946 0.2576]);

end


end
```

CIRCULAR ARRAY IN MATLAB

```
%This function is to calculate the antenna gain of a circular array
%given the following parameters:
%xx - x coordinate of the antenna
%yy - y coordinate of the antenna
%zz - z coordinate of the antenna
%Rx - x coordinate of the angle of interest
%Ry - y coordinate of the angle of interest
%Rz - z coordinate of the angle of interest
%W - room size in width
%L - room size in length
%step - resolution of how accuracy the output should be
%nTheta - nulling direction in  elevation angle
%nPhi - nulling direction in azimuthal angle
%debug mode on = 1/off = 0


function [G_est] = circularGain4A_NULL(xx,yy,zz,Rx,Ry,Rz,...
                    W,L,nTheta,nPhi,debug)
a = 1;
N = 20;                  %number of antenna element
th = [0:100]*pi/100;
```

```
ph = [0:100]*2*pi/100;


pinc = 2*pi/N;


Gmax = 14;


[theta(1),phi(1)] = get3Angle(xx,yy,zz,Rx,Ry,Rz);


if(debug >= 1)
    fprintf('********************\n');
    fprintf('DOA Angle th=%f, ph=%f\n',theta(1)*180/pi,phi(1)*180/pi);
    fprintf('NULL Angle th=%f, ph=%f\n',nTheta*180/pi,nPhi*180/pi);
end


for q=1:length(nTheta)
     theta(q+1) = nTheta(q);
     phi(q+1) = nPhi(q);
end


%-----------------calculate optimal weight---------------%%
NoOfsamples = 100;
lamda = 1;                        % c/f = 1
variance = 1/10;                  % Noise variance
d = lamda/2;                      % distance between elements
beta = 2 * pi;                    % Beta is phase propagation
                                  %     factor B = 2 pi / lamda
degr = pi/180;
```

```matlab
rdeg = 180/pi;

numplot = 360;

alpha=linspace(0,2*pi,numplot);


for n = 1 : N
    U_d(n,1) = exp(-1j*2*pi*(sin(theta(1)).*...
                cos(phi(1)-(n-1)*pinc)));
end


Covar_d = conj(U_d)*conj(U_d');


S = conj(U_d);


NoOfsignals = length(nTheta);


for n = 1 : N
    for k =1 : NoOfsignals
        U_i(n,k) = exp(-1j*2*pi*(sin(nTheta(k)).*cos(nPhi(k)-(n-1)*pinc)));
    end
end


Covar_n = variance * eye(N);


Covar_i = zeros(N);


for k = 1 : NoOfsignals
        Covar_i = Covar_i + conj(U_i(:,k))*conj(U_i(:,k)');
```

```
end



Covar = Covar_n + Covar_d + Covar_i;



W_opt = inv(Covar) * S;
W_optc = conj(W_opt');
Y = zeros(180,360);


for n = 1: N
    for t = (1:180)
        for p = (1:360)
            X(q,t,p) = exp(-j * (q-1) * 2 * pi/lamda * ...
                        d * cos(degr*theta));
            X(n,t,p) = exp(-1j*2*pi*(sin(degr*t).*...
                        cos(degr*p-(n-1)*pinc)));
            Y(t,p) = Y(t,p) + W_optc(n)*exp(-1j*2*pi*...
                        (sin(degr*t).*cos(degr*p-(n-1)*pinc)));
        end
    end
end


AF = Y;
%------------------
AFn = abs(AF).^2/max(max(abs(AF).^2));
G_est = 10*log10(AFn.*10^(Gmax/10));
```

```matlab
if(debug >= 1)
%      figure(1);
%      plot(th*180/pi,AFn(:,ceil(phi(1)/(2*0.0314)+1)));
%      title(strcat('Beamforming at ',int2str(theta(1)*180/pi),', max gain
%      is ',int2str(DOA_gain)));
    DOA_gain = G_est(floor(theta(1)*rdeg+1),floor(phi(1)*rdeg+1));
    fprintf('-----\nDOA Gain is %f\n',DOA_gain);
    if(length(theta)>1)
        NULL_gain = G_est(floor(theta(2)*rdeg+1),floor(phi(2)*rdeg+1));
        fprintf('NULL Gain is %f\n',NULL_gain);
    end


    ci =0;
    for i=1:10:W
        ci = ci+1;
        cj=0;
        for j=1:10:L
            cj=cj+1;
            [t,p] = get3Angle(i,j,50,500,500,300);
            g2d(ci,cj)=G_est(floor(t*rdeg+1),floor(p*rdeg+1));
        end
    end


    surf([1:100],[1:100],g2d);


    plane_max = 0;
    plane_min = 20;
```

146

```matlab
        plane_max_id = [0 0];
        plane_min_id = [0 0];
        for i=1:180
            for j=1:360
                if(i>=116)
                    if(plane_max < G_est(i,j))
                        plane_max = G_est(i,j);
                        plane_max_id = [i,j];
                    end
                    if(plane_min > G_est(i,j))
                        plane_min = G_est(i,j);
                        plane_min_id = [i,j];
                    end
                end
            end
        end
        fprintf('plane Maximum Gain = %f , \nAngle th = %f, ...
                ph = %f\n\n',plane_max,plane_max_id(1),...
                plane_max_id(2));
        fprintf('plane Minimum Gain = %f , \nAngle th = %f, ...
                ph = %f\n\n',plane_min,plane_min_id(1),...
                plane_min_id(2));

end


end
```